(42)

A Numerical Model Investigation of the Effects of Proposed Confined Disposal Facilities on New Bedford Harbor, Massachusetts

by

R. Michael Lohse

B.S., Mechanical Engineering, Northwestern University, 1993

Submitted to the Department of Ocean Engineering
in partial fulfillment of the requirements for the degrees of

Master of Science

and

Master of Engineering in Marine Environmental Systems

at the

MASSACHUSETTS INSTITUTE OF TECHNOLOGY

February 1997

Author .....
Department of Ocean Engineering
October 11, 1996

Certified by .....
Dr. E. Eric Adams
Senior Research Engineer, Ralph M. Parsons Laboratory
Department of Civil and Environmental Engineering
Thesis Supervisor

Accepted by .....
Professor J. Kim Vandiver
Professor of Ocean Engineering
Chairman, Departmental Committee on Graduate Studies

A Numerical Model Investigation of the Effects of Proposed Confined Disposal Facilities on New Bedford Harbor, Massachusetts

by

R. Michael Lohse

Submitted to the Department of Ocean Engineering
on October 11, 1996, in partial fulfillment of the
requirements for the degrees of
Master of Science
and
Master of Engineering in Marine Environmental Systems

Abstract

New Bedford Harbor sediments are contaminated with polychlorinated biphenyls (PCB), a result of four decades of poor environmental and industrial regulation. Surrounding towns are now faced with dredging and properly disposing over 400,000 cubic yards of contaminated sediments from the harbor. One likely option for disposal is the construction of confined disposal facilities (CDF) along the shoreline of the harbor, which will lead to changes in the hydraulics of the harbor.

A numerical model of New Bedford Harbor has been developed and calibrated using analytical techniques presented in this thesis as well as observations from previous studies. Existing baseline conditions have been modeled under normal and extreme meteorological forcing, and the velocity fields from this model have been compared to those from models incorporating proposed CDF sites in alternative arrangements under equivalent forcings. Each CDF siting scenario has been analyzed based on sediment erosion criteria to determine potential environmentally impacted areas. Recommendations regarding an optimal arrangement of the CDFs are based on quantitative (e.g., maximum velocity fields) and qualitative (e.g., A vs. B) analyses. Upper estuary CDFs are shown to result in velocities in excess of the critical resuspension velocity under normal baseline conditions (i.e., non-extreme events). This suggests that the CDFs are better sited in the lower harbor, where they not result in adverse effects on the flow velocities. Furthermore, areas in the lower harbor have been identified that provide practical siting alternatives such that they do not interfere with harbor traffic.

Thesis Supervisor: Dr. E. Eric Adams
Title: Senior Research Engineer, Ralph M. Parsons Laboratory
Department of Civil and Environmental Engineering

Acknowledgments

Many people have been extremely helpful in the pursuit of this thesis. First and foremost, I would like to thank Dr. Eric Adams for taking me on as a thesis advisee. I am also grateful to Dr. Judy Peterson for believing in me and my work and providing valuable insight for this thesis as my pseudo-advisor; I will always be indebted to Dr. Peterson for her advice and support.

Special thanks to Professor Judy Kildow, without whom I would not have had the opportunity to explore the environmental monitoring field in such depth. Other faculty thanks to Professor Carmichael, Dr. Mazel, and Professor Milgram for their assistance along the way.

In addition to faculty, several other graduate students have made this thesis better in one way or another. Thanks to Ling Tang for his patience and help in working and modifying the ECOM-si code. Thanks also to the rest of the Adams lab for providing valuable input.

I would like to thank my family members for supporting me in my decision to go to graduate school as well as Adèlle Smith for providing *in situ* support and friendship in a sometimes unforgiving environment. Thanks also to Todd Jackson who provided welcome distractions during my work.

Outside of the Institute, I offer my thanks to Dr. Rich Signell of USGS for introducing me to the ECOM-si model, as well as his colleagues, including John Evans of USGS, who provided several useful tools for analyzing the ECOM-si data.

Contents

List of Figures

List of Tables

Chapter 1

Introduction

1.1 Overview

Anthropogenic stresses on the productivity and sustainability of the New Bedford Harbor estuarine and Buzzards Bay marine ecosystems have severely impacted local commercial fishing and shipping industries. The disposal of carcinogenic polychlorinated biphenyls (PCBs) and heavy metals into the New Bedford Harbor over the period of four decades along with poor sewage treatment methods have led to widespread contamination of harbor sediments, with PCB's concentrated in some areas as high as 40,000 ppm, or 4% by weight (USEPA 1992). The contaminants have spread throughout the inner harbor, sorbed to small sediment particles that eventually accumulate in benthic organisms and man-made navigation channels. A hurricane barrier, built at the mouth of the New Bedford Harbor restricts flushing out of the harbor; however, significant quantities of the contaminated sediments have been moved out of the harbor into Buzzards Bay by years of tidal action.

In 1982, the United States Environmental Protection Agency (USEPA) designated New Bedford Harbor as its first Superfund site, providing federal funds for remediation measures. The USEPA clean-up has been divided into three phases, which focus on 1) hot spots, 2) sediments with PCB concentrations greater than 50 ppm, and 3) sediments with PCB concentrations greater than 10 ppm (USEPA 1992a). The first phase was completed in September of 1995, removing approximately 10,000 cubic

yards of contaminated sediment material, treating and storing it at a pilot confined disposal facility on the New Bedford waterfront until permanent sites can be located and developed. When completed, the three-phase clean-up will have removed over 400,000 cubic yards of contaminated sediment material (USEPA 1995), requiring a single large disposal site or several smaller sites. Though many options and alternative methods have been tested via pilot studies, USEPA officials favor the construction of confined disposal facilities (CDF) along the New Bedford shoreline. Concerns from the public, however, have delayed the siting and construction of these CDFs. The final two clean-up phases cannot be started (or completed) until storage facilities are built to house the contaminated material.

Public concerns over the siting of the CDFs also have postponed maintenance dredging of navigation channels indefinitely because these sediments are also contaminated and must be stored in confined facilities. The volume of contaminated sediments from the maintenance dredging of navigation channels (to project depths plus overdepth) is estimated at approximately 1.1 million cubic yards, 800,000 cubic yards of which is located inside that hurricane barrier and is most likely unsuitable for open ocean disposal (O'Donnell 1996). Because of the prohibitive costs involved with the dredging and disposal of this volume of contaminated material, critical navigation areas have been identified, and a priority dredging plan has been proposed, wherein the total volume is approximately 500,000 cubic yards total (inside and outside the barrier). Without necessary maintenance dredging, fully loaded and/or deep draft (e.g., $>$ 30 feet) commercial shipping vessels cannot navigate the waterways safely and cannot continue to operate at a profit. Because of shoaling in the navigation channels, ship owners have resorted to operating 1) only partially loaded vessels (e.g., salt ships operating at 2/3 capacity), 2) smaller vessels, or 3) only during high tide (Taylor 1996). All three of these options reduce efficiency, and subsequently profits. To further compound the local economic problems, New Bedford's staple fishing industry has declined in recent years because of overfishing in New England waters. Nearby fishing grounds rich in lobster and shellfish have also been closed because of the PCB contamination.

Timely siting of the confined disposal facilities and removal of contaminated sediments from the harbor will benefit the harbor's ecological resources as well as New Bedford's economy. This thesis seeks to provide qualitative and quantitative information that will assist federal and local authorities in the siting of the CDFs along the harbor shoreline. The siting of CDFs is expected to alter circulation patterns as well as current velocities in the harbor. Increased current velocities from reduced channel cross-sections may lead to resuspension of contaminated sediment material. In addition, flushing rates, especially local flushing rates from the upper estuary, are likely to be affected because of a reduction in channel volume. Flushing rates provide an indication of how long resuspended sediment particles remain in an area before settling out to the bottom.

Simple and numerical modeling techniques are employed to estimate the impacts of CDFs on harbor circulation and sediment resuspension under specific climatic events, namely extreme runoff and wind events. Analysis of these simple models helps to direct more complex numerical modeling efforts. Examination of the results from each climatic scenario (with and without CDFs) provides valuable information that may eventually drive an optimal placement of the CDFs, in which critical current velocities necessary to suspend sediment into the water column are minimized by systematic placement of each CDF site.

1.2 New Bedford Harbor Description

New Bedford Harbor, located approximately 50 miles south of Boston, is situated between the town of Fairhaven and the city of New Bedford in southern Massachusetts (Figure 1-1). The harbor is a tidal estuary, at the mouth of the Acushnet River and on the northwestern side of Buzzards Bay, which connects to the bay via a gated hurricane barrier that was completed in 1966 to protect the harbor from tidal storms.

New Bedford Harbor is divided into upper and lower halves by U.S. Route 6, which connects New Bedford and Fairhaven via the New Bedford/Fairhaven Bridge (see Figure 1-1). The lower harbor has a fetch length of approximately 1,800 meters

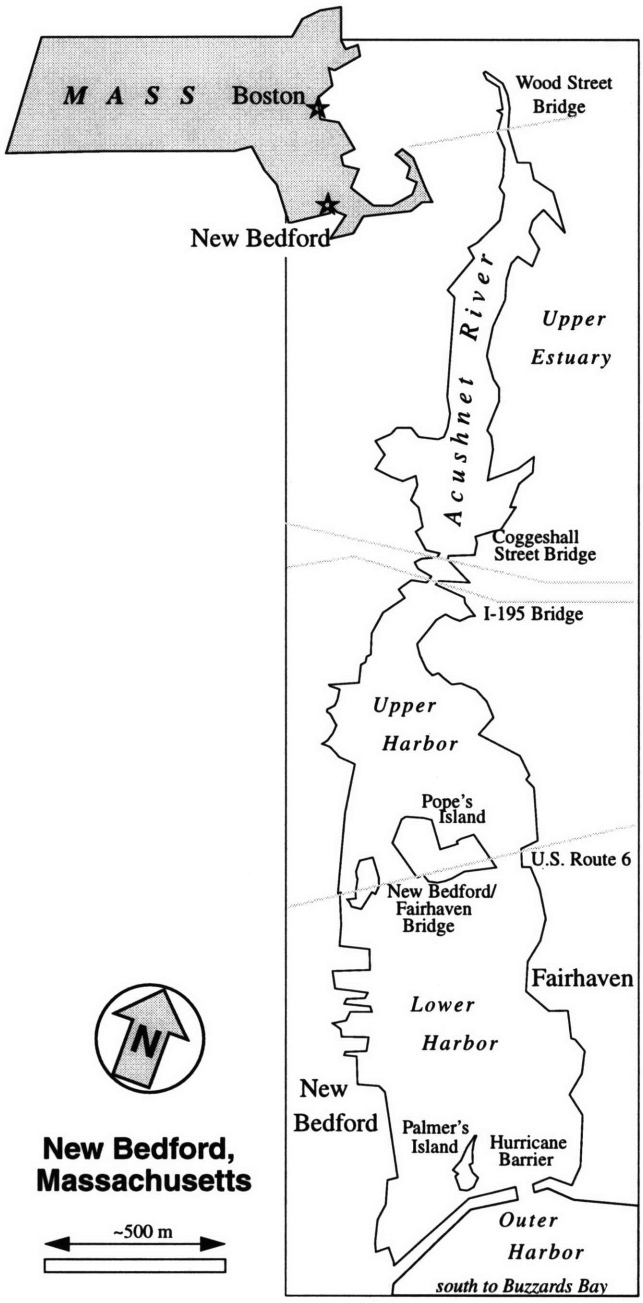

Figure 1-1: **New Bedford Harbor, MA**
New Bedford borders on the west side of the harbor and Fairhaven borders on the east, with Buzzards Bay to the south.

and a width of 1,100 meters with mean low water (MLW) depths ranging from an average of 6 feet in the NE and SW corners to an average of 30 feet along most of the western shoreline; depths along the eastern shore are, on average, 10 to 15 feet deep (NOAA Navigational Chart #13232, NOAA 1991). A 30 foot deep navigation channel crosses the lower harbor diagonally from the hurricane barrier through the New Bedford/Fairhaven Bridge openings. The upper harbor extends approximately 1,500 meters north of the Coggeshall Street Bridge and varies in width from 1,100 meters at U.S. Route 6 to just under 300 meters south of the Coggeshall Street Bridge. Depths in the upper harbor are shallower, on average, than the lower harbor, ranging from areas of 4 and 7 feet in the majority of the upper harbor to over 30 feet in a small and localized commercial shipping turning area and over 20 feet in a narrow navigation channel that leads upriver (NOAA 1991). North of the Coggeshall Street Bridge, the Acushnet River upper estuary extends over 2,200 meters to the Wood Street Bridge at an average width of 300 meters, and a linearly decreasing depth from 11 feet at the Coggeshall Street Bridge to one foot deep just south of Wood Street Bridge (NOAA 1991).

At the mouth of the lower harbor, a hurricane barrier spans the harbor width, restricting flow and traffic to a 150 foot wide, 30 foot deep, opening. In addition to the hurricane barrier, the Coggeshall Street Bridge restricts flow to an opening width of 62 feet at MLW (NOAA 1991) and 110 feet at MHW (Teeter, 1988) and a depth of approximately 11 feet at MLW (NOAA 1991) and 19 feet at MHW (Teeter, 1988). The New Bedford/Fairhaven Bridge, while a constriction to harbor traffic at 150 feet, does not restrict flow significantly.

1.3 Historical Background

Throughout history, New Bedford and its harbor have been home to many large scale industries. Once the whaling center of New England during the early to mid-1800's, New Bedford also supported several early shore-based industries that sprung up when the demand for whale oil declined because of the discovery of petroleum.

The early to mid-1900's saw massive garment and textile mills dotting the waterfront, using the harbor for the transport of raw materials and goods. The mills, however, closed down in the middle of the 20th century, leaving massive waterfront warehouses vacant. Commercial fishing, a historic staple industry in New Bedford, peaked in the mid-1980's when fish stocks in Georges Bank and surrounding Massachusetts waters were abundant. Rapid declines in fish stocks from overfishing in the late 1980's and early 1990's, however, saw the subsequent, but predicted decline of yet another New Bedford staple industry.

1.4 Contaminated Sediments

During the middle of this century, companies such as Revere Copper and Brass, a metalsmithing operation, Cornell-Dublier and Aerovox, both electrical capacitor manufacturers, moved to the New Bedford waterfront. Lack of environmental legislation during this time led to widespread discharges by manufacturers and surrounding towns. The harbor acted as a sink for particulates and associated contaminants over the years (Summerhayes *et al.* 1977). Elevated levels of copper, lead, and polychlorinated biphenyls (PCBs) in the harbor sediments have been directly linked to these industrial discharges as well as combined sewage overflows, storm drains, and runoff. Presumably once localized "hot spots" near the industrial waterfront sites, contaminated sediments have been spread around the harbor and out into nearby Buzzards Bay by many years of tidal action and migratory benthic organisms. Because of the PCB contamination, nearby fishing grounds have been closed, resulting in lost revenues. Since further input of PCBs has ceased, a reverse process occurs in which the sediments act as the source of pollutants back into the water column, especially during storm events that generate higher-than-average tidal ranges and/or waves. Net seaward transport of PCBs through the Coggeshall Street Bridge of 1.55 and 0.91 kg/tidal cycle were measured by USACE (1986) and USEPA (1983), respectively, confirming the upper estuary location of the PCB source.

1.5 EPA Superfund Cleanup

In response to the contamination of the New Bedford Harbor, the U.S. Environmental Protection Agency (USEPA) designated the site as the nation's first Superfund site in 1982, providing federal funds for remediation of the contaminated sediments. Averett *et al.* (1989) estimate the volume of sediments with PCB concentrations in excess of 5,000 ppm is approximately 11,000 cubic yards, with roughly 9,000 cubic yards in the top foot of sediment; the volume of sediments with PCB concentrations from 50-5,000 ppm is approximately 120,000 cubic yards with 100,000 cubic yards in the top foot of sediment; and the volume of sediments with PCB concentrations in excess of 50 ppm is approximately 360,000 cubic yards.

Many years of risk assessment and planning investigated numerous remediation alternatives. Among the methods to dispose of the PCB-contaminated sediments were open ocean disposal, offshore incineration, bioremediation (i.e., using microbes to "eat" the PCBs), upland disposal, chemical breakdown of the PCBs, *in-situ* disposal, capping, and in-harbor disposal; some of the proposed methods have been tested using small pilot studies. Foremost on the list of remediation actions was the removal of PCB hot spots; this became the first phase of the superfund clean-up. Phase I (also ROD I, Record of Decision I) of the Superfund operations concluded in September of 1995 by dredging the 10,000 cubic yards in areas designated as hot spots, i.e., PCB concentrations in excess of 4,000 ppm (USEPA 1992b). Phase II (ROD II) of the cleanup effort will dredge approximately 415,000 cubic yards of sediments with PCB concentrations in excess of 10 ppm in the upper estuary (including sediments in excess of 50 ppm in the Fairhaven salt marshes), and 60,000 cubic yards in the lower harbor that have concentrations of 50 ppm or greater (USEPA 1995). Phase III (ROD III) will focus on those areas outside and south of the hurricane barrier, near the Cornell-Dublier site, with concentrations in excess of 10 ppm.

Figure 1-2 shows PCB concentrations in New Bedford Harbor. Concentrations are summed over a depth of 6 inches for the harbor and 12 inches for the upper estuary (north of the Coggeshall Street Bridge); concentrations outside of the Acushnet

Rivers and Harbors Act of 1899	33 U.S.C.A 401 *et seq.*
Clean Water Act	CWA-33 U.S.C.A. 1251 *et seq.*
Marine Protection, Research and Sanctuaries Act	MPRSA-16 U.S.C.A. 1431 *et seq.*
National Environmental Policy Act of 1969	NEPA-42 U.S.C.A. 4321 *et seq.*
Massachusetts Public Waterfront Act	91 M.G.L.A
Massachusetts Environmental Policy Act	MEPA-30 M.G.L.A. 62-62H
Federal Coastal Zone Management Act of 1972	CZMA-16 U.S.C.A 1451 *et seq.*
Wetland Protection Act	WPA-131 M.G.L.A. 40

Table 1.1: **Federal and state dredging and disposal legislation (from Dolin and Pederson 1991)**

River boundary (solid line) represent contaminated wetlands. Of the hot spots, approximately 3 acres (1.2 ha) contained PCB concentrations greater than 10,000 ppm (Francingues *et al.* 1988). The contaminated material from the Phase I cleanup has been treated at a pilot CDF on the New Bedford shoreline until a final decision is made concerning remediation of the material. The EPA had planned on incinerating the highly contaminated sediments, but local opposition has postponed any incineration. Federal, state, and local legislation involving dredging and disposal are listed in Table 1.1 (Dolin and Pederson 1991).

1.6 Disposal Options

Alternative methods of containment and disposal were the focus of a Feasibility Study by the USEPA in 1990 (USEPA 1990) and a Supplemental Feasibility Study in 1992 (USEPA 1992a, 1992b, 1992c). The USEPA Feasibility Study proposed five alternatives for the disposal of contaminated sediments from the New Bedford Harbor (from Francingues *et al.* 1988):

1. Channelizing the Acushnet River north of the Coggeshall Street Bridge and capping contaminated sediments in the remaining open-water areas.

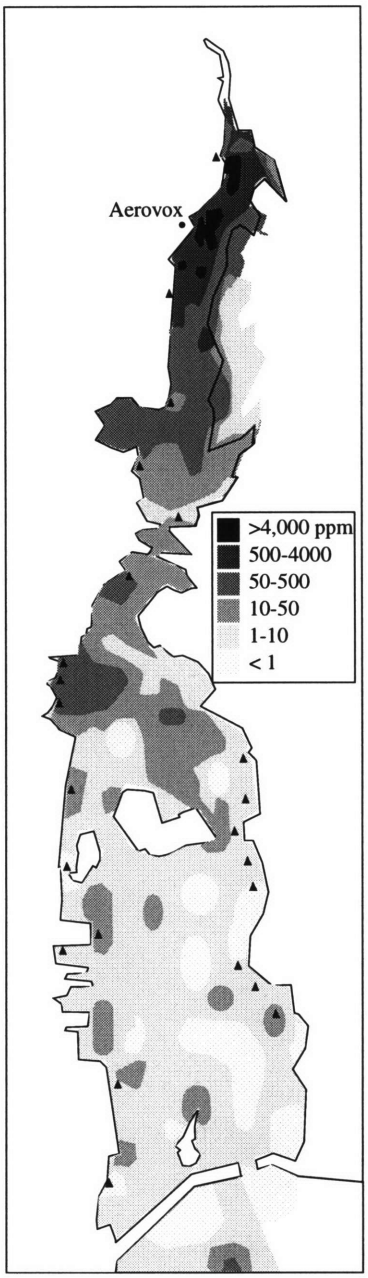

Figure 1-2: **PCB Concentrations (ppm), New Bedford Harbor, MA**
Black triangles represent combined sewer overflows (CSO) and/or storm drain outfalls. Depth: 0-6 inches for lower harbor and 0-12 inches for upper estuary (north of Coggeshall Street Bridge) (after USEPA 1990).

2. Dredging contaminated sediments and disposing of them in a partially lined containment site in the northern part of the estuary along the eastern shore [i.e., confined disposal facilities].

3. Same as the second option except that the containment site would be lined on the bottom, as well as on the sides [i.e., confined disposal facilities].

4. Dredging contaminated sediments and disposing of them in an upland containment site.

5. Dredging contaminated sediments (which lay over clean sediments) and dredging clean sediments, temporarily storing both before returning the contaminated sediments to a specially constructed cell in the channel bottom and covering with clean capping material. This alternative is termed contained aquatic disposal (CAD).

Upland disposal of the contaminated material requires ground transportation by truck, incurring high costs and increased contamination risks from overland transport. Open ocean disposal of the dredged material is not feasible because the sediments are contaminated, they do not meet water quality standards (Clean Water Act Section 404), and they are in violation of Section 103 of the Marine Protection, Research and Sanctuaries Act (MPRSA). In the case of open ocean disposal, bulk sediment analyses are performed on dredged material prior to disposal by the US Army Corps of Engineers. The sediments are analyzed for eight metals (As, Cd, Cr, Cu, Pb, Ni, Hg, Zn), total PCBs, pesticides, and PAHs according to USEPA protocols (Germano *et al.* 1994). Because sediments cannot be disposed of in open waters, and overland transport introduces human health risks and increased cost, proposed alternatives for the containment of contaminated sediments favor shoreline confined disposal facilities (CDFs) as suggested in options #2 and #3 above because they are the most cost effective and pose the least risk to the environment.

USEPA, state, and local planners have identified several potential sites along the harbor waterfront in which to confine the contaminated sediments. These potential

CDF #	Location	CDF Volume (cy)
CDF 1	NW of Coggeshall St. Bridge	270,000
CDF 1A	NW of Coggeshall St. Bridge	30,000
CDF 1B	NW Upper Estuary (Aerovox)	90,000
CDF 3	NE of Coggeshall St. Bridge	134,000
CDF 7	Herman Melville (SW of CSB)	181,000
CDF 10/10A	Standard Times Field	267,000
CDF 4	NE of Coggeshall St. Bridge	20,000
CDF 8	Adjacent to Pope's Island	42,000

Table 1.2: **Approximate Locations and Volumes of Potential CDF Sites (EPA 1992b), cy = cubic yards, capacities represent wet volumes**

locations are shown in Figure 1-3 and should be considered approximate. The approximate capacities of each of the CDFs are listed in Table 1.2, and represent the total solids storage space required. Averett *et al.* (1989) have used bulking factors, the ratio of wet to dry (i.e., settled) volumes of dredged material, of 1.4-1.57 for the New Bedford CDFs. The volume of *in-situ* dredged material to be contained within each CDF listed in Table 1.2, then, can be estimated by dividing each CDF volume by approximately 1.5. Each CDF has been designed to have 8-11 feet of storage capacity with a 2 foot ponding depth and 2 feet of freeboard on top of that (Averett *et al.* 1989).

Siting of CDFs along the harbor shoreline, however, will alter the geometry of the harbor. The modification of the hydraulics, or hydromodification, of the harbor by the siting of CDFs is likely to lead to changes in tidal current velocities, flushing rates, and sediment transport within the harbor. Uninformed placement of these CDFs may also lead to increased sediment suspension and further contamination of the surrounding harbor. Numerical modeling efforts suggest that strategic placement can produce favorable results in the form of decreased current velocities and suspended sediment loads.

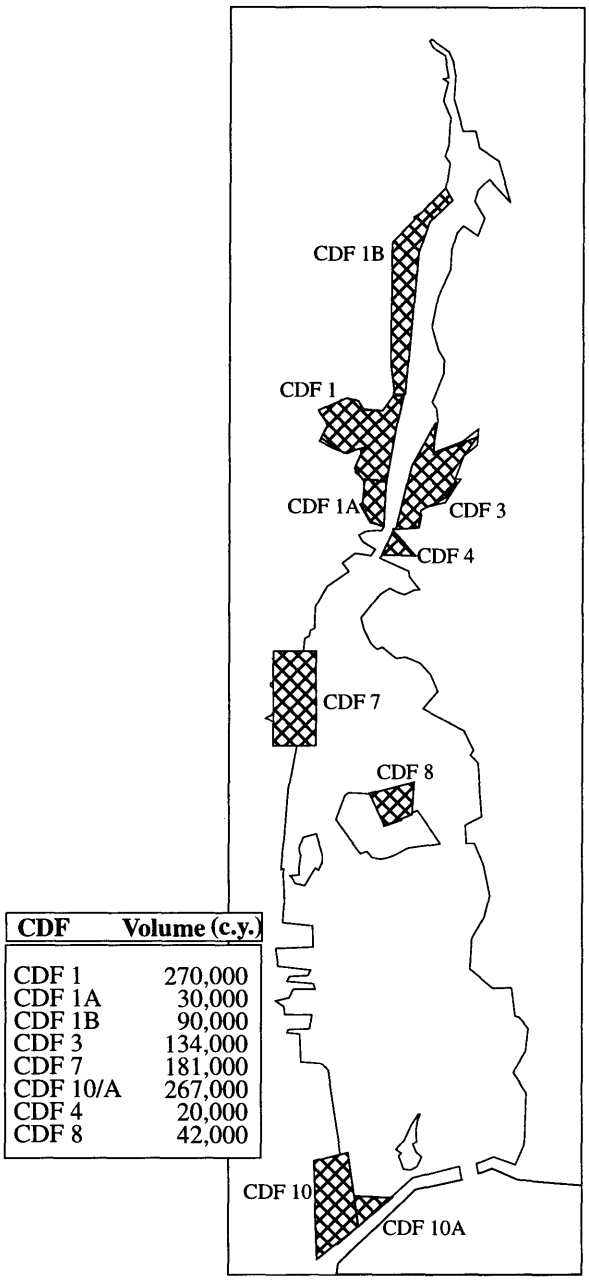

CDF	Volume (c.y.)
CDF 1	270,000
CDF 1A	30,000
CDF 1B	90,000
CDF 3	134,000
CDF 7	181,000
CDF 10/A	267,000
CDF 4	20,000
CDF 8	42,000

Figure 1-3: **Potential Confined Disposal Facilities (after USEPA 1992b)**

Chapter 2

Purpose, Approach, and Background for this Study

2.1 Purpose

This thesis is concerned with the effects that the siting of confined disposal faciliites (CDF) will have on harbor circulation. Specifically, this study will address the impacts that the CDFs will have on 1) current velocities, 2) residence time, and 3)sediment resuspension under different climatic conditions: namely, normal, extreme freshwater runoff (flood), and extreme wind (hurricane) events. In addition, this study investigates an optimal placement of CDFs along the harbor shoreline to minimize adverse environmental impacts. The following five subsections outline the approach taken in this thesis.

2.2 Approach

Previous Studies This study draws upon previous studies and analyses therein, in lieu of new field studies, to provide calibration data and observations for baseline (i.e., no CDFs) scenarios. Many studies have investigated the transport, fate, and effects of PCBs in New Bedford Harbor, see ASA (1986) and Battelle (1990), and still others have focused on the environmental impacts that dredging the PCBs will

have on adjacent ecosystems (Teeter 1988, USACE 1990). Teeter (1988), as part of a larger engineering feasibility study (EFS) by USACE, uses a numerical model to study the effects of dredging, specifically, the sediment plume and resulting transport of PCBs from dredging operations. Part of the USACE study was to determine the most feasible options for dredged material disposal, as described Section 1.6. With the USACE model, Teeter (1988) also investigated the effects of maintenance dredging operations by increasing the model's depths by one meter in navigation channels. Because these studies pre-date discussions concerning the containment of the dredged material, neither the ASA, Battelle, nor USACE models investigations addressed the possible impacts that the construction of CDFs will have on harbor circulation patterns. A review of some of the existing studies can be found in Section 2.3.

Critical Sediment Parameters As part of the USACE (1990) EFS, bulk sediment analyses were performed on material dredged from New Bedford Harbor. Heavers (1983 as referenced in ASA 1986) as part of a separate study, performed flume tests on New Bedford Harbor sediments. From these two analyses, critical sediment parameters, leading to resuspension, are calculated, e.g., critical shear stress and velocity, which are used to identify probable resuspension events in the simple and numerical model simulations. Sediment criteria appear in Chapter 3.

Simple Models Simple one-dimensional and analytical models are used to estimate the effects of the CDFs on dominant forcing factors (i.e., tidal, wind and freshwater runoff), resuspension, and residence time (see Chapter 4). These simple models include a tidal prism analysis as well as several techniques outlined in the USACE *Shore Protection Manual.*

Numerical Modeling Numerical modeling techniques are employed in Chapter 5 to investigate the impacts of the CDFs on harbor circulation and sediment resuspension. The simple analytical models from Chapter 4 are used to drive the development of the numerical modeling efforts. The simple models also serve as an initial calibration tool for the numerical model. As in Chapter 4, the numerical model is used

to more accurately simulate the effects of the CDFs on dominant forcing factors (i.e., tidal, wind and freshwater runoff), resuspension, and residence time simulates current patterns and the changes in them caused by the construction of the CDFs. Furthermore, modeling provides a cost-efficient method for testing different CDF-siting scenarios with relatively simple changes to the numerical model. Because of New Bedford's susceptibility to hurricanes and the subsequent storm surges, torrential rains and runoff, state and local officials involved with the siting and construction of the CDFs must be aware of the effects that the CDFs will have on the rest of the harbor.

Conclusions Conclusions and recommendations based on the modeling efforts are given in Chapters 6.1 and 7. These chapters will also address several issues that have not been answered by previous modeling efforts.

Issues Several questions are addressed in this thesis, focusing on the environmental impacts of the CDFs on the harbor, but also addressing the functionality of the harbor.

- Will the siting of the CDFs increase tidal-, wind-, and/or freshwater-driven velocities in the harbor waterways such that an increased level of sediment is resuspended in the water column?
- Will the siting of the CDFs affect local flushing rates and residence times within the harbor?
- Is there an optimum arrangement of the CDFs that will minimize the impact on harbor velocities and sediment entrainment?

2.3 Previous Studies

Since the discovery of high levels of pollutants in New Bedford Harbor in the mid-1970's, several studies have been carried out in the harbor to assess the transport,

fate, and effects of PCBs from the contaminated harbor sediments on and into nearby ecosystems. Applied Science Associates (ASA) and Woods Hole Oceanographic Institution (WHOI) are among the organizations that have performed surveys in New Bedford Harbor. In addition to measuring physical parameters, such as tidal elevation and velocities, ASA and Aquatec, Inc., another consulting agency, independently conducted dye studies to determine the original source of the PCBs.

This section gives a brief description of the data that were collected for each of the three studies as well as several other data that have been collected. This thesis draws upon these previous studies, in lieu of collecting additional field measurements, and several references are made to these previous efforts throughout this study. These previous studies also help to refine the models (analytical and numerical) developed for this thesis by providing observational data at locations throughout the harbor. Figure 2-1 shows the locations of each field study.

2.3.1 Field Measurements

Summerhayes *et al.* (1977) and (1985) from Woods Hole Oceanographic Institution (WHOI) examined the PCB and heavy metal concentrations in the sediments of New Bedford Harbor and Buzzards Bay. Summerhayes *et al.* (1977) obtained field data from two (2) stations: the New Bedford/Fairhaven Bridge and the hurricane barrier, referenced in Summerhayes *et al.* (1977, 1985) as **H4** and **H5**, respectively, and shown in Figure 2-1. At both locations, current velocities, water temperature, salinity, and dissolved oxygen levels were recorded for surface and bottom waters over a complete tidal cycle during 8 and 9 June 1976. In a separate but related study, Summerhayes *et al.* (1985) theorized that estuaries act as sinks for industrial waste which sorbs onto sediment particles. Summerhayes *et al.* (1985) found positive correlations between contamination levels and the clay fraction of the sediments within the estuary using some of the data collected during the earlier 1976 study.

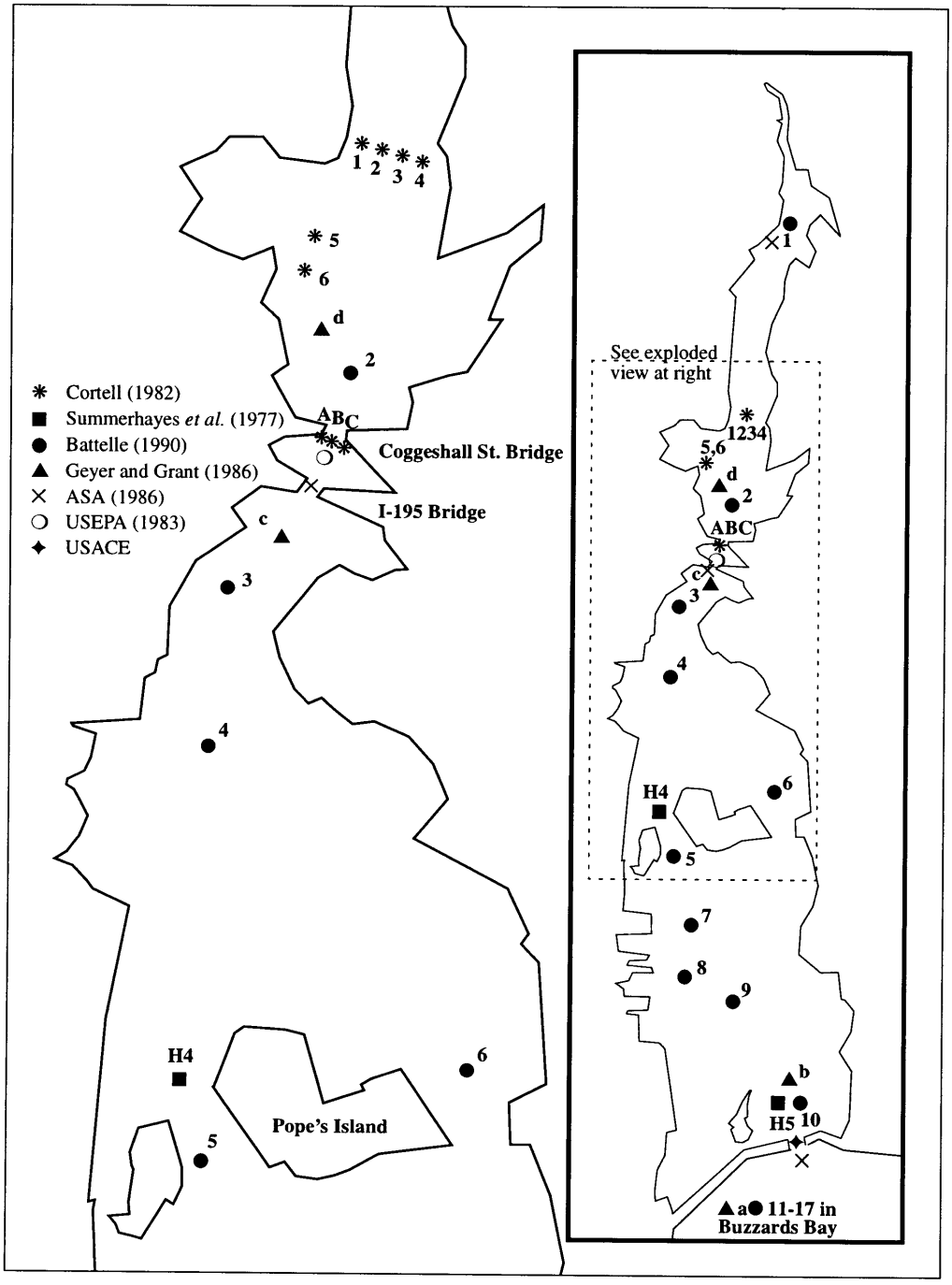

Figure 2-1: **Locations of Previous Studies (after Battelle 1990)**

Geyer and Grant (1986), contracted by Battelle Ocean Sciences, took measurements of tidal height at three (3) stations within the harbor on 23 and 31 July 1986: 1) just north of the hurricane barrier; 2) just south of the Coggeshall Bridge; 3) just north of the Coggeshall Bridge; referenced in Geyer and Grant (1986) as stations **b**,**c**, and **d**, respectively. Station **b** was also equipped with a current meter to record current velocities. These three stations can also be seen in Figure 2-1.

Applied Science Associates, ASA, (1986 and 1987) examined PCB transport from the Aerovox facility, in the upper estuary of the Acushnet River, into the harbor. Hourly measurements of current velocities and tidal heights were taken at three (3) locations on 20 June 1986, including the hurricane barrier, the I-195 Bridge (current speed only), and near the Aerovox facility (see Figure 2-1). In December 1986, ASA also conducted a dye study in the harbor; a description of the dye study can be found later in Section 2.3.2.

Cortell (1982), a Massachusetts consulting firm, took hourly current measurements at nine (9) locations in the Harbor on 13 November 1981 and 11 December 1981. Seven (7) of these stations included four (4) locations just north of the Coggeshall Street Bridge, referenced in Cortell (1982) as stations **1**, **2**, **3**,and **4**, and three (3) stations located directly under the Coggeshall Street Bridge (east, mid-span, west), referenced as **A**, **B**, and **C**. Figure 2-1 shows these stations.

U.S. Environmental Protection Agency, (USEPA 1983) has been cited in ASA (1986) and Battelle (1990) as conducting a field study on 11 and 12 January 1983 and collecting current velocities at the Coggeshall Bridge.

U.S. Army Corps of Engineers, since the completion of the hurricane barrier in 1966, has maintained a tide guage at this location, measuring tidal heights, as well as recording other meterological data such as wind speed and direction. Wind data are also recorded by New Bedford Airport and Greene Airport in Warwick, RI. The USACE also conducted an Engineering Feasibility Study from 1988 to 1990 to

Type of Data	Date of Survey	#	Location Station Reference	Reference
TH,V CTD+O	6/8-9/76	2	HB,US6 H4,H5	Summerhayes *et al.* (1977)
TH	7/23,31/86	3	HB_n B CB_s, CB_n C,D	Geyer/Grant (1986)
TH, V	6/20/86	3	HB, I195, AX N/A	ASA (1986)
DS	12/15-23/86	45	N/A	ASA (1986)
V	11/13, 12/11/81	9	7@CB 1-4,ABC	Cortell (1982)
V	1/11-12/83	1	CB N/A	EPA (1983)
W	indef.	2	airports N/A	NB and Warwick,RI
W,TH	indef.	1	HB N/A	USACE
DS	2/26/91-3/19/91	N/A	N/A	Aquatec, Inc. (1991)

Table 2.1: **Summary of Existing Data**
Type: TH = tidal heights, V = current velocities, DS = dye study, CTD+O = temp, salinity, and DO, W = wind;
Location: HB = Hurricane Barrier, CSB = Coggeshall Bridge, US6 = US Route 6, AX = Aerovox, I195 = I-195, $XX_{n/s}$ = just north/south of location.

identify dredging and disposal options (USACE 1990 and Teeter 1988). Table 2.1 summarizes these previous studies.

2.3.2 Dye Studies

There were two dye studies performed in the New Bedford Harbor to investigate the origins and impact of PCBs:

ASA (1987) released a dye study near the Aerovox facility in the upper estuary from 15-29 December 1986 to measure residence times and flushing rates. A Rhodamine-WT dye was released continuously for eight and a half days, with dye concentrations measured and recorded at 45 stations throughout the harbor, both at a surface and several subsurface levels, from 15-29 December 1986 during low tide. Sampling locations from ASA (1987) can be found in Figure 2-2. Additional information on the ASA dye study can be found in Section 6.3.

Aquatec, Inc. (1991) conducted a second dye study from 26 February to 19 March 1991. Rhodamine WT Dye was released just below the surface simultaneously at two sites in the harbor, in the upper estuary near Aerovox and outside the hurricane barrier near Cornell-Dublier, for the period of one tidal cycle (approximately 12 hours). Dye injection rates for the Aerovox and Cornell-Dublier discharges were 0.93 and 0.82 g/s, respectively. Dye concentrations were measured at low slack tide from 27 February until 3 March 1991. Salinity and temperature data were also collected during these times, however salinity data for the upstream sampling (north of the Coggeshall Street Bridge) were erroneous. Salinity and temperature profiles for the lower harbor show a well mixed condition for the lower harbor. Sampling transects from Aquatec (1991) can be found in Figure 2-2.

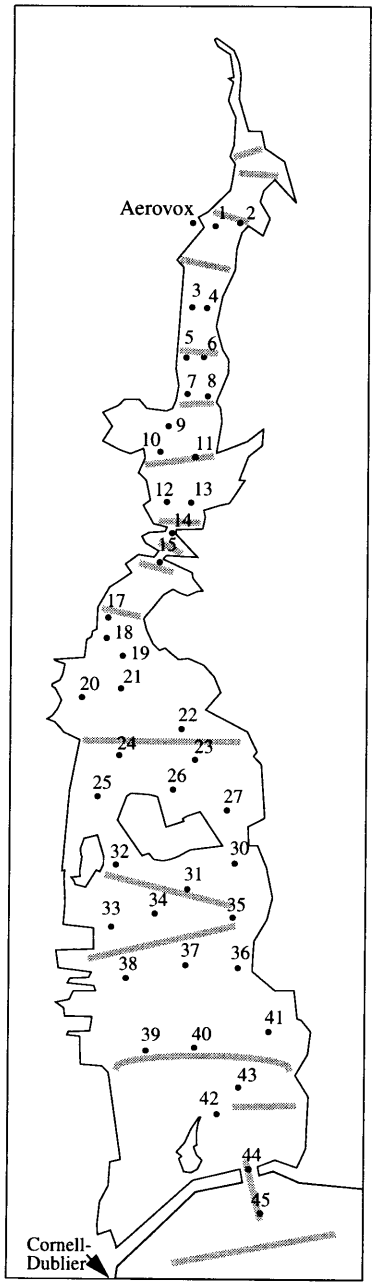

Figure 2-2: **Dye Study Sampling Locations**
Numbers indicate ASA (1987) sampling locations;
grey lines represent Aquatec (1991) sampling transects

Chapter 3

New Bedford Harbor Sediments

New Bedford Harbor sediments are susceptible to resuspension into the water column by elevated current speeds. Resuspension is an important issue because contaminants (e.g., PCBs) generally sorb onto sediment particles, and with the resuspension of sediment particles come PCBs, further contaminating the surrounding harbor and Buzzards Bay ecosystems. With the introduction of CDFs, current velocities are likely to change. Though remediation dredging efforts will clean up hot spots as well as surrounding sediments, it is impossible (and unreasonable) to remove all traces of PCB contamination. With educated placement of the confined disposal facilities, velocities can be reduced, reducing the risk of further contamination.

USEPA (1983) and Teeter (1988) have measured a net seaward transport, or flux, of PCBs past the Coggeshall Street Bridge at a rate of 0.91 and 1.55 kg/tidal cycle, respectively. Total suspended material (TSM) was measured to have a net *landward*, or upstream, transport of 6,700 and 2,200 kg/tidal cycle, respectively (USEPA and USACE). Measurements of TSM at several stations along the harbor by Teeter (1988) indicate that the TSM concentration increases as one proceeds upriver; Figure (3-1), after Teeter (1988), shows this relationship.

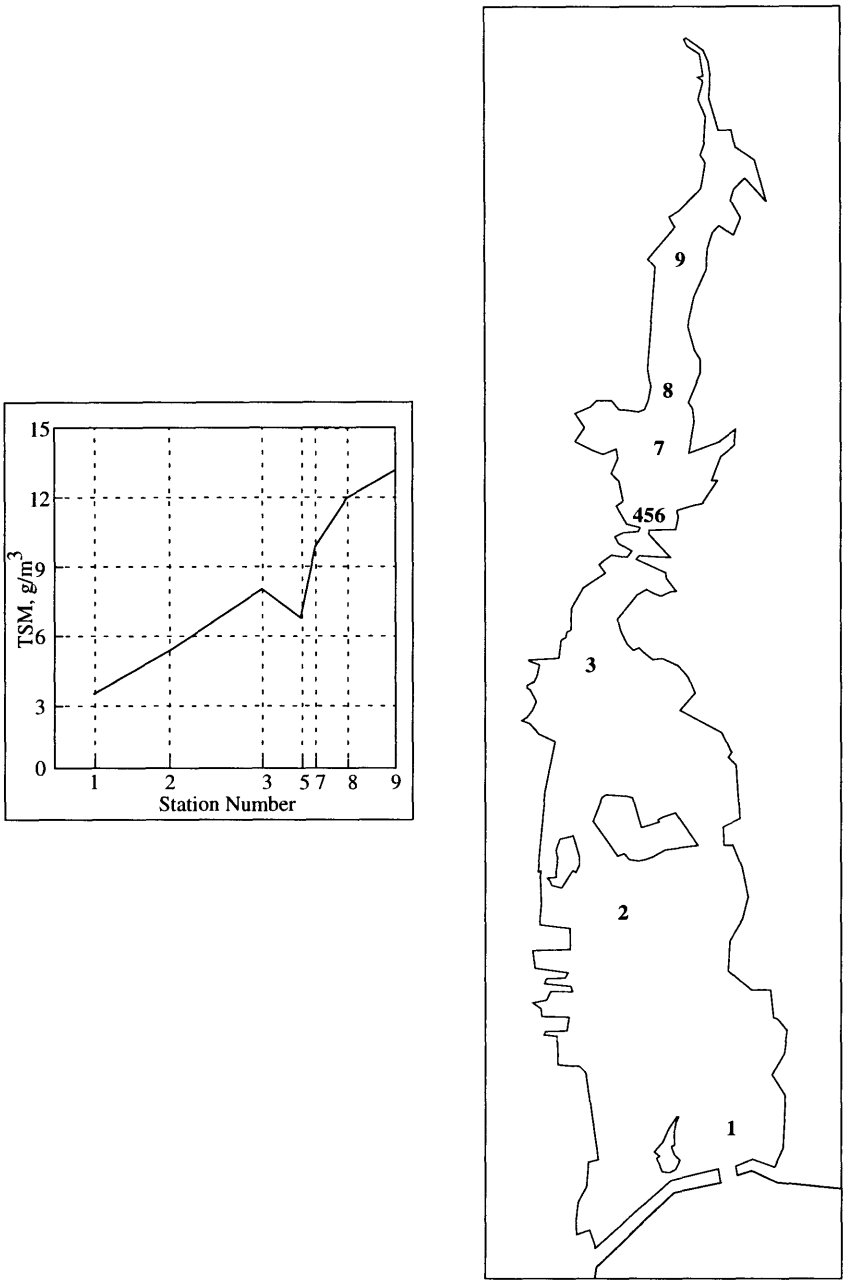

Figure 3-1: **Total Suspended Material (TSM) (after Teeter 1988)**

3.1 Sediment Properties

Sediments in the New Bedford Harbor have been characterized by Summerhayes *et al.* (1985) as being muddy in the harbor and navigation channels; this is especially prevalent near the west bank, which offers protection from winds. Summerhayes *et al.* (1985) also identified sandy areas, such as those near the hurricane barrier, which had been scoured by currents.

Summerhayes *et al.* (1985) report a clay to mud ratio of 0.18 in the harbor and a significantly higher ratio of 0.34 in Buzzards Bay. Most of the mud fraction is silt, with increasing concentrations of silt upriver. From sediment grab samples, Summerhayes *et al.* (1985) have found a two to three centimeter thick layer of loose, non-cohesive material, similar to that found by Rhodes and Young (1970) in Buzzards Bay, which they described as a *moving carpet* over the bottom that could be easily resuspended.

Evaluation and testing of New Bedford Harbor sediments for their susceptibility to erosion and deposition was done by USACE (1986) and Teeter (1988). Erosion, or resuspension, of New Bedford sediments occurs when individual sediment particles are displaced from the sediment bed by a shear stress, τ_b, above some critical shear stress, τ_c. Teeter (1988) defines particle resuspension, E, in terms of an erosional rate, M, and the ratio between τ_b and τ_c as in Equation (3.1):

$$E = M\left(\frac{\tau_b}{\tau_c} - 1\right), \tau_b > \tau_c \tag{3.1}$$

One of many methods of calculating the settling velocity, W_s, the rate at which a particle settles to the sediment bed after being resuspended in the water column is given by Equation (3.2) for *enhanced settling-concentration range* (Ariathurai *et al.* 1977):

$$W_s = A_1 C^n \tag{3.2}$$

where, W_s is the settling rate or velocity, A_1 is a constant, C is the suspended sediment concentration, and n is generally equal to 1.33, or 4/3. The concentration range

Variables	Sediment Fraction (SF) SF-1	SF-2	SF-3
Deposition			
τ_{cd}, N/m^2	0.42	0.33	0.043
A_1	6.4 x 10^{-3}	3.2 x 10^{-3}	1.8 x 10^{-5}
W_s, mm/s	2.02	1.04	0.006
Erosion			
τ_c,N/m^2	0.6	0.6-0.16	0.060
M, $g/m^2/min$	–	–	0.25

Table 3.1: **New Bedford Harbor Sediment Property Coefficients (from Teeter 1988)**

over which Equation (3.2) applies is from a lower bound of 10 to 200 mg/l up to an upper bound of 2,000 to 75,000 mg/l, and it varies with the cohesive properties (e.g., diameter) of the sediments. Teeter (1988) defines deposition as the product of settling flux and deposition probability summed over each sediment fraction (Mehta *et al.* 1986):

$$D = \sum_{i=1}^{k} P_i W_{s_i} C_i \tag{3.3}$$

where, k is the number of fractions, i is the sediment fraction #, P is probability that an aggregate reaching the bed will remain there, W_s is the settling velocity (from Equation. 3.2), and C is the concentration just above the bed. P is defined in Teeter (1988) such that it varies linearly from 0 at a critical shear stress for deposition, τ_{cd}, to 1 at zero shear bed stress, τ_b.

Teeter (1988) characterized composite New Bedford Harbor sediment samples into sediment fractions 1, 2, and 3 (Table 3.1) . Sediment fraction #3 (SF-3) comprised 39% of the total sediment deposit during water tunnel tests. In other words, during resuspension tests, 39% of the sediment that was resuspended was SF-3; the remainder of the resuspended material was considered SF-2. Sediment material that was not suspended in the water tunnel tests was considered SF-1. For most of the water tunnel tests, weight percentages of the sediment fractions were consistent at 30%, 30%, and 40%, for SF-1, SF-2, and SF-3, respectively. Empirically measured erosional and

depositional coefficients for Equations (3.1), (3.2), and (3.3) from tests conducted by USACE (1988) can be found in Table 3.1.

3.2 Critical Shear Stress

Theoretically, shear stress is given by Equation (3.4):

$$\tau = \mu \frac{du}{dz}, \tag{3.4}$$

where μ is the dynamic viscosity, u is the mean flow velocity, and z is defined in the upward direction from the sediment bed. A shear velocity, u^*, can be defined in terms of the mean shear stress at the bed, τ_o, and the fluid density, ρ, as

$$u^* = \sqrt{\tau_o / \rho} \tag{3.5}$$

The mean wall shear stress, τ_o is related to the mean velocity, $\overline{u}$, by Equation (3.6) (Fischer *et al.* 1979):

$$\tau_o = \frac{1}{8} f \rho \overline{u}^2, \tag{3.6}$$

Combining Equations (3.5) and (3.6), the ratio of the mean velocity and shear velocity can be defined in terms of the Darcy-Weisbach friction factor:

$$\frac{\overline{u}}{u^*} = \sqrt{\frac{8}{f}} \tag{3.7}$$

3.3 Critical Shear Velocity

Rearranging Equation (3.6) for $\overline{u}$ and replacing shear stress, τ_o, with the critical shear stress, τ_c gives a relation for a critical velocity, u_{crit}:

$$u_{crit} = \left(8 \frac{\tau_c}{\rho f} \right)^{\frac{1}{2}} \tag{3.8}$$

Using values of τ_c from Table 3.1 and using a frictional coefficient $f = 0.015$ to 0.02 from Teeter (1988) yields a critical velocity range of 15 to 55 cm/s, depending on the diameter of the sediment particles:

$$u_{crit} = \left(8\frac{(0.06\ to\ 0.6)}{(\ 1025\ kg/m^3)(0.015\ to\ 0.02)}\right)^{\frac{1}{2}} = 15 - 55\ cm/s \qquad (3.9)$$

This range of values agrees well with earlier studies, e.g., a critical, or threshold, current velocity, determined empirically by Heavers (1983 as reference in ASA 1986). Heavers found that at an average flow velocity of $\overline{V} = 20$ cm/s, no New Bedford Harbor sediment particles were resuspended, but at $\overline{V} = 30$ cm/s, erosion was significant. From this study and others, ASA (1986) estimated the critical velocity for New Bedford sediments at approximately $u_{crit} = 28$ cm/s. This value falls within the range specified in Equation (3.9), and has been used throughout this thesis as the critical, or threshold, velocity in determining the effects of the CDF-siting on the harbor's circulation.

Chapter 4

Simple Models and Dominant Forcing Factors

Factors influencing harbor circulation include tidal motion, wind-generated waves, and freshwater runoff down the Acushnet River. The impact of each forcing function varies within the harbor depending on the geometry and bathymetry. In deeper areas, tidal influence is stronger, but in shallower areas wind and freshwater effects have been shown to have significant effects (ASA 1986). This section highlights the relative impact of each forcing function on New Bedford Harbor circulation.

4.1 Vertical Stratification

Density differences due to stratification in the estuary are not considered to be a significant circulation mechanism because the harbor is generally well mixed. While not a dominant circulation mechanism, stratification may increase the residence time of the harbor because of poor mixing.In the upper estuary, top to bottom salinity differences have been measured at 1 ppt; however, this difference may be as large as 18 ppt after rainfall. Typically, the salinities in the upper estuary range from 26 to 30 ppt, but may be as low as 12 ppt at the surface after rainfall (USEPA 1983). The lower harbor is also vertically well mixed with top to bottom salinity differences of 1 to 2 ppt; salinities in the lower harbor are slightly higher than those in the upper

estuary. Ellis *et al.* (1977) reported that the longitudinal salinity gradients were small for the harbor. Salinity profiles taken during an ASA (1987) dye study are given in Figure 4-1. These profiles, measured 22 December 1986, show vertical stratification in the upper layers (< 0.5 meters) of water, with significant top-to-bottom salinity differences occurring north of the Coggeshall Street Bridge, mostly. The upper estuary stratification is most likely residual runoff from a storm that passed through the area on 19 December 1986, increasing the Acushnet River flow rate to 3.7 m3/s from its average annual flow rate of 0.85 m3/s. Below 3 meters, the harbor is well mixed and no stratification is visible. Additional information on this dye study can be found in Section 6.3.

4.2 Tidal Circulation

Tidal forcing is the dominant mechanism driving circulation in New Bedford Harbor, and it is least limited geographically within the harbor, i.e., its effects are significant even in the upper portions of the Acushnet river. A tidal pumping action has been determined to be responsible for the net-seaward flux of PCBs through the Coggeshall Street Bridge. A tidal prism analysis has been performed for New Bedford Harbor and has shown that current velocities exceed an empirically measured u_{crit} (see Section 3), the critical threshold velocity for sediment resuspension, during maximum ebb tide under normal meteorological conditions. The tidal prism analysis, presented below, indicates that the effect of siting CDFs in the upper estuary results in increased velocities at some locations and reduced velocities at others.

New Bedford Harbor's circulation is primarily tidally driven, with some influence by winds and freshwater flow during storm events. The M_2, the principal lunar semi-diurnal (twice a day) tidal constituent, dominates the tidal forcing with approximately 85% of the tidal energy (Signell 1987). The amplitudes of the S_2, the principal solar semi-diurnal constituent, and N_2, the lunar elliptic semi-diurnal constituent, tides are each about 20% of the M_2 tide (see Table 4.1), and the interference among these three constituents accounts for spring and perigean tides being approximately 20% stronger

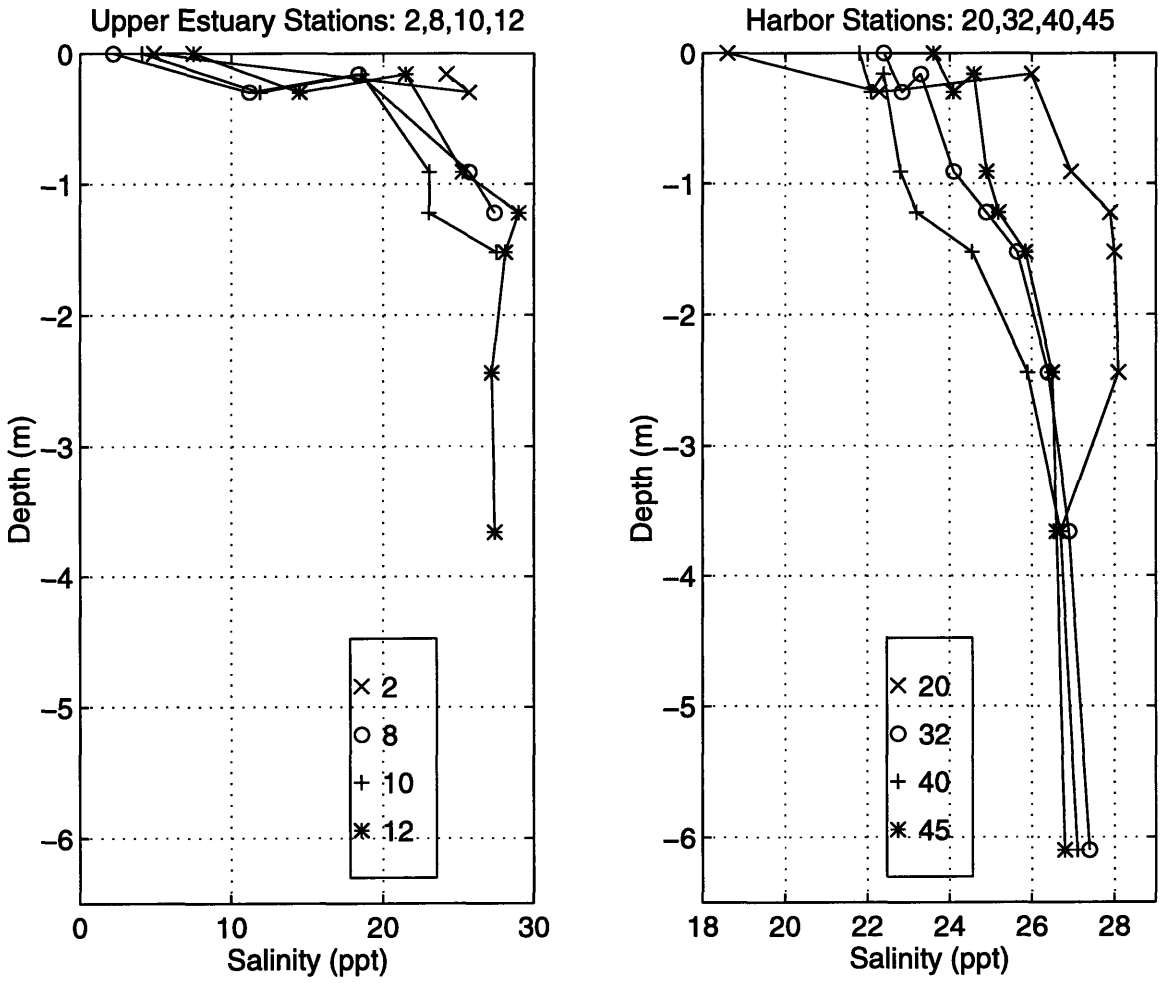

Figure 4-1: **Salinity Profiles from New Bedford Harbor**
Station numbers refer to those in Figure 2-2 (from ASA 1987)

Tidal Constituent	Period (hours)	Amplitude (meters)	Modified Epoch, K' (degrees)
M_2	12.42	0.5356	218.6
N_2	12.66	0.137	206.6
S_2	12.00	0.130	234.6
M_4	6.21	0.078	107.7
K_1	23.93	0.062	95.2
S_a	365.25 (days)	0.054	156.5
O_1	25.82	0.049	128.8
K_2	11.96	0.040	234.4
μ_2	12.87	0.031	205.5

M_2	lunar constituent: (principal) semi-diurnal
N_2	lunar constituent: (elliptic) semi-diurnal
M_4	lunar constituent: (shallow water overtide of principle)
S_2	solar constituent: (principal) solar semi-diurnal
K_1	lunisolar constituents: (diurnal)
K_2	lunisolar constituents: (semi-diurnal)
S_a	solar annual constituent
O_1	lunar diurnal constituent
μ_2	variational constituent

Table 4.1: **NOAA/NOS Tidal Constituents for New Bedford Harbor,MA Principal tidal constituents and their relative periods, amplitudes and phase lag for New Bedford Harbor, Massachusetts.**

than normal and neap and apogean tides being 20% weaker; every seven (7) months or so, the interaction of these three constituents also leads to a perigean-spring tide that is 40% above normal (Signell, 1987).

Speer (1984), as referenced in Signell (1987), suggests that the M_4 component can lead to assymetry in the tidal curve, depending on its relation with the M_2 tide, and may affect those processes, such as sediment transport, which are non-linearly-dependent on the current. The phase difference between the M_2 and M_4 tides ($\theta_d = 2\theta_{M_2} - \theta_{M_4}$) provides some indication about the relative strengths of the flood and ebb tides.

Using values for M_2 and M_4 from Table 4.1, the phase phase difference, θ_d, can be shown to be greater than 270^o suggesting that the tidal current is flood dominant, with a longer and slower ebb followed by a shorter and quicker flood. Field

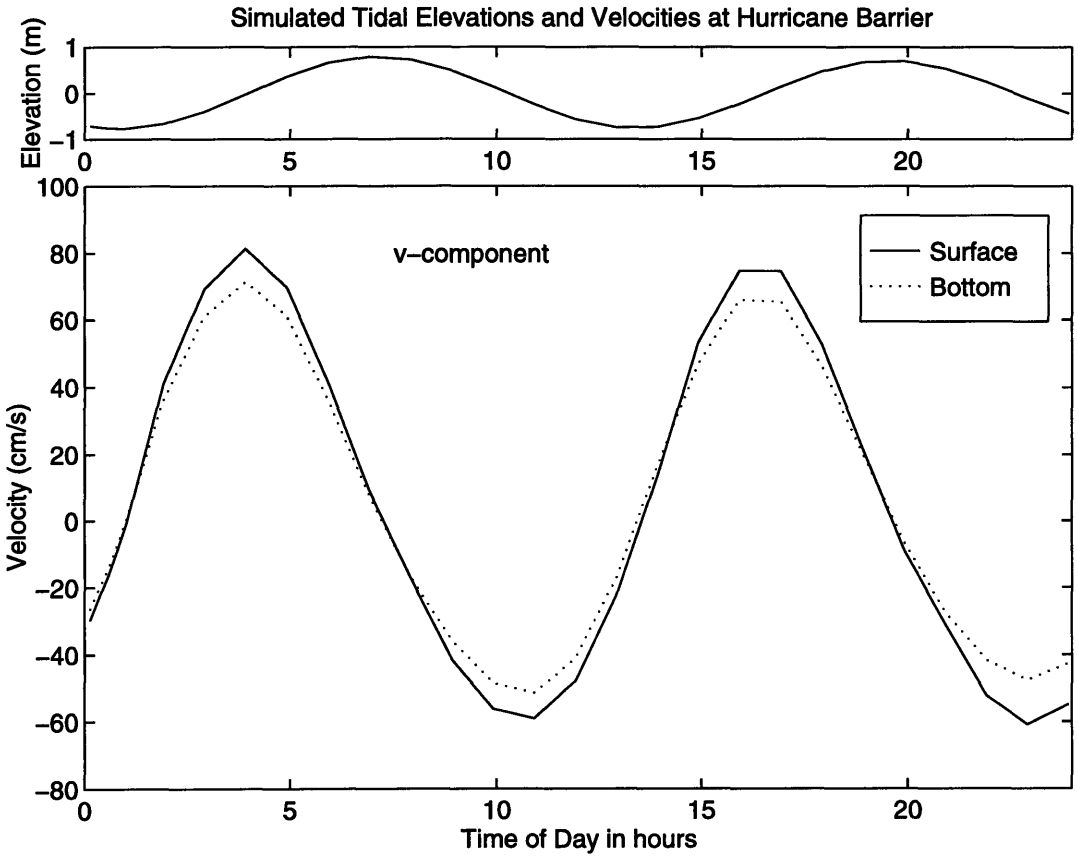

Figure 4-2: **Simulated one-day tidal cycle at hurricane barrier Note 1) the sharper flood/rounder ebb assymetry and 2) the 90^o phase difference between the velocity (bottom) and elevation (top).**

observations (and modeling efforts) support this theory with higher flood velocities and temporally sharper flood tides and lower ebb velocities and temporally rounder ebb tides. Figure 4-2 shows the predicted (i.e., modeled) v-component (longitudinal) of the velocity vector for the hurricane barrier over a single day. Note the slightly sharper peak at maximum flood (positive velocity) compared with the more gradual peak at maximum ebb. Another interesting aspect of the New Bedford Harbor tidal cycle (Figure 4-2) is the 90^o phase difference between maximum tidal elevations and velocities, with the velocity cycle leading the elevation cycle by approximately three (3) hours.

4.2.1 Tidal Prism Analysis

A tidal prism analysis has been performed to approximate tidally-induced current velocities in the Acushnet River estuary. A tidal prism is the volume of water that is brought into an estuary or inlet during the flood stage of a tidal cycle. An upstream prism, then, is the portion of the volume that is upstream of a location, x, if x is defined along the major axis of an estuary or channel. An estimate of the upstream tidal prism volume at any location, x, $\overline{P(x)}$, is given by the following equation:

$$\overline{P(x)} = A_s h_{tide}, \tag{4.1}$$

where A_s is the surface area of the channel upstream of location x, and h_{tide} is the tidal range (3.7 feet in New Bedford). The maximum tidal ebb velocity, $u(x)_{max}$, that is generated by the upstream prism volume flowing seaward past a point, x, can be estimated by the following equation:

$$\overline{\overline{u}}(x)_{max} = \frac{\pi \overline{P(x)}}{A_c(x)(T/2)}, \tag{4.2}$$

where $A_c(x)$ is the cross-sectional area at location x, T the tidal period, and the double bars over $u(x)_{max}$ indicate that the value may be considered an upper bound estimate. Cross-sectional areas and surface areas were digitized from NOAA (1991). Since the M_2 tide is the dominant constituent with a period 12.42 hours, $T/2$ is

Location	Prism Velocity (cm/s)	Max. Observed Ebb Velocity (cm/s)
Aerovox (CDF1b)	14	5,7 (ASA, 1986)
CDF1	11	8 (Teeter, 1988)
CDF1 and 3	11	8 (Teeter, 1988)
Coggeshall St. Bridge	73	62,99 (EPA,83 Cortell,82)
CDF7	13	18 (Summ. et al.,77) 37 (USACE 88)
US Rte 6	16*	24 (Summ. et al.,77)
hurricane barrier	120	75,98,122 (ASA,86 USACE,61/70)

* average velocity of 3 openings

Table 4.2: **Tidal Prism Analysis: Baseline Tidal Velocities**

approximately 6.25 hours for these tidal prism calculations. Figure 4-3 illustrates the components of a tidal prism analysis.

Scenario 1: New Bedford Baseline Harbor A tidal prism analysis has been calculated in this thesis for New Bedford Harbor without the addition of contained disposal facilities. Table 4.2 summarizes the tidal prism-calculated, maximum ebb flow velocities and field observations for a number of locations in the harbor and estuary. Discrepancies between observed and calculated velocities near US Route 6 occur because the prism model assumes a single lumped cross-sectional area.

Table 4.2 clearly shows the effect of the two harbor constrictions (i.e., hurricane barrier and Coggeshall Street Bridge). The tidal prism-calculated velocities agree fairly well with the observed and measured values, given their high variability, with

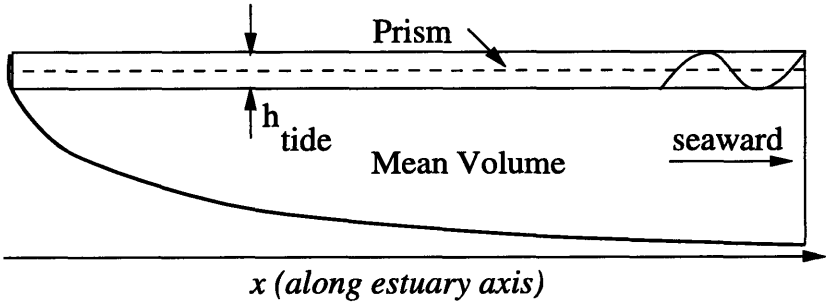

Figure 4-3: **Components of a Tidal Prism**

Location	Baseline Velocity (cm/s)	CDF Velocity (cm/s)
Aerovox (CDF1b)	14	28
CDF 1	11	9
CDF 1 and 3	11	17
Coggeshall St. Bridge	73	45
CDF 7	13	9
US Rte 6	16*	14*
Hurricane barrier	120	112

* average velocity of 3 openings

Table 4.3: **Tidal Prism Analysis: Baseline vs. CDFs**

the exception of the upper estuary near Aerovox. Figure 4-4 graphically shows the relationship between the calculated and observed values. The discrepancy between the tidal prism analysis and observed measurements for the Aerovox facility may be a result of a poor assumption regarding the upward limit of the tidal excursion. Because of the shallow water depth near Aerovox (on the order of 1 to 3 feet deep at MLW), the water flow may be slowed by bottom friction; this is something that the tidal prism analysis cannot reproduce accurately. Additionally, the prism model assumes that the cross-sectional areas, A_c, are constant, which is not true for shallow areas. Because of this assumption, the prism model is sensitive to small variations in tidal height resulting in over- and underestimation of prism velocities.

Scenario 2: New Bedford Harbor with CDFs Incorporating the largest upper Acushnet River confined disposal facilities, including CDFs 1, 1b, 3, and one upper harbor facility, CDF 7, (see Figure 1-3), into the tidal prism analysis offers some insight into the impact of building CDFs at the selected locations. These four CDFs represent current proposals of USEPA officials. CDF 10 in the lower harbor, however, is not in the current proposals, and thus has not been incorporated into this initial analysis but does appear in later calculations. Table 4.3 summarizes and compares the tidal prism-calculated maximum ebb velocities for the baseline and CDF conditions.

Table 4.3 provides a comparison between the two scenarios. Because the CDFs do

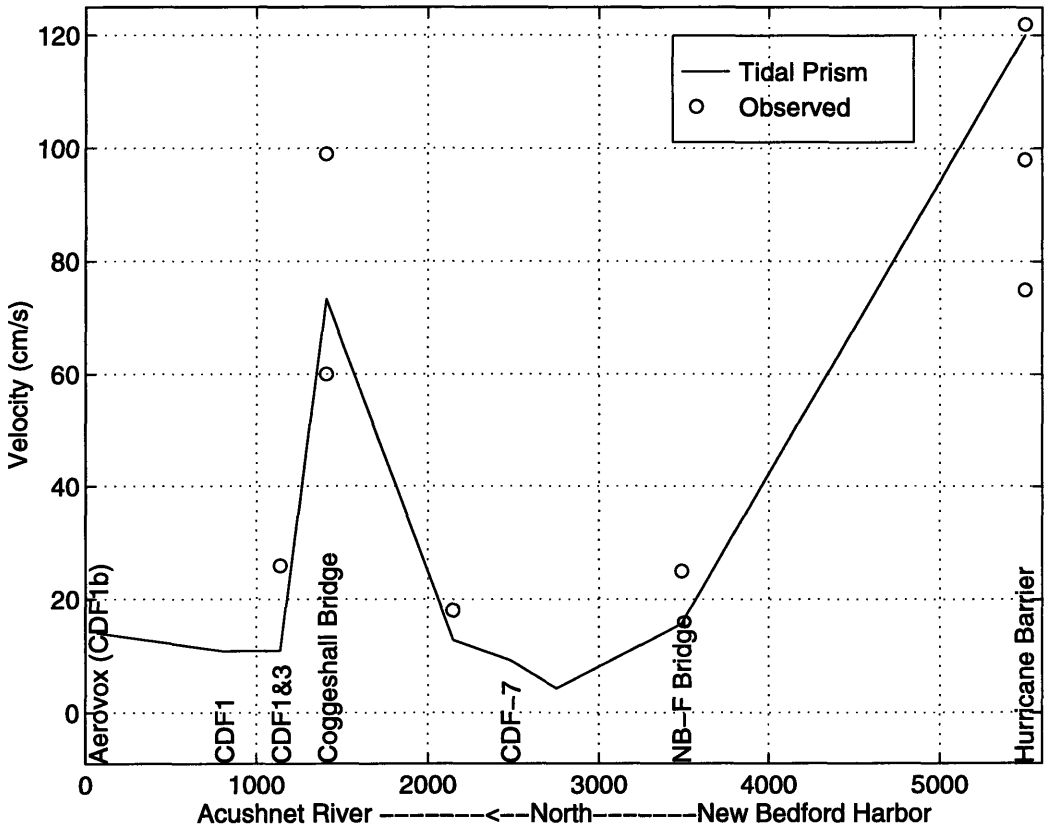

Figure 4-4: **Tidal Prism Analysis and Observed Velocities**

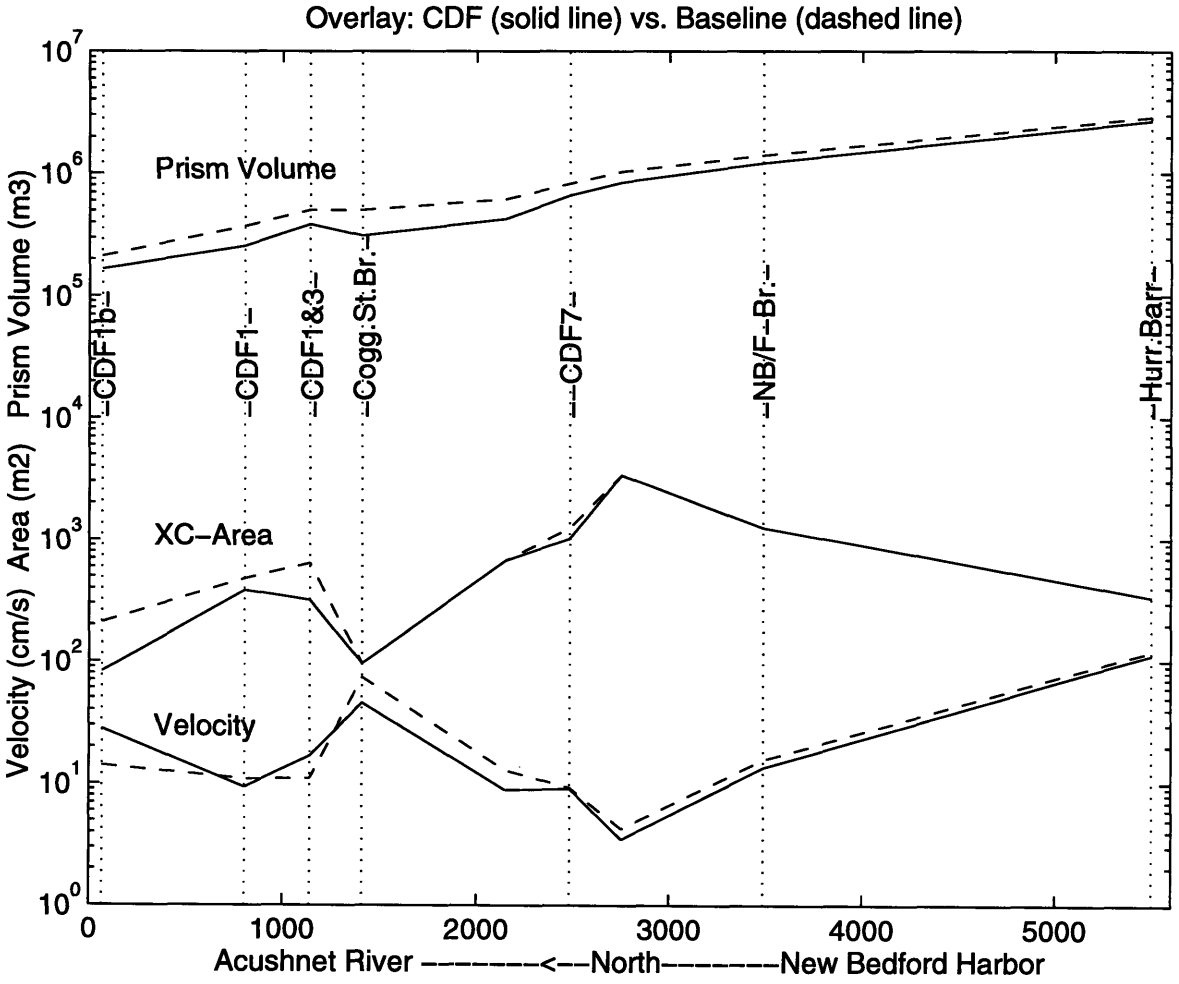

Figure 4-5: **Tidal Prism Analysis**

not exist, there cannot be field measurements with which to compare values; however this type of modeling does lend itself to "A to B" comparisons of the two scenarios. Interestingly, some velocities increase, while others decrease; the increased velocity at CDF 1b is the result of a reduction in the cross-sectional area by half at that location. From one-dimensional channel flow, one can expect that for half of the original cross-sectional area with a constant flow rate, the velocity will double (as seen in Table 4.3). Similarly, the location between CDF 1 and CDF 3 experiences increased velocity because of reduced cross-section. The decreased velocity at the Coggeshall Street Bridge is a direct result of this reduction in the upstream tidal prism near CDF 1b. Figure 4-5 graphically shows the relationship among the prism volume, cross-sectional area, and the resulting velocities for the two scenarios, i.e., baseline and CDFs.

Effects of Individual CDFs The relative impacts of the individual CDFs is shown in Figure 4-6. In this case, CDF 10 is included for comparison purposes; in Figure 4-6 CDF 10 can be assumed to be co-located with the hurricane barrier (see Figure 1-3). From Figure 4-6, it is clear that CDF 1 and 1b in the upper estuary have the most significant impact in this area as expected. CDF 1 and 1b result in velocity increases that are 250% and 200% of the baseline velocities (35 and 28 vs. 14 cm/s), respectively, because of reductions in cross-sectional areas. The reduced prism in the upper estuary leads to a decreases in downstream velocities on the order of 85% of the baseline velocity (62 vs. 73 cm/s) at the Coggeshall Street Bridge and only 97% of baseline at the hurricane barrier. CDF 7 also has significant effects on the velocities in the vicinity of the CDF on the order of 150% of baseline (14 vs. 9 cm/s). Increasing CDF 7 by 18 m^2 to simulate a slightly larger facility leads to increases of approximately 175% of baseline (16 vs. 9 cm/s). This larger CDF 7 is labeled in Figure 4-6 as **CDF7BIG**. CDF 10 appears to have to least effect on harbor velocities, resulting in a 3% decrease in the hurricane barrier ebb velocity.

As previously discussed in Sections 1.1 and 1.6, the total volume of material from the Phase II Superfund operation will be over 400,000 cubic yards. Add 500,000

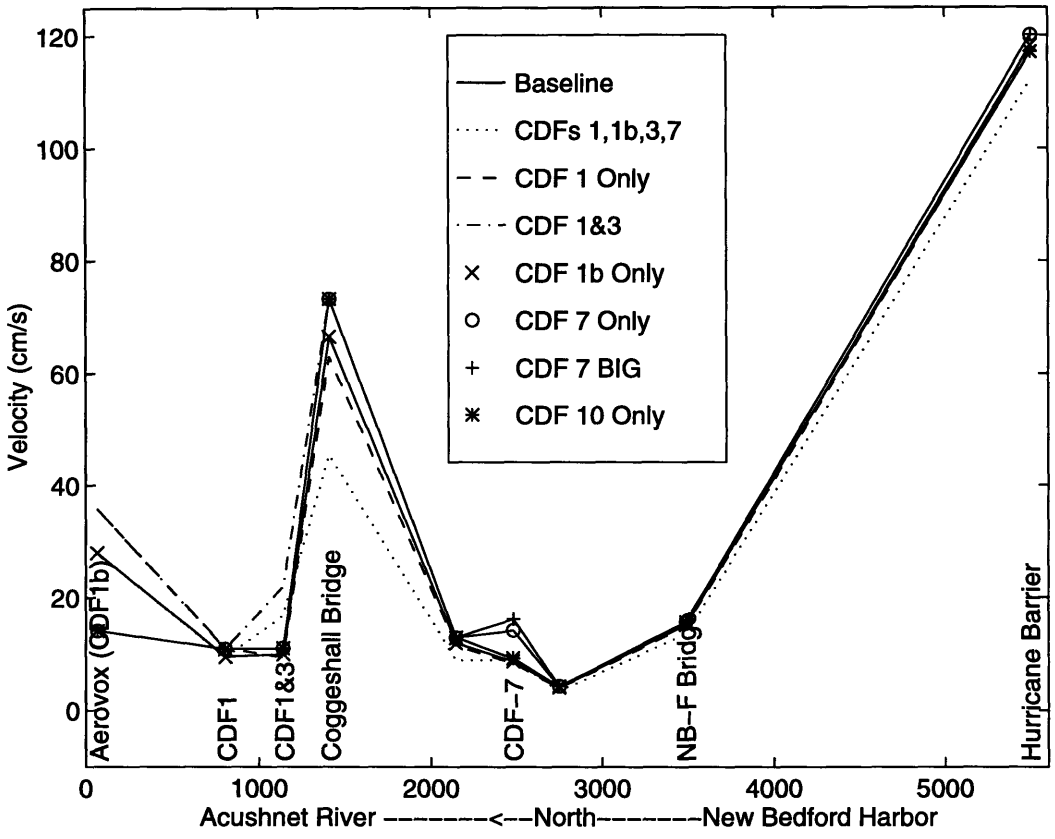

Figure 4-6: **Tidal Prism: Impacts of Individual CDFs**

cubic yards of material from maintenance dredging operations (assuming all priority dredging is within the hurricane barrier), and the total amount of sediment approaches one-million cubic yards. Currently, the largest facility will hold only 270,000 cubic yards (CDF 1), suggesting that single CDF will not confine all of the dredged material from the harbor. It is reasonable, therefore, to model multiple CDFs based on the total volume of material.

From the tidal prism analysis, arrangement with CDF 10 appears to have the least impact on the surrounding harbor velocities. Both CDF 7 and CDF 7BIG velocities, while significant increases from the baseline conditions, do not exceed u_{crit}. Combined, CDFs 7 and 10 will hold approximatly 450,000 cubic yards, enough for the Superfund dredging operations. Additionally, CDF 10 is sited in such a place (near the hurricane barrier) where it does not interfere with harbor traffic. Furthermore, neither CDF 7 nor CDF 10 result in elevated velocities in the upper estuary where the risk for resuspension and PCB contamination is greatest.

4.3 Wind-Generated Circulation and Waves

Wind is the second dominant mechanism for circulation in New Bedford Harbor. The speed of wind-generated currents may exceed u_{crit} under storm conditions, i.e., moderately high winds, in the lower harbor, and just above normal conditions in the upper areas of the harbor. Even under normal conditions, it should be noted, the wind has a significant effect in driving circulation in the harbor. Winds are a critical element to this study because they are the principle ingredient to hurricanes which plague the eastern seaboard of the United States during the late summer and fall every year. While a storm surge, created by the low pressure field of a hurricane, is usually the most destructive element to coastal towns and harbors, New Bedford Harbor is protected by a hurricane barrier; as such, this study focuses on the effects created by the winds only.

Winds alter the tidally-driven circulation in New Bedford Harbor by applying a shear stress on the water surface. This shear stress may result in a condition known

as setup on enclosed water bodies, e.g., New Bedford Harbor with a closed hurricane barrier, in which there is an increase in water height at the far end of a wind-driven fetch, and a decrease in height at the near end, from which direction the wind is blowing. Wind also generates waves, which subsequently produce orbital velocities in the water column below the waves. This section describes these conditions in detail and calculates wind speeds which are required to generate wave heights that result in sediment-suspending critical orbital velocities, u_{crit}. This section also calculates setup heights for New Bedford Harbor for normal and storm events, and discusses possible effects of siting CDFs along the shoreline.

Prevailing Wind Conditions Data indicate that the winds in New Bedford generally originate from the northwest in the winter and the southwest in the summer, with wind speeds typically ranging from 4.2 m/s to 5.4 m/s and an average annual wind speed of 4.8 m/s (ASA, 1986 and Signell, 1987).

Prevailing wave height information in New Bedford Harbor is not something that is recorded by the Corps of Engineers. Some observations have been taken, but mostly during storm events.

Extreme Wind Events More important than daily wind conditions are the storm-related impacts that the New Bedford Harbor experiences during an extreme weather event such as a hurricane. A hurricane, by definition, produces winds in excess of 60 mph, and because winds can gust up to 70 mph (31 m/s) (Batelle 1990 and ASA 1986) and even 186 mph (83 m/s) as recorded during a 1938 hurricane (ASA 1986), precautions should be taken when modifying the harbor. It should be noted that these latter values are only gust speeds and will not necessarily generate sufficient wave heights to cause resuspension of sediments.

During a storm events in New Bedford (not necessarily hurricanes), sustained winds of speeds in excess of 15 m/s occur once or twice per month and last for one to two days (Battelle 1990). Given this wind speed, even the deepest areas of the New Bedford Harbor (e.g., 30 feet), orbital velocities can reach 77 cm/s, well in excess of

u_{crit} (28 cm/s).

For one such storm, while measuring PCB flux through the Coggeshall Street Bridge, Teeter (1988) reported waves as high as 0.92 meters just north of the bridge. The waves were driven by gusts up to 48 km/hr (30 mph), and they were restricted to the deeper main channel. A 1962 report from USACE, cited by Summerhayes *et al.* (1985), suggests that wind-driven wave heights will not exceed six (6) feet in New Bedford Harbor, most probably during extreme wind events.

Fetch Length and Maximum Fetch Length USACERC (1977) defines a fetch as a region in which the wind speed and direction are *reasonably* constant (e.g., if variations in speed and direction are less than 5 knots (2 m/s) and 15 degrees, repectively). Fetch length is used by USACERC (1977) to estimate setup, wave heights, and the overall impact of a wind. Generally an embayment is either fetch- or duration-limited meaning that the effects of winds (e.g., waves heights, setup, general circulation) blowing over the water body are bounded by the maximum distance or time over which the wind can act (fetch and duration limited, respectively). Under these conditions, there are maximum wave and setup heights that cannot be exceeded because of the limited distance or time.

The prevailing wind speeds for New Bedford are within 2 m/s of one another, suggesting that the winds can be considered reasonably constant for any given non-storm event time period. The maximum fetch length for New Bedford Harbor is the distance from the Hurricane Barrier to the New Bedford/Fairhaven Bridge, and the maximum fetch for the upper estuary is from the Coggeshall Street Bridge to the Wood Street Bridge.

Effective Fetch Length The effective fetch length over which wind can affect a body of water is reduced by obstructions (e.g., land masses or islands) in, along, or at the opposite end of that body of water. An effective fetch length can be calculated based on a series of radial measurements from a site onshore outward at six (6) degree intervals (e.g., $0°, \pm 6°, \pm 12°, \ldots, \pm 42°$) from a central (0°) radial that defines

the direction of the wind. The total fetch length is summed over the radial distances, X_i, and then divided by the sum of the angles to give an effective fetch length:

$$F_{effective} = \frac{\sum X_i cos\alpha}{\sum cos\alpha}, \tag{4.3}$$

where α is the angle deviation from the wind direction and X_i is the distance from the onshore site along a radial at each angle α to the point where it hits an obstruction. The cosine of the angle is used to weight the radial distances relative to the central radial which has a weighting factor of unity. As the angles increase, the weight, or importance, of the angle's radial distance decreases.

Applying Equation (4.3), effective fetch length, to the lower New Bedford Harbor, (between the hurricane barrier and the New Bedford-Fairhaven Bridge), with northwest (NW) and southwest (SW) winds provides effective fetch lengths which are approximately 70% of the maximum fetch length. Equation (4.3) gives effective fetch lengths of approximately 4,200 feet, with effective fetch lengths from the northwest and southwest of 4,140 and 4,250 feet, respectively.

4.3.1 Circulation

Winds may alter current velocities and directions under normal and storm conditions. Under non-storm conditions, the harbor becomes most susceptible to wind forcing during slack water, when the tidally-driven current speeds are small or zero. During severe storm events, the hurricane barrier at the mouth of the harbor is closed to protect the harbor from tidal surge. This makes the harbor into an enclosed waterbody, with varying inputs of freshwater from the Acushnet River. In such situations, the harbor may experience setup or setdown from winds, making winds (and sometimes freshwater runoff) the primary circulation mechanism.

Wind Setup Wind setup is defined as a rise above normal water levels that is caused by wind stress on the water surface over a given fetch length. Setup is important to consider because it can increase the upstream prism volume (above that

of the tidal prism), and thus increase the ebb flow velocities above those calculated by Equation (4.2). Setdown, the decrease in water level at one end of a waterbody due to setup at the other may decrease depths, making an area more susceptible to wave-generated orbital velocities and sediment resuspension (see Section 4.3.2).

From USACERC (1977), wind setup, ΔS, can be calculated from the following equation:

$$\Delta S = \frac{kn\rho_a W^2 F}{\rho g d} cos\theta, \tag{4.4}$$

where,

$k \sim 0.003$ (constant)

$n = 1 + \frac{\tau_s}{\tau_b}$

$1.15 \leq n \leq 1.30$ and $n_{typical} = 1.25$

τ_s = surface shear stress

τ_b = bottom shear stress

ρ_a = air density

W = wind velocity

F = fetch length (total length of estuary)

θ = angle between the wind and fetch axes

ρ = water density

d = average depth of fetch

In Equation (4.4), fetch length refers to the total length of a water body and is unaffected by obstructions. This definition is in contrast to that of fetch for wave generation, where obstructions in the water body may reduce the maximum fetch length. The fetch length used in this calculation is the distance from the Hurricane Barrier to Wood Street in the upper estuary, or approximately 5,500 meters. Applying wind setup equation (4.4) to New Bedford Harbor, with F = 5,500 m, d = 4.6 m (average), n = 1.25, $k \sim 0.003$, ρ_a = 1.225 kg/m^3, ρ = 1025 kg/m^3, and W = 15 m/s, gives a maximum setup height (e.g., at $\theta = 0°$) of ΔS = 0.123 meters, or 12.3 cm. For northwest and southwest winds ($\theta = 45°$), ΔS = 9 cm.

A setup of 12 cm over the entire estuary (hurricane barrier to northern reaches of the Acushnet River) gives a setup of approximately 5 cm from the Coggeshall Street Bridge north. A 5 cm head, could theoretically result in a velocity of over 100 cm/s. Using an ASA (1986) simulated setup value of 28 mm for the entire estuary, or 13 mm north of the Coggeshall Street Bridge, gives a velocity of 50 cm/s. It should be noted that these are maximum possible theoretical values based on the difference in height, i.e., the head, and are probably overestimations.

Wind Direction*	Setup/Setdown	Circulation
North	28 mm in upper estuary Sharp increase north of Coggeshall St. Bridge	CCW gyre around Pope's Is. max. current velocity 1.6 cm/s small CCW eddy N. of CSB
Northwest	22 mm	CCW gyre around Pope's Is.
West	4 mm on west side	CCW gyre around Pope's Is. 1 cm/s east of Pope's Is.
Southwest	setdown of 18 mm in upper estuary setup of 2 mm SW of Palmer Is.	CW gyre around Pope's Is. 0.6 cm/s
South	analogous to North	CW gyre around Pope's Is.
Southeast	analogous to Northwest	CW gyre around Pope's Is.
East	analogous to West	CW gyre around Pope's Is. CCW eddy north of Palmer Is. CW eddy N. of CSB
Northeast	analogous to Southwest	CCW gyre around Pope's Is. CW eddy N. of CSB

Table 4.4: **ASA Wind Sensitivity Studies (1987)**
*Wind direction indicates direction in which wind is blowing towards, CCW = counter-clockwise, CW = clockwise, CSB = Coggeshall Street Bridge.

The siting of CDFs will constrict cross-sections in the upper estuary. As such, setup, when winds driving it cease, may result in velocities in excess of u_{crit} through these new constrictions. Additionally, setup may result in increased flooding in the wetland areas of the upper estuary and increased contamination because the CDFs will have reduced the storage volume of the river.

The effect of wind in controling circulation patterns has been modeled by ASA (1987). Winds from the north and south generate gyres around Pope's Island, altering current velocities on the east and west sides of the island. ASA (1987) also found that north to east blowing winds created eddies north of the Coggeshall Street Bridge. In their model, ASA applied a wind forcing (stress) of 1 dyne/cm^2, ramping it up from zero to one over two hours using a cosine ramp function and holding the sea level boundary condition at the Hurricane Barrier fixed at mean sea level.

The ASA wind sensitivity studies, summarized in Table 4.4, indicate that the

harbor, which is oriented mostly north-south, is most susceptible to winds from the north and south, with setup heights that are approximately five times that from east and west winds. These relations follow from Equation (4.4) for calculating wind setup, in which the setup height is directly proportional to the fetch length, and the fetch length is 5 to 6 times the width. Holding values for fetch length and depth constant from previous setup calculations of Equation (4.4) at 5500 and 4.6 meters, respectively, the ASA (1987) values for setup (±28 mm) with a north/south wind correspond to a wind speed of approximately 7.2 m/s.

Wave Refraction, Reflection, and Diffraction Potentially, the introduction of CDFs may cause refraction, reflection, and diffraction of wind-generated waves; however since winds in New Bedford Harbor typically originate from the west, the western shore CDFs, i.e., all CDFs except CDFs 3 and 4, will most likely be unaffected and ineffective at altering the wave patterns. Numerical modeling efforts, in Section 5, are used to identify significant changes in circulation patterns.

4.3.2 Wave-Induced Orbital Velocities

Using existing wind data for New Bedford, maximum wave heights have been determined and horizontal excursion velocities have been calculated from methods outlined in USACERC (1977). Winds blowing across the surface of a body of water generate waves which are a function of the wind speed and duration, as well as the fetch length and depth of the body of water. Deep water wave orbitals (depth/wavelength $< 1/2$) occur in circular patterns which exponentially decrease in diameter with depth, while shallow water wave orbitals (depth/wavelength $< 1/20$) occur in elliptical patterns with uniform major, i.e., horizontal, axes and decreasing minor, i.e., vertical, axes with depth. For shallow water, the maximum horizontal excursion distance, $2A$, i.e., twice the major axis of the ellipse, is given by

$$2A = \frac{H_s T_s \sqrt{gd}}{2\pi d}, \tag{4.5}$$

Depth/Maximum Fetch	Wave Height	Orbital Velocity
Prevailing Winds, W = 10 mph		
Upper Estuary:		
3 ft/5,500 ft	0.38 ft	0.62 ft/s (18.9 cm/s)
10 ft/5,500 ft	0.40 ft	0.36 ft/s (10.9 cm/s)
Lower Harbor:		
30 ft/6,000 ft	0.45 ft	0.23 ft/s (7.1 cm/s)
Observed Wave Heights with W = 10 mph		
10 ft/6,000 ft	3.02 ft	**2.7 ft/s (82.5 cm/s)**
10 ft/6,000 ft	6 ft	**5.38 ft/s (164 cm/s)**

Table 4.5: **Orbital Velocities for Prevailing Winds in New Bedford Harbor** For the fixed depth calculations a 10 MPH wind has been used, and for the observed wave heights, a depth of 10 feet has been used. **Velocity in bold** $> u_{crit}$.

where where d is the depth, g is gravity, and H_s is the significant wave height, and T_s is the significant wave period. The maximum horizontal velocity, U_{max}, in the fluid generated by the wave is given by

$$U_{max} = \frac{H_s\sqrt{gd}}{2d} \tag{4.6}$$

Orbital Velocities from Prevailing Winds Table 4.5 shows the approximate orbital velocities for prevailing winds and observed wave heights in the harbor. Some of the wave height values in Table 4.5 have been estimated using forecasting curves from USACERC (1977) which correlate wave height to fetch length, wind speed, and depth; this is the reason fetch length appears in Table 4.5. USACERC (1977) uses English units, so these will be used throughout the calculations. Prevailing winds range from 4.2 to 5.4 m/s (10 to 12 mph); however there is little distinction between these two values in the USACERC (1977) shallow-water forecasting curves, so a 10 mph wind has been used. For this reason, the table estimates the wave heights and orbital velocities resulting from a 10 MPH wind for three common harbor depths: 3, 10, and 30 feet. Orbital velocities for two observed wave heights, 3.02 feet (Teeter 1988) and 6 feet (USACE from Summerhayes *et al.* 1985) are calculated using

Location	Depth	Wave Height	Fetch Length	Wind Velocity
Upper Acushnet	3 ft (1 m)	0.5 ft (0.2 m)	5,500 ft	13 mph (6 m/s)
Lower Acushnet	10 ft (3 m)	1.0 ft (0.3 m)	5,500 ft	23 mph (10 m/s)
Lower Harbor	30 ft (10 m) 30 ft (10 m)	1.5 ft (0.5 m) 1.5 ft (0.5 m)	4,200 ft (F_{eff}) 6,000 ft (F_{max})	35 mph (15.6 m/s) 32 mph (14.3 m/s)

Table 4.6: **Wind Velocities and Wave Heights Required for Resuspension**

Equation (4.6).

Table 4.5 indicates that under "normal" conditions, i.e., 4.2 m/s$< W <$ 5.4 m/s, orbital velocities do not exceed u_{crit} of 28 cm/s. Both observed (storm) wave heights, however, result in orbital velocities that exceed u_{crit}.

Critical Wind Generated Current Velocities From Section 3 on New Bedford Harbor sediments, an empirical critical velocity, u_{crit}, range of $20-30 cm/s$ was found by Heavers (1983 as referenced in ASA 1986) for sediment suspension, and a critical velocity was estimated by ASA (1986) to be approximately 28 m/s.

The following method was used to interpret this critical velocity in terms of meteorological conditions:

1. Equation (4.6), the maximum horizontal orbital velocity generated by a wave, was rearranged to solve for the significant wave height, H_s, based on a critical velocity of 28 cm/s and three common depths in the harbor (3, 10, and 30 feet).

2. Wind velocities necessary to create the wave heights that were calculated in the first step were determined using **Forecasting Curves for Shallow-Water Waves**, from USACERC (1977), which correlates fetch length, wave height and period, and wind speed for constant shallow-water depths.

From the calculations shown in Table 4.6, for the lower harbor, a fetch of 6,000 feet and a depth of 30 feet requires a 32 mph (14 m/s) wind to generate 1.5 foot waves. These 1.5 foot waves are necessary to generate a horizontal orbital velocity of 28 cm/s

to suspend sediment. As previously mentioned, storms with wind speeds of 15 m/s and wind durations of 1-2 days occur once or twice per month, on average. Results from Table 4.6, therefore, suggest that the lower harbor experiences resuspension events at least once to twice per month just from winds.

For the upper estuary, a 13 mph (6 m/s) wind is necessary to suspend sediments. This wind speed is just slightly higher than the prevailing wind speeds, suggesting that even small storms will resuspend sediments.

4.4 Freshwater Runoff

Freshwater runoff from the Acushnet River has the most impact in the upper estuary because of the smaller cross-sections. During storm events, higher runoff rates are responsible for increasing the flushing of the upper estuary. The increased freshwater flow may, however, increase vertical stratification (see Section 4.1) which may affect the residence time (see Section 4.5). The introduction of CDFs along the shoreline of the upper estuary will reduce the cross-sections of the river as well as reducing the volume of water that the upper estuary can accommodate. Changes in surface elevation are most significant in shallow areas where the increases may be a substantial percentage of the stillwater height. Runoff has the least effect in the lower harbor, where tidal mechanisms dominate circulation; however, freshwater flow may add a significant volume of water to the total prism, resulting in elevated ebb flow velocities.

Under normal weather conditions, e.g., non-storm events, freshwater runoff has little effect, with annual average flow rates of 0.85 m^3/s (Cortell 1982). Under these conditions, the Acushnet River experiences velocities of approximately 3 to 5 cm/s (ASA 1986); this value also accounts for tidal forcing. This relatively low flow rate of 0.85 m^3/s is in contrast to storm and post-storm situations when runoff rates may be as high as 18.4 m^3/s (NUS 1984 as referenced in Battelle 1990) for 100 year storm events. These storm-related runoff rates have a significant effect in the upper harbor, where cross-sectional areas are smaller. In addition to the river flow, there are several combined sewage overflow (CSO) pipes which feed into the harbor at many locations

along it. These CSOs have been observed to flow quite freely after rain events, though none of them are monitored or measured (Beaudoin 1996).

Maximum Freshwater Induced Velocities Increased freshwater runoff into the Acushnet River immediately after extreme weather events increases velocities within the upper portions of the river. One-hundred year flood flow rates up to 18.4 m^3/s have been modeled in ASA (1986), resulting in river flow velocities of approximately 11 cm/s. ASA (1986) combined the normal condition values of 3-5 cm/s with this storm value of 11 cm/s to give a total maximum velocity of 16 cm/s. This value is approximately half of the velocities necessary to suspend sediments (28 cm/s).

The cross-sectional area of the Acushnet River adjacent to the Aerovox site and proposed CDF 1b is approximately 95 m^2. A maximum flow rate of 18.4 m^3/s gives a velocity of approximately 19 cm/s. With the proposed CDF 1b, the cross-sectional area of the river at this point will be reduced by about two times to approximately 45 m^2, resulting in velocities of 39 cm/s, in excess of u_{crit}. Under normal tidal conditions, the result of the CDF siting would increase the velocity to 23 cm/s, still below u_{crit} of 28 cm/s, but within the range of 20-30 cm/s defined by Heavers (1983 as referenced in ASA 1986). This area is particularly important because it is one of the "hottest" PCB-contaminated sites in New Bedford, and increased water velocities may suspend PCB-contaminated sediments into the water column.

4.5 Residence Time

Residence time, τ, is defined as the length of time that a slug, or volume, of water stays within a bay or estuary. The inverse of the residence time is called the flushing rate, and it is the rate at which the slug of water leaves the bay or estuary. Residence time is an estuary-specific parameter that changes with geometry, bathymetry, and climatic conditions. It is also location-specific within an individual estuary and can change depending where the slug of contaminant or conservative tracer is introduced. Especially important for polluted embayments, residence time gives an estimate of

how quickly the water body exchanges its volume of contaminated water with clean water from outside (i.e., the ocean). Additionally, residence time, when considered with current and fall velocities, gives an indication of how long and far resuspended sediment particles travel before settling. Figure 4-7 shows the velocity components of a sediment particle.

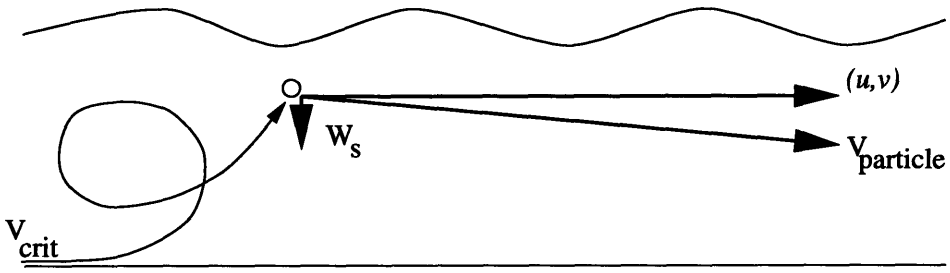

Figure 4-7: **Particle Velocity Components**

Because settling time, W_s, is usually much smaller than current velocities, the sediment particle will travel farther in the horizontal plane than in the vertical. As an example, using a settling velocity from Table 3.1 in Section 3 of 0.006 mm/s and a water depth of one (1) meter, as might be found in the upper Acushnet River estuary, gives a settling time of approximately 46 hours (1.9 days). The direction of the tide changes every 6.25 hours, however, and a particle with $W_s = 0.006$ mm/s will settle only 13.5 cm. This small distance is in contrast to the 1125 meters that the particle may travel in the horizontal plane under a 5 cm/s current for the same amount of time. The longer a particle stays suspended in the water column, the greater the chance that it will be flushed from the estuary.

The residence time of an estuary is influenced by tides, winds, and rainfall. An increase in tidal ranges, e.g., during spring tides, increases the amount of water that enters the estuary, and decreases the residence time. An increase in rainfall and the subsequent runoff from the Acushnet River and numerous combined sewage overflows (CSO) alters the flushing characteristics of the harbor. Increased runoff may result in vertical stratification of the water column which, under some circumstances, may increase the residence time of bottom layers of water and decrease the residence time of

surface layers. For conservative tracer dye that is mixed with freshwater and released on the surface, the effect of increased runoff will most likely reduce the residence time because the runoff mixes with the surface water to dilute the surface concentrations. Conversely, for PCBs that have sorbed onto resuspended sediment particles in the upper estuary, residence time may be increased for a stratified water column because the particles could become trapped beneath the pycnocline and move upstream as discussed in Section 3. Wind is a secondary factor to tidal and runoff effects in controlling residence time. Depending on direction, duration, and magnitude, winds can increase or decrease the residence time by altering circulation patterns within an estuary.

4.5.1 Estimation Techniques for Residence Time

Three methods are presented for estimating residence time: tidal prism, dye study, and freshwater fraction. Among these methods, the tidal prism is perhaps the simplest, but least accurate. The measurement of dye concentrations over a period of several tidal cycles is a more accurate technique; the injection of the dye can be done instantaneously or continuously over several days. Finally, if dye is not available, the salt in the system, also considered a conservative substance, can be used; this is called the freshwater fraction method.

Tidal Prism Method

Using the concept of a tidal prism as in Section 4.2.1, where P is the prism volume defined by the surface area of an inlet, bay, or estuary and the difference in height between high and low tides, and T is the tidal period, the flow rate from this prism is given by

$$Q = \frac{P}{(T/2)} = AV, \tag{4.7}$$

the rightmost equation being that of one-dimensional channel flow where A is the cross-sectional area and V is the velocity.

The tidal prism method estimates the time for the entire volume, or $P + \forall$, where $\forall$ is the MLW volume, to flow out of the estuary at flow rate Q from (4.7) during ebb tide ($T/2$):

$$\tau_{res} = \frac{\forall + P}{Q} = \frac{\forall + P}{2P/T} = \frac{(\forall + P)T}{2P}, \tag{4.8}$$

The tidal prism method is considered a lower bound for residence time because it assumes that the entire volume of water in the estuary is exchanged with new water; this method does not account for return flow back into the estuary.

Conservative Dye Study

Residence time calculations using measured concentrations from a dye study are generally more reliable than estimations made using tidal prism methods, though much more costly. Three methods are presented for analysis: one using dye injected as an instantaneous slug and two using dye introduced continuously for several tidal cycles. In all three methods, the measured dye concentrations are integrated spatially over the harbor. Two of the methods are equivalent and all three are equivalent if the waterbody can be considered well mixed. If the waterbody is not well mixed, the calculation of residence time depends on the location of dye injection.

Instantaneous Injection Measurements for the instantaneous injection are made over time and begin almost immediately. For a waterbody that is not well mixed, the instantaneous injection residence time calculation is sensitive to dye input location. For the instantaneous point source (see Figure 4-8), residence time is calculated by Equation (4.9), where M_o is the initial mass of the tracer, and $M(t)$ is the spatially integrated mass, i.e., concentration as a function of time, $c(t)$, integrated over the volume of the tracer:

$$\tau = \frac{\int_0^\infty M(t)dt}{M_o}, \tag{4.9}$$

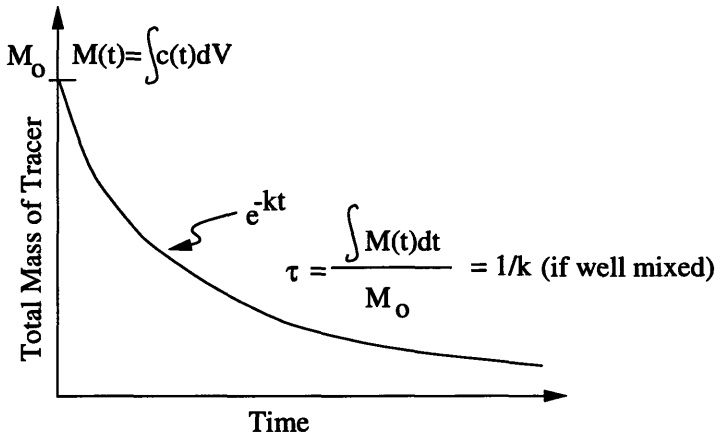

Figure 4-8: **Instantaneous Tracer Mass Time Series**

where

$$M(t) = \int_V c(t)dV \tag{4.10}$$

Continuous Discharge For a continuous discharge, two methods have been used to compute residence time. The first assumes that the dye has been released for a long enough time for concentrations to have reached steady-state throughout the waterbody. Residence time can be estimated from the following equation, where c_{ss} is the steady-state concentration spatially integrated over volume, i.e., the steady-state mass, M_{ss}, in the system, and $\dot{m}_{in}$ is the input rate of the dye:

$$\tau = \frac{\int c_{ss}dV}{\dot{m}_{in}} = \frac{M_{ss}}{\dot{m}_{in}} \tag{4.11}$$

It can be shown that the residence time computed by Equation (4.11) is identical to that computed by Equation (4.9). Assuming a well mixed regime, residence time for a continuous discharge can also be estimated by fitting an exponential curve (a straight line on a semilog plot) to the decline of the tracer mass in the form of e^{-kt}, where t is time following cessation of the dye release, and residence time is equal to $1/k$ as in Figure 4-9. This is equivalent to the approach for an instantaneous release and may be less accurate than that in Equation (4.11) because it adds smoothing with the line fit.

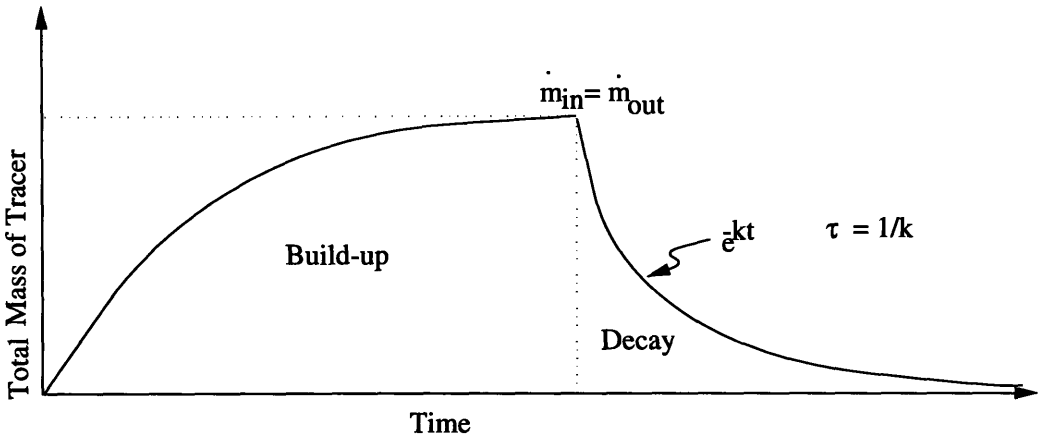

Figure 4-9: **Continuous Tracer Mass Time Series**

To the extent that the waterbody is not well mixed (and no waterbody is truly well mixed), this approach will predict a different residence time than Equation (4.11) depending on the location of the dye release. This is because if the waterbody is not well mixed, the dye mass will have assumed a spatial distribution throughout the waterbody (at the time the release stops), which is not the same as for the instantaneous injection. For example, if the discharge is to the upper (closed end) of the waterbody, the center of mass will tend to be closer to the open boundary when the dye release is stopped. This suggests that the instantaneous injection should give a slightly longer residence time. The opposite would be true for a discharge near the mouth (open end) of the estuary.

Figure 4-9 shows the build-up and decay periods of the mass of the conservative dye during and after discharge, respectively.

Freshwater Fraction Method

Essentially the same as a continuous discharge (Equation 4.11), the freshwater fraction method considers freshwater, instead of dye, as the tracer. The method calculates the fraction, f_x, of a given volume which is freshwater, and then divides the sum of these volumes by the input rate of freshwater into the estuary as in Equations (4.12), (4.13), and (4.14):

$$f_x = \frac{(\sigma - s_x)}{\sigma}, \tag{4.12}$$

where σ is the ocean salinity and s_x is the salinity of the volume fraction. Then,

$$\forall_{f_x} = f_x \forall_x, \tag{4.13}$$

where $\forall_{f_x}$ is the freshness-weighted volume fraction, leading to a residence time of

$$t_f = \frac{\Sigma \forall_{f_x}}{R}, \tag{4.14}$$

where R is the flow rate of any freshwater input (e.g., the Acushnet River).

Calculations for New Bedford Harbor Equation (4.8) gives a residence time of 50 hours, or 2.1 days, using prism and harbor volumes estimated from NOAA (1991). Other tidal prisms have been calculated for New Bedford Harbor, with values for a residence time of 1.9 to 2.2 days. From these calculations, a lower limit can be estimated at approximately 2.0 days. The variability in these values is most likely a result of differences in discretizing surface areas and volumes from navigational charts.

Recall from earlier calculations in this chapter that sediments suspended in the water column have a settling time of approximately 1.9 days (46 hours), similar to the lower limit of the residence time. This indicates that a particle that is suspended in the upper estuary has a reasonable chance of being flushed out of the harbor before settling.

An alternative method of calculating residence time is the modified tidal prism, developed by Ketchum (1951), which factors in the length of the tidal excursion. An estuary can be divided into tidal-excurion-length sections, with the high-tide volume of an upstream segment equal to the low-tide volume of an adjacent downstream segment. Using this method, Case (1989) estimated the residence time for New Bedford Harbor at 20.8 days; however, using the same method to measure concentrations from a dye study, Case found that the values were an order of magnitude larger than those

Reference	Method	Residence Time (days)	Comments
ASA (1987)	Dye Study	2.4	continuous
Case (1989)	Freshwater Fraction	4.0	recent rainfall
Case (1989)	ASA Dye Study	3.2 ±0.2	continuous
Case (1989)	Tidal Prism	2.2	
Case (1989)	Modified Tidal Prism	20.8	10x too high?
Cochrane (1992)	Aquatec Dye Study	4 ±1	instantaneous
Lohse (1996)	Tidal Prism	2.1	

Table 4.7: **Residence Time Calculations for New Bedford Harbor**

actually measured.

Case (1989) also used a freshwater fraction method to calculate residence time (see Equations 4.12, 4.13, and 4.14). Using this method, Case calculated a residence time of 4.0 days, assuming a freshwater discharge rate of 0.85 m^3/s. A rainfall that occurred a few days prior to the salinity measurements, making surface waters fresher than normal, may have decreased the residence time slightly; this suggests that a slightly higher residence time would exist during non-storm events.

A residence time of 2.4 days has been calculated for New Bedford Harbor by ASA (1986) from a continuous dye study by measuring the decline of mass of a conservative tracer over several tidal cycles after the dye injection stopped. Another analysis of the ASA (1986) dye study data by Case (1989), estimates slightly higher values of 3.0 to 3.4 days. Cochrane (1992) analyzed an instantaneous dye study performed by Aquatec (1991) and calculated a residence time of four (4) days, plus or minus one day. This slightly higher value agrees with prior arguments that less mass escapes during an instantaneous injection, resulting in higher residence times. Table 4.7 summarizes the residence time calculations for New Bedford Harbor. From Table 4.7, not including the modified tidal prism method, it can be seen that the instantaneous dye study gave the longest estimate, followed by the continuous dye study analyses, which were slightly shorter, and tidal prim methods which gave the lowest estimates.

Confined Disposal Facilities The introduction of CDFs along the western shoreline of the harbor (see Figure 1-3) will certainly reduce the overall volume of the harbor as well as the tidal prism, though not sufficiently to alter the harbor residence time estimations significantly. Considering the CDFs collectively (i.e., CDF 1, 1b, 3, 7), Equation (4.8) gives a residence time of 52 hours, or 1.25 hours longer than the baseline condition. Local to each CDF, residence times may be reduced by as much as 8 hours and increased by as much as 1.25 hours. The decrease in local residence time occurs in the upper estuary, where CDF 1b reduces the local prism volume by approximately 40% as well as the local total volume by approximately 25%.

4.6 Summary of CDF Effects on Harbor Forcing

The previous sections in this chapter have shown the effects of CDFs on the harbor circulation. This section summarizes these effects on the dominant forcing factors as well as residence time, which is driven by a combination of the tidal, wind, and freshwater effects.

Tidal

- Reduction of prism volumes and cross-sections
- Elevated velocities in upper estuary, e.g., 28 vs. 14 cm/s
- Reduced velocities in the lower harbor, e.g., 45 vs. 73 cm/s at the Coggeshall Street Bridge and 120 vs. 112 cm/s at the hurricane barrier
- CDF 7 and CDF 10 provide the best arrangement.

Wind and Waves

- Negligible effect on wind-generated waves
- CDFs and setup may result in flooding of wetlands in upper estuary
- Elevated velocities from release of setup

Freshwater

- Increase flushing and velocities during flood events, e.g., 19 vs. 39 cm/s
- Elevated current velocities may resuspend PCBs

Residence Time

- Slight increase in harbor residence time
- Slight decrease in upper estuary residence time

Chapter 5

Numerical Modeling: ECOM-si

This chapter describes the numerical finite difference model, ECOM-si, and describes the input and output files associated with it. Model grid information pertaining to this thesis is also presented as well as modifications to the standard grid arrangement. Additionally, runtime parameters are presented and discussed in terms of the New Bedford model.

5.1 Model Description

ECOM-si is a time-dependent, three-dimensional, estuarine, coastal and ocean model (semi-implicit), ECOM-si, developed by Blumberg and Mellor (1980, 1987). This model has been used in a number of studies including Blumberg and Mellor (1983) on the South Atlantic Bight, Oey, *et al.* (1985a, b, c) on the Hudson-Raritan estuary, Blumberg and Mellor (1985) on the Gulf of Mexico, Galperin and Mellor (1990a, b) on Delaware Bay, River, and adjacent continental shelf, Blumberg and Goodrich (1990) on Chesapeake Bay, and Blumberg, Signell, and Jenter (1993) on Massachusetts Bay.

The 3-D model solves the governing circulation model equations by finite difference methods (described later). With a horizontally and vertically staggered lattice of grid points, the model uses an implicit numerical scheme in the vertical direction (Roache, 1972; Appendix A) and a semi-implicit scheme in the horizontal direction (Casulli, 1989, 1990 and Cheng and Casulli 1991) for the barotropic mode. Prognostic variables

calculated include free surface, η, velocity components, u, v, ω, temperature, salinity, concentration, and two turbulence coefficients (Blumberg 1991). The finite difference equations conserve energy, mass and momentum.

The model uses a bottom-following σ-coordinate system, for the vertical dimension such that the number of grid points in the vertical is independent of depth, with σ ranging from σ=0 at the surface, $z = \eta$, to σ = -1 at the bottom, $z = -H$, where $\eta(x, y)$ is the surface elevation and $H(x, y)$ is the bottom topography. The σ-coordinate system is given by the following relation:

$$\sigma = \frac{z - \eta}{H + \eta} \tag{5.1}$$

The σ-coordinate system also allows for better resolution of important surface and bottom Ekman layers across a sloping shelf (Blumberg, 1991). However, rapid changes in σ-layer thickness from continental shelf to deep basin result in artificial numerical diffusion, both vertically upward and downward in the grid. In addition, the model uses a horizontal, orthogonal, curvilinear coordinate system. From Blumberg (1991), the equations of motion are as follows (in σ-curvilinear coordinates), where ξ_1 and ξ_2 are abitrary horizontal curvilinear orthogonal coordinates, U_1 and U_2 represent the ξ_1 and ξ_2 velocity components, and h_1 and h_2 are the curvilinear grid cell length scales in the ξ_1 and ξ_2 directions, respectively:

Continuity Equation:

$$h_1 h_2 \frac{\partial \eta}{\partial t} + \frac{\partial}{\partial \xi_1}(h_2 U_1 D) + \frac{\partial}{\partial \xi_2}(h_1 U_2 D) + h_1 h_2 \frac{\partial \omega}{\partial \sigma} = 0 \tag{5.2}$$

where

$$\omega = W - \frac{1}{h_1 h_2}\left[h_2 U_1 \left(\sigma \frac{\partial D}{\partial \xi_1} + \frac{\partial \eta}{\partial \xi_1}\right) + h_1 U_2 \left(\sigma \frac{\partial D}{\partial \xi_2} + \frac{\partial \eta}{\partial \xi_2}\right)\right] - \left(\sigma \frac{\partial D}{\partial t} + \frac{\partial \eta}{\partial t}\right) \tag{5.3}$$

The continuity equation (5.2), when integrated over depth while using a kinematic

boundary equation at the surface leads to the free surface equation (Blumberg 1991):

$$h_1 h_2 \frac{\partial \eta}{\partial t} + \frac{\partial}{\partial \xi_1} \int_{-H}^{\eta} (U_1 h_2 D) dz + \frac{\partial}{\partial \xi_2} \int_{-H}^{\eta} (U_2 h_1 D) dz = 0 \tag{5.4}$$

The Reynolds Equation for the ξ_1 coordinate (similar for ξ_2) is:

$$\begin{aligned}
&\frac{\partial (h_1 h_2 D U_1)}{\partial t} + \frac{\partial}{\partial \xi_1}(h_2 D U_1^2) + \frac{\partial}{\partial \xi_2}(h_1 D U_1 U_2) + h_1 h_2 \frac{\partial \omega U_1}{\partial \sigma} \\
&\qquad + D U_2 \left(-U_2 \frac{\partial h_2}{\partial \xi_1} + U_1 \frac{\partial h_1}{\partial \xi_2} - h_1 h_2 f \right) \\
&= -g D h_2 \left(\frac{\partial \eta}{\partial \xi_1} + \frac{\partial H_o}{\partial \xi_1} \right) - \frac{g D^2 h_2}{\rho_o} \int_{\sigma}^{0} \left(\frac{\partial \rho}{\partial \xi_1} - \frac{\sigma}{D} \frac{\partial D}{\partial \xi_1} \frac{\partial \rho}{\partial \sigma} \right) d\sigma \\
&\quad - D \frac{h_2}{\rho_o} \frac{\partial P_a}{\partial \xi_1} + \frac{\partial}{\partial \xi_1} \left(2 A_M \frac{h_2}{h_1} D \frac{\partial U_1}{\partial \xi_1} \right) + \frac{\partial}{\partial \xi_2} \left(A_M \frac{h_1}{h_2} D \frac{\partial U_1}{\partial \xi_2} \right) \\
&\qquad + \frac{\partial}{\partial \xi_2} \left(A_M D \frac{U_2}{\xi_1} \right) + \frac{h_1 h_2}{D} \frac{\partial}{\partial \sigma} \left(K_M \frac{\partial U_1}{\partial \sigma} \right)
\end{aligned} \tag{5.5}$$

where A_M is the horizontal viscosity defined by Smagorinsky (1963) as

$$A_M = \alpha \Delta x \Delta y \left[\left(\frac{\partial U}{\partial x} \right)^2 + \left(\frac{\partial V}{\partial y} \right)^2 + \left(\frac{\partial U}{\partial y} + \frac{\partial V}{\partial x} \right)^2 \right]^{\frac{1}{2}} \tag{5.6}$$

and the notation for Equation (5.6) is based on the Cartesian coordinate system and conventional variable names, and α has ranged from 0.01 to 0.5 in various models, but is typically equal to 0.10 (Blumberg 1991).

The transport of a conservative tracer, C, is given by:

$$\begin{aligned}
&h_1 h_2 \frac{\partial (CD)}{\partial t} + \frac{\partial}{\partial \xi_1}(h_2 U_1 C D) + \frac{\partial}{\partial \xi_2}(h_1 U_2 C D) + h_1 h_2 \frac{\partial (\omega C)}{\partial \sigma} \\
&= \frac{\partial}{\partial \xi_1} \left(\frac{h_2}{h_1} A_H D \frac{\partial C}{\partial \xi_1} \right) + \frac{\partial}{\partial \xi_2} \left(\frac{h_1}{h_2} A_H D \frac{\partial C}{\partial \xi_2} \right) + \frac{h_1 h_2}{D} \frac{\partial}{\partial \sigma} \left(K_H \frac{\partial C}{\partial \sigma} \right)
\end{aligned} \tag{5.7}$$

where A_H and K_H are the vertical diffusivity and vertical eddy diffusivity, respectively. Transport equations for temperature, salinity, turbulent kinetic energy, and the turbulent macroscale are similar to Equation (5.7).

The horizontal viscosity, in this version of ECOM-si is given according to the

Smagorinsky (1963) formulation and varies between 1 and 50 m^2s^{-1}. The vertical eddy viscosity and diffusivity coefficients are evaluated using the level 2-1/2 turbulence closure model developed by Mellor and Yamada (1982) as modified by Galperin *et al.* (1988), in which the vertical eddy coefficients are calculated from turbulence transport equations for the turbulence kinetic energy and turbulence length scale.

On the open boundaries, the surface elevation is determined by a Sommerfield radiation condition (Blumberg, 1991), modified by a restorative term (Blumberg and Kantha, 1985) so that the boundary elevation does not drift from a mean value. For tidally-driven boundaries, the model is forced using six (6) harmonic constituents: S_2, M_2, N_2, K_1, P_1, and O_1. For inflow through a boundary, temperature and salinity data sets are used, whereas for outflow through the boundary, conditions are calculated from a simple horizontal advection equation from interior-calculated data. To avoid discontinuity and conserve mass when flow direction changes, an exponential relationship with a specified e-folding is assumed between the advected boundary value and data prescription (Blumberg, 1991). Additionally, the ECOM-si model may be forced by surface wind stress, atmospheric pressure gradients, heat flux, salinity flux, and freshwater discharge. ECOM-si treats freshwater run-off as a discharge rate at a specified location. Temperature, salinity, and depth of discharge are input parameters for the model to drive density-induced mixing. In its barotropic (2D) module, ECOM-si is also capable of handling flooding and drying of wetlands.

5.1.1 Model Adjustments

Previous studies using the ECOM-si model have relied on lower resolution and larger grid cell sizes on the order of 1 to 10's of kilometers (see Blumberg and Mellor (1983), Oey, Mellor and Hires (1985) and Galperin and Mellor (1990a,b) for further discussion). The model has been shown to represent circulation patterns quite well at these resolutions; however a need exists to resolve complex coastlines and rivers with details of less than 1 kilometer.

To model narrow waterways in the Hudson-Raritan Estuary, Oey, Mellor and Hires (1985), incorporated non-dimensional width factors, $b(x)$ and $b_T(x)$, into the

governing equations to represent the ratio of the river width to the grid cell size; a later study of the Delaware Bay and river system by Galperin and Mellor (1990a,b) also utilized these non-dimensional factors. Though not explicitly stated in either Oey *et al.* (1985) or Galperin and Mellor (1990a,b), b_T appears to represent the width at the surface while b is the average width of the subsurface channel; generally, $b(x) = b_T(x)$. As an example, for shallow marsh areas, where the surface width is large, and the average subsurface width may be slightly smaller, $b_T > b$. These non-dimensional factors are incorporated into depth-averaged versions of the governing equations in which $v = 0$ and the y-derivatives have been dropped:

$$\frac{\partial}{\partial t}(\overline{u}Db) + \frac{\partial}{\partial x}(\overline{u}^2 Db) + gDb\frac{\partial \eta}{\partial x} = \tau_x^w b - kb\overline{u}|\overline{u}| \tag{5.8}$$

$$\frac{\partial}{\partial t}(\eta b_T) + \frac{\partial}{\partial x}(\overline{u}Db) = 0 \tag{5.9}$$

where $\overline{u}$ is a depth-averaged horizontal component of the velocity vector and τ_x^w is a horizontal component of the wind stress.

Using these equations, Oey *et al.* (1985) defined a variable width river along a (single) uniform grid cell width (see reference for more detailed explanation). The parameter, b, changes according to the actual width of the river and can be greater or less than unity. The modifications used by Oey *et al.* (1985), however, are not part of the standard package of subroutines in the ECOM-si model, and therefore requires significant programming effort to implement. As such, other modeling techniques have been pursued in this thesis, as discussed in Section 5.2.1.

5.2 Model Inputs

5.2.1 Model Grid

The model's grid is input from a *model_grid* file that defines grid cell size (i.e., width, height, and depth), grid cell coordinates, and, if desired, the angle from due east. This last option exists for curvilinear grid layouts and for uniformly oriented rectangular

grids.

A grid for the New Bedford circulation model has been developed using NOAA Navigational Chart #13232 (NOAA 1991) to map harbor geometry and bathymetry. The New Bedford Harbor geometry has been discretized and mapped onto a simplifed non-uniform cartesian grid, as shown in Figure 5-1. Figure 5-2 shows the model bathymetry. The model's water surface area shows good agreement with measurements by ASA (1986). For this study, a 16 (ξ_1) by 25 (ξ_2) by 10-σ layer model domain has been developed. Grid spacing in the ξ_1 (east-west) direction has been held fixed at 100 meters for all grid cells, and ξ_2 (north-south) spacing varies from 100 to 600 meters. For the majority of the harbor geometric features, constrictions, and proposed confined disposal facilities, a 100 meter horizontal grid pattern provides adequate resolution; exceptions, discussed later in this section, occur at constrictions in the harbor such as the Hurricane Barrier, Coggeshall Street Bridge, and the I-195 Bridge. To account for non-uniform grid spacing, the mixing coefficients in the ECOM-si model vary proportionally to maintain a uniform grid Reynolds number (Blumberg, 1991). CDFs are modeled by simply filling in water cells to make them land cells. The grid provides sufficient detail in the locations of the potential contained disposal facilities (CDFs) to investigate the sensitivity of the harbor model to the siting of the CDFs. The locations of the CDFs are shown in Figure 1-3; CDF grid #1 is shown in Figure 5-3, and CDF grid #2 is shown in Figure 5-4.

Time Step Limitations The dimensions of a grid cell (e.g., length, width, and depth) are important because they control the internal time step of the model according to the Courant-Friedrichs-Levy (CFL) criteria, where the time step, $\Delta t(I, J)$, at each grid cell (I, J), is given by the following equation:

$$\Delta t(I,J) = \frac{0.5}{\sqrt{gH(I,J)\left(\frac{1}{(H_1(I,J))^2} + \frac{1}{(H_2(I,J))^2}\right)}} \tag{5.10}$$

where, g = gravity; $H(I, J)$ = depth of grid cell (I, J) in meters; $\sqrt{gH(I,J)}$ = speed of the gravity wave over depth H; $H_1(I, J)$ = grid cell (I, J) width in meters in ξ_1

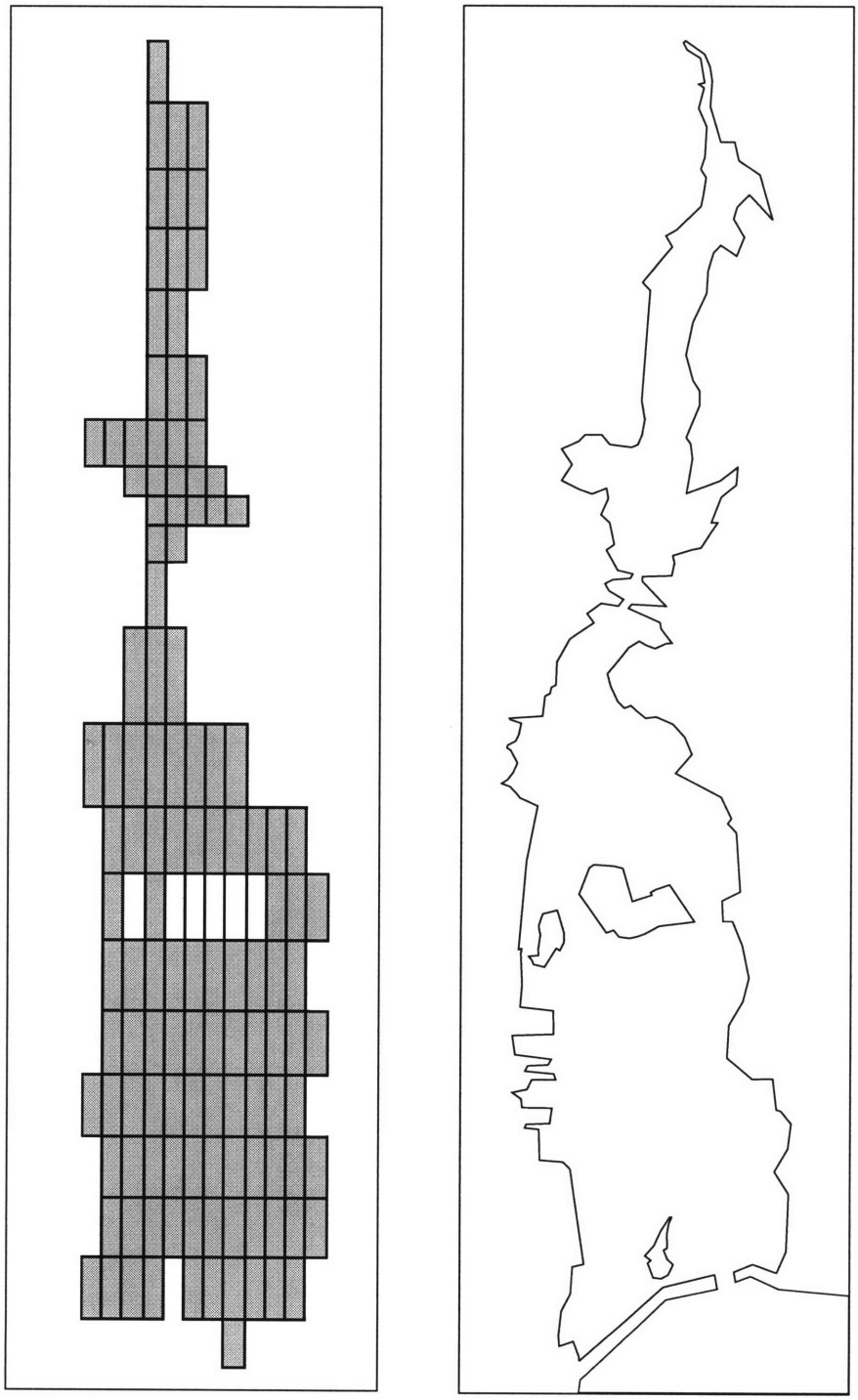

Figure 5-1: **New Bedford Harbor Model Grid**

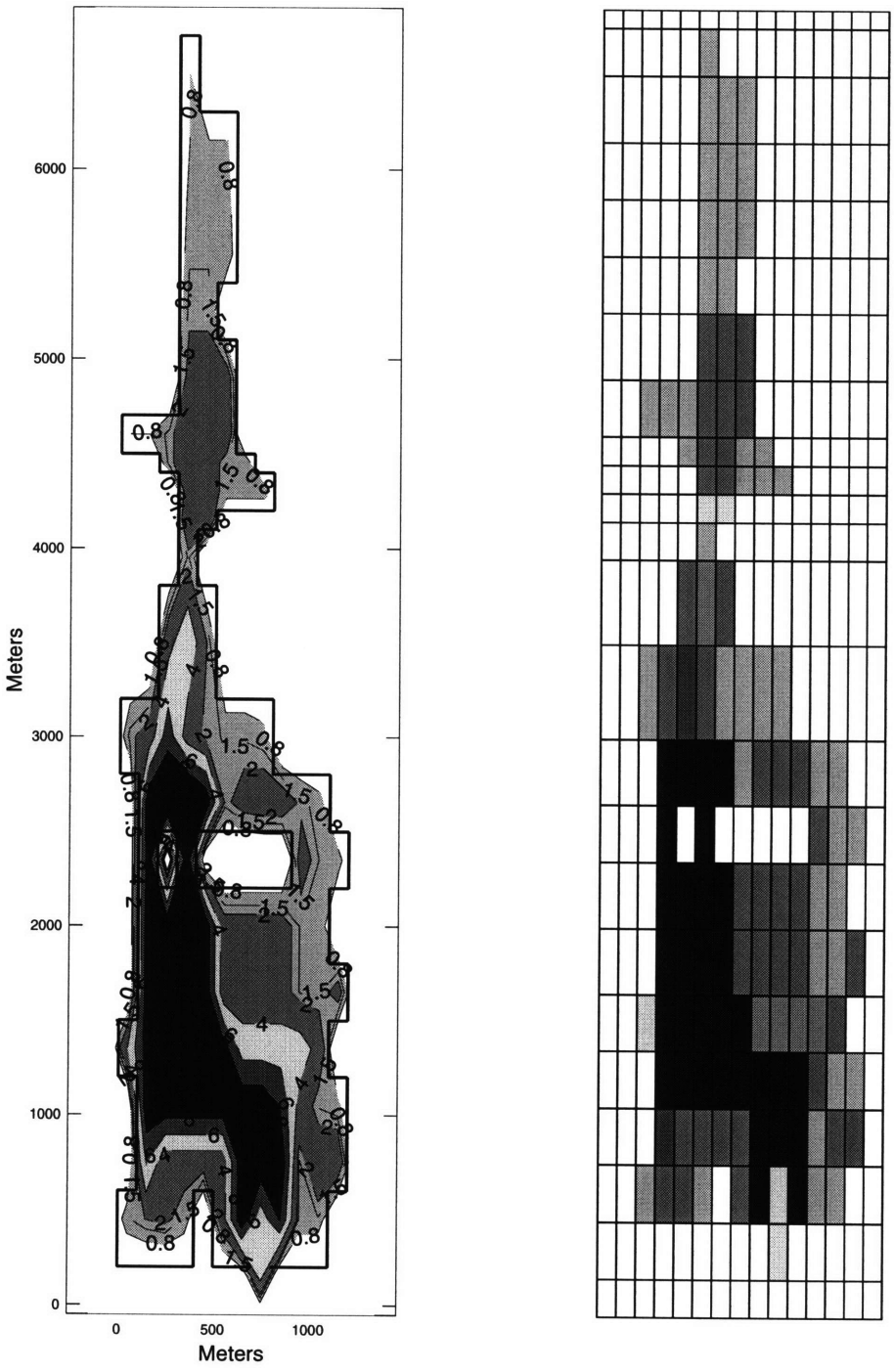

Figure 5-2: **New Bedford Harbor Model Bathymetry**

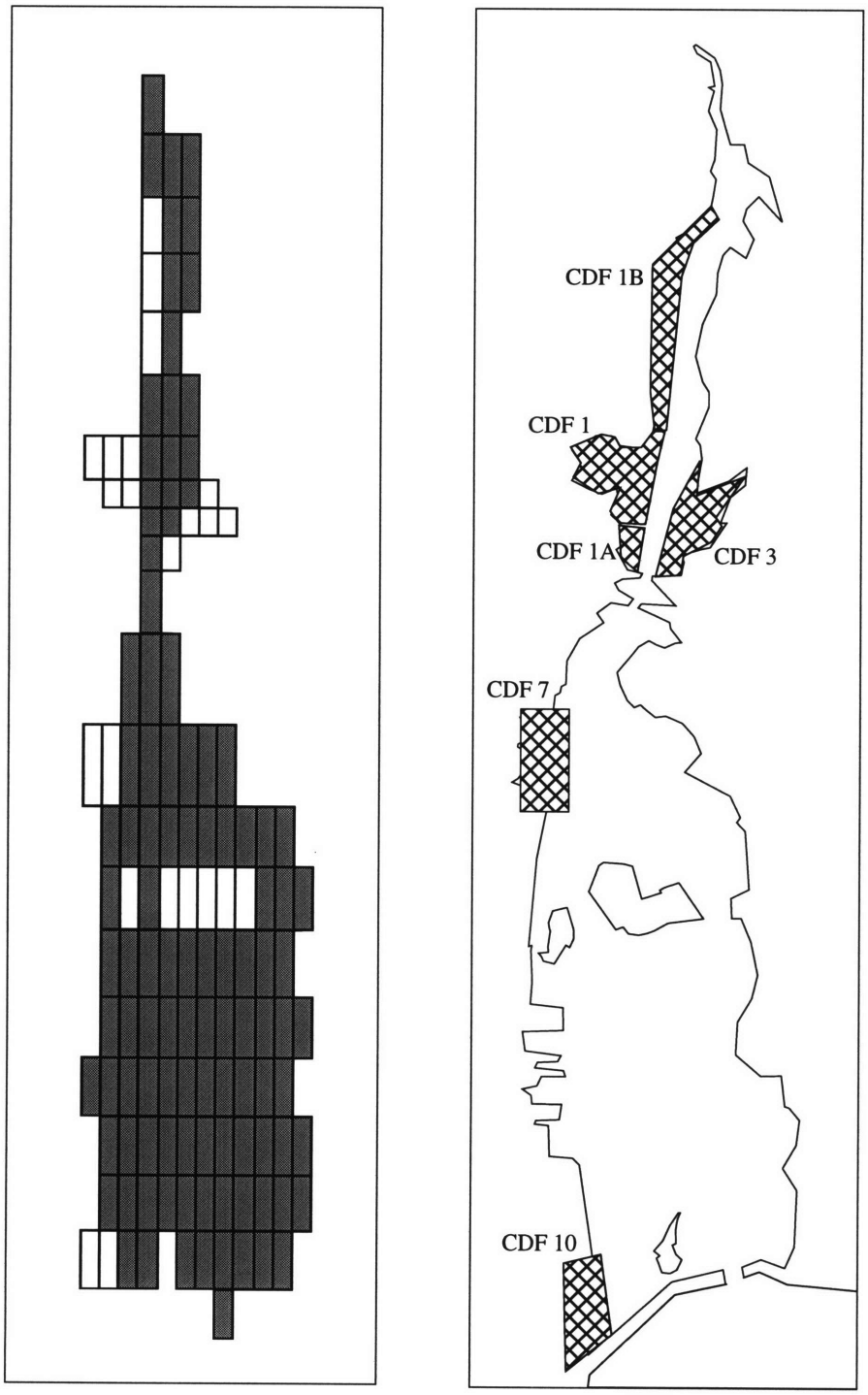

Figure 5-3: **New Bedford Harbor Model CDF Grid #1**

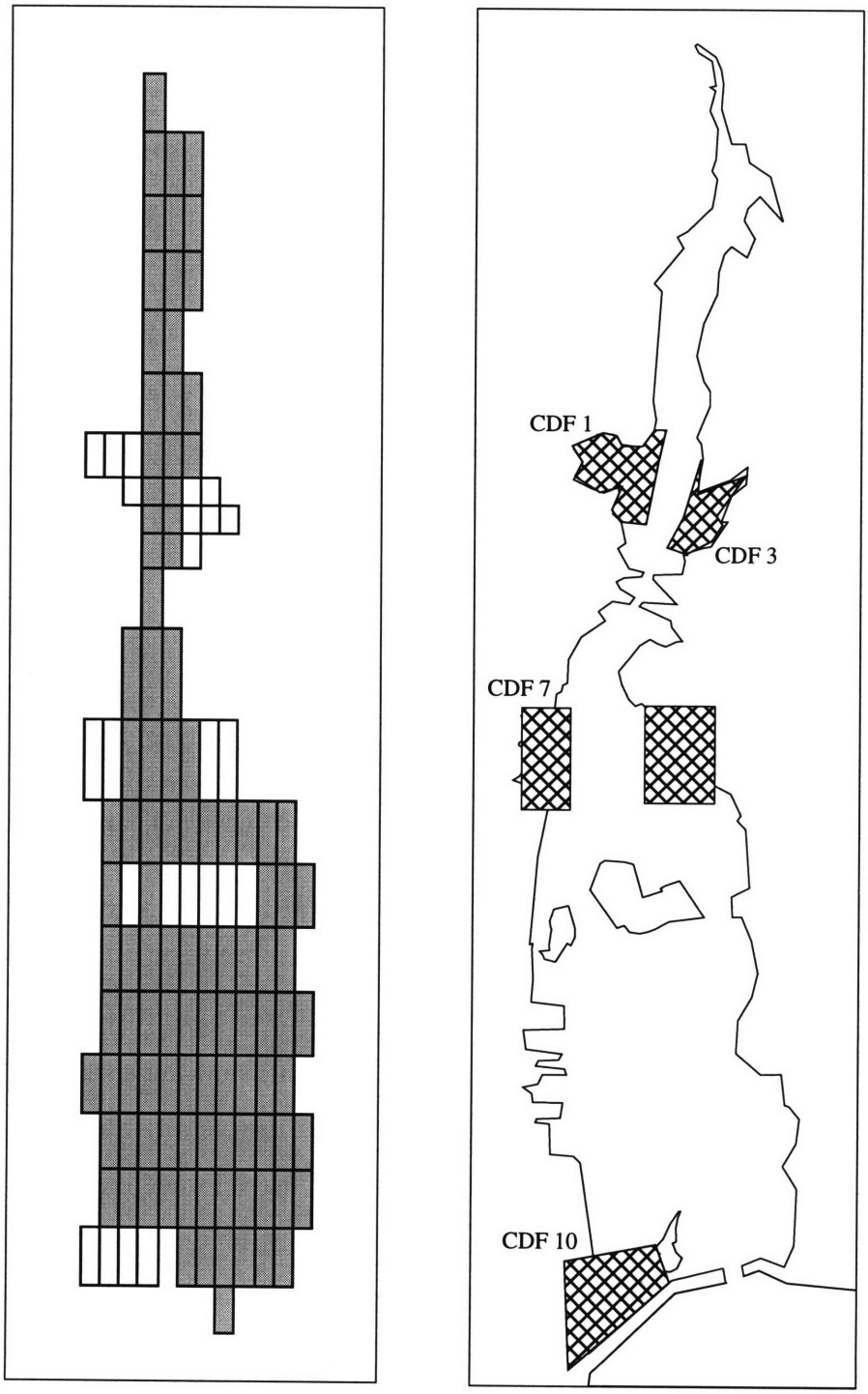

Figure 5-4: **New Bedford Harbor Model CDF Grid #2**
CDF Arrangement #2 removes CDF 1b from the upper estuary, shrinks CDF 1 slightly, increases CDF 10, and adds an additional CDF north of Pope's Island.

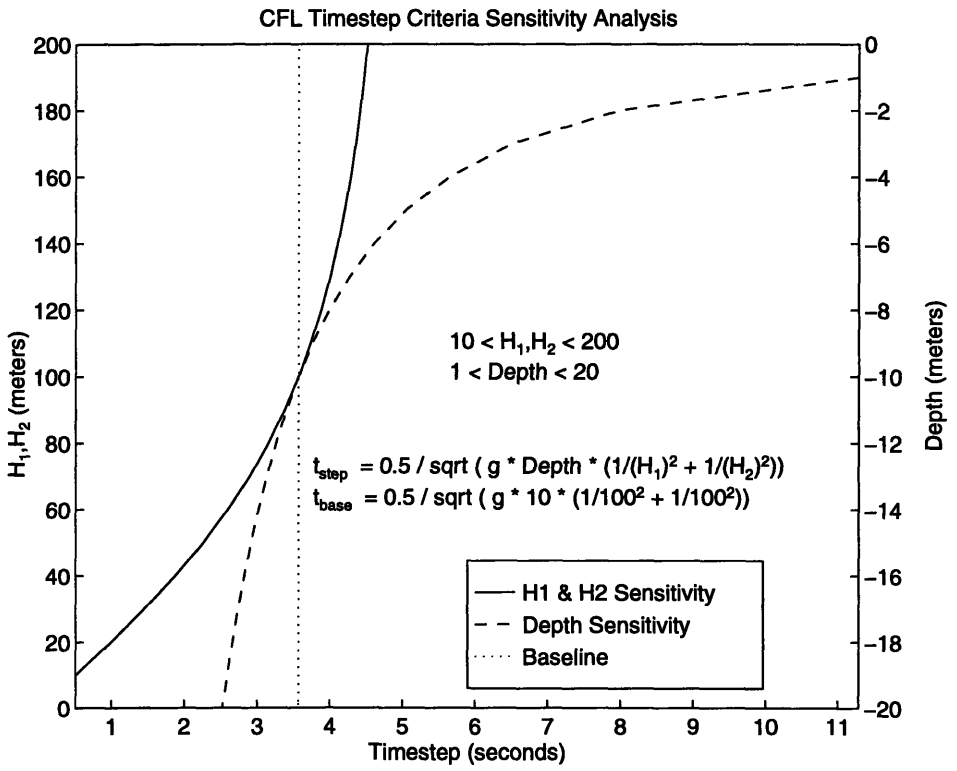

Figure 5-5: **CFL Timestep as a function of depth and width**
Holding H_1 (or H_2) and the depth constant at 100 and 10 meters, respectively, and varying H_2 (or H_1) between 10 and 200 meters results in the solid curve. The dashed curve results from holding both H_1 and H_2 constant at 100 meters and varying the depth between 0 and 20 meters. Dotted line represents a baseline grid cell with dimensions 100 x 100 x 10 meters

direction; and $H_2(I, J)$ = grid cell (I, J) width in meters in ξ_2 direction.

Figure 5-5 is a sensitivity analysis of Equation (5.10) showing a strong dependence on depth, and a weaker dependence on H_1 and H_2. A sample "baseline" timestep value of approximately 3.5 seconds has been calculated given the following parameters: $H_1 = 100$, $H_2 = 100$, and depth = 10 meters; the 10 meter depth of this baseline grid cell is representative of the deepest areas in New Bedford Harbor. For harbor constrictions (e.g., the Coggeshall Street Bridge, the Hurricane Barrier, and the I-195 Bridge), where widths may be 50 meters or less and result in timesteps on the order of 1-2 seconds, model modifications must be made to increase the timestep and model efficiency. Some of these modifications by Oey *et al.* (1985) have been described in

Constriction Location	Width (m) (MLW/MHW)	Depth (m) (MLW/MHW)	Δt from Eqn. 5.10 with $\xi_1 = 100\ m$
CSB	19/ N/A	2.6*/3.9*	1.85/1.51
I-195	19/43^{++}	5.1/6.5^{++}	1.32/2.47
HB	46/46	9.1/10.4*	2.21/2.07

Table 5.1: **New Bedford Harbor Constriction Dimensions**
Coggeshall Street Bridge (CSB), I-195 Bridge, Hurricane Barrier (HB). Depths estimated from 1989 NOAA Navigational Chart. *Estimate. $^{++}$From ASA (1986).

Section 5.1.1, but other techniques have been employed, as discussed later.

Model Grid Modifications For the smaller constrictions in the harbor, modifications were made to the model geometry and/or bathymetry to maximize the CFL timestep (from Eqn. 5.10). As previously mentioned, the Coggeshall Street Bridge (CSB), the Hurricane Barrier, and the I-195 Bridge have openings with widths of less than 50 meters; their dimensions are given in Table 5.1. An ASA (1986) survey of the I-195 channel (at MHW) can be seen in Figure 5-6.

The cross-sectional areas of the I-195 opening at MHW and MLW are approximately 183 m^2 and 176 m^2, respectively, or about 180 m^2 on average. Because this thesis is concerned with changes in circulation patterns and velocities resulting from the siting of CDFs along the shoreline, it is important that the model preserve the cross-sectional area so that the relation for one-dimensional channel flow, $V = Q/A$, also remains unchanged, where V, the velocity from flow rate Q through cross-sectional area A.

With this cross-sectional area restriction, another method of representing narrow waterways, in addition to methods presented by Oey *et al.* (1985) in Section 5.1.1, is to model them as shallower and wider waterways, thus providing a larger and more efficient timestep. A rectangular approximation of the width and depth of the I-195 Bridge are 30 and 6 meters, respectively, also shown in Figure 5-6 preserving the 180 m^2 cross-sectional area. The equivalent time step, Δt, from Equation (5.10), for this 30 by 60 meter cell is slightly less than 2 seconds. Lumping the two constrictions

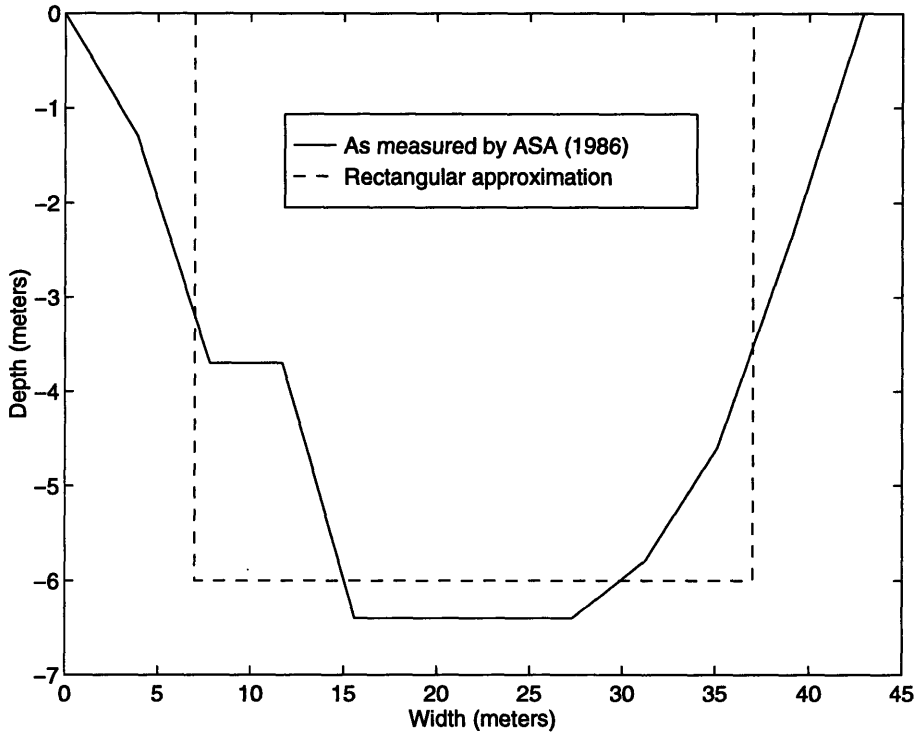

Figure 5-6: **Cross-section of Channel Under I-195 Bridge**
The solid line denotes measurements made in ASA (1986) and dashed line indicates a rectangular (30 by 6 meters) approximation.

of the CSB and I-195 Bridges together into a single 100 meter wide by 1.8 meter deep (and 300 meters long) grid cell, which also maintains the prescribed cross-sectional area, gives a more reasonable timestep of just over 7.5 seconds; these two (lumped into one) constrictions no longer define the limiting timestep.

There may be some consequences from making this type of engineering judgement regarding the model layout. While a single grid of 180 meters wide by 1 meter deep gives a CFL timestep of almost 14 seconds, the effect of bottom friction on the flow (especially on the phase of the tidal flow) may be significant (Galperin and Mellor 1990a), resulting in a reduced or out-of-phase tidal velocity field. Another consequence of the artificial depth of the CSB/I-195 grid cell may be a reduction in the free-surface elevation upstream of the constriction. In other words, the shallow grid cell may impede the traveling tidal wave up the estuary. Model runs indicate that the artifical shallowness of the CSB/I-195 grid cell does not result in a reduction of free-surface elevation amplitude or a change in phase.

Time Step An internal timestep of 4.0 seconds was chosen for the model, limited by a 100 x 300 x 12.3 meter deep grid cell just north of the New Bedford/Fairhaven Bridge (U.S. Route 6); depths are the greatest in this area because it serves as a commercial shipping turning basin.

5.2.2 Model Runtime Input

ECOM-si is driven by a separate data input file that defines meteorological, hydrodynamic, and atmospheric conditions. The *run_data* file contains all runtime information including the time step and output times. It also contains initial and time-variable temperature and salinity conditions, as well as time-variable on-shore discharge information (e.g., a river) and time-variable off-shore discharge information (e.g., an outfall pipe). Open boundary tidal forcing is specified in terms of six tidal harmonics and phases (as discussed in Section 5.1) or a time series of elevations, and meteorological forcing is input in terms of time-variable wind direction and speed.

Hydrodynamic Characteristics Vertical mixing is controlled by a turbulent closure submodel (described in Section 5.1). The background mixing can be adjusted by varying the vertical diffusivity constant, **umol**. Modeling efforts to compare the ECOM-si model to conservative dye tracer studies in Boston Harbor by Chan (1995) indicate that the ECOM-si model does not resolve the vertical mixing of the dye study. Chan varied **umol** between 1 x 10^{-6} and 7.5 x 10^{-5} m^2/s and found that a value of 1 x 10^{-6} m^2/s underpredicted the vertical mixing resulting in a lower-than-observed residence time. While a value of **umol**= 7.5 x 10^{-5} m^2/s resulted in a residence time (3.95 days) close to the dye study (3.75 days), it also did not predict the vertical structure well. As such, Chan (1995) chose a value of **umol**= 5 x 10^{-5} m^2/s, which underestimated the residence time (3.26 days), but predicted the vertical structure better. Given these results, a value of **umol**= 5 x 10^{-5} m^2/s was used for the dye study modeling efforts in this thesis, and a more typical value of **umol**= 1 x 10^{-6} m^2/s was used for modeling harbor circulation. A vertical Prandtl number, the ratio of horizontal viscosity to horizontal diffusivity, of 1.0 is used in all modeling efforts.

A horizontal mixing coefficient, i.e., α in Equation (5.6), of 0.05 and a horizontal Prandtl number of 1.0 are used in all of the modeling efforts. ECOM-si uses a non-dimensional bottom friction coefficient which is one-eighth of the Darcy-Weisbach friction factor; a value of 0.0026 was chosen to reflect estimates by Graber (1987) along with a bottom roughness coefficient, z_o, of 0.003. This bottom roughness coefficient is used to define the bottom friction coefficient according to the following equation:

$$BFRIC = MAX\left[\frac{k^2}{(ln(z/z_o)}, 0.0026\right] \tag{5.11}$$

where $k = 0.4$ is the von Karman constant (Blumberg 1991), and 0.0026 refers to the Graber (1987) estimates.

Model Forcing Initial temperature and salinity conditions have been approximated from conditions described in ASA (1987). River flow has been modeled as a freshwater on-shore discharge with a flow rate of 0.85 m^3/s, the average annual flow rate for the Acushnet River as discussed in Section 4.4. The open boundary has been

forced with six tidal harmonics, the amplitudes and phases of which can be found in Section 4.2. Winds have been mostly neglected in the model because of their variability and lack of detailed data. In the model runs, a 1 m/s wind from the southwest has been used because ASA (1986) wind sensitivity studies indicated that the harbor is sensitive to winds from this direction (see Section 4.3) and the southwest wind also represents a prevailing wind direction.

5.3 Model Output

The model was run using two different output formats. For the dye study model, location (e.g., x, y, z), concentration, and σ-level were output in ASCII text format. Concentration data were processed using MATLAB. For the circulation models, output was produced in a binary *network Common Data Form*, or NetCDF format, developed by the Unidata Program Center. The NetCDF format allows for quick access to 3- and 4-D, e.g., (x, y, z, t), data as well as several operators that allow for efficient processing (Jenter and Signell, 1992). Data processing of elevation, velocity, temperature, salinity fields were performed using MATLAB via MexCDF, a mex-file interface between NetCDF and MATLAB, developed by Chuck Denham of the USGS, Woods Hole, MA, and modified by Jim Mansbridge of CSIRO to increase MexCDF's efficiency. Numerous MATLAB m-file routines have been borrowed from Rich Signell and Chuck Denham of USGS, to analyze the ECOMsi-generated NetCDF data, the output of which included u, v, and w velocity components as well as elevation, salinity, and temperature fields.

Chapter 6

New Bedford Harbor Modeling Results

6.1 Model Simulations

This chapter details the numerical modeling efforts in this thesis including model calibration and results. To validate the model, an ASA (1987) dye study has been simulated; this validation appears in Section 6.3. In the remaining sections, three conditions (baseline, flood, and hurricane) have been modeled with and without confined disposal facilities (CDF). The baseline case refers to normal harbor conditions, while flood refers to excess runoff from the Acushnet River, and hurricane refers to hurricane-force winds (no tidal surge); each case is explained in detail in Section 6.4.1. Each case is examined individually at first and then compared with present-day baseline (i.e., no CDFs) conditions. Criteria against which two cases are compared include changes in the velocity fields and changes in general circulation patterns. The model grid shown in Figure 5-1 has been used for all non-CDF cases, and Figure 5-3 has been used as CDF Case #1 to compare with CDF Case #2 in Figure 5-4.

The first CDF scenario (Figure 5-3) includes CDFs 1, 1a, 1b, 3, 4, 7, and 10 (see Figure 1-3). In addition to CDFs 1, a slighly smaller CDF 3, and CDF 4, the second CDF scenario, CDF Case #2, (Figure 5-4) incorporates a larger CDF 10 in the southwestern corner of the lower harbor as well as a new CDF sited north of

Pope's Island. The latter of these has been modeled based on modeling results from baseline and CDF Case #1 scenarios. These models showed a low-flow condition in this area suggesting that the siting of a CDF would not greatly impact circulation or elevate velocities.

The 16 by 25 by 10-σ models have been run primarily on 115 MHz SUN Sparc 4 and 5 workstations; 24 hour model runtime takes approximately 90 minutes on these workstations. Earlier runs have been run on a 25 MHz DEC Personal Workstation 5000/25; 24 hour model runtime takes approximately 9 hours. All model scenarios have been ramped up to full conditions over the first three (3) hours of runtime, and they have been run for two (2) full days under normal conditions (see baseline explanation) prior to applying extreme forcing (i.e., excessive runoff or winds) for one to two days. Section 6.4.1 details the analyses of a single day of runtime (i.e., the third runtime day) for baseline, flood, and hurricane scenarios.

6.2 Model Calibration

The model has been calibrated to measurements and observations made by previous studies (see Section 2.3) as well as simple model calculations in Section 4.2. Given a reasonable (i.e., for the coarse model grid) comparison between observed and modeled velocity fields, the model will be assumed to be able to adequately predict changes in the circulation patterns caused by changes in the geometry of the harbor (i.e., CDFs). Table 6.1 shows a comparison of the tidal prism and observed velocities from Section 4.2.

In general, agreement is good between the observed and modeled velocities. Both the tidal prism analysis and numerical model appear to overpredict the velocity field in the upper estuary. There is significant variability in the tidal range of New Bedford Harbor, depending on the time of year, which may explain some of the differences. The reasonable agreement among the observed, prism analysis, and modeled values indicates that the model adequately predicts the velocities in several locations within the harbor, and that it should also provide valid velocity fields when geometric changes

Location	Prism Velocity	Max Observed^{++} Ebb	Flood	ECOM-si Ebb	Flood
Aerovox (CDF1b)	14	<5	<5	9.5	6
CDF1 and 3	11	13	15	14	13
Coggeshall St. (I-195)	73	62	91 (60/85)	56	65
CDF7	13	18	18	13	16
US Rte 6	16*	n/a	15-23	10	12.5
Pope's Island East	16*	n/a	n/a	8.5	7.2
Hurricane Barrier	120	75(122,64)	85	51	71

* average velocity of 3 openings; $^{++}$See Section 2.3 for ref.

Table 6.1: **ECOM-si Baseline Tidal Velocity Calibration**

are made to the model (i.e., CDFs).

6.3 Dye Study Validation

6.3.1 ASA Dye Study

A dye study performed by Applied Science Associates (ASA) in December 1986 has been used to validate the New Bedford ECOM-si model. ASA released a Rhodamine-WT dye-tagged continuous disharge of freshwater in the upper estuary near the Aerovox facility (see Figures 1-1 and 2-2). The freshwater was released over an 8.5 day period at a rate of 1580 cm^3/s with a dye concentration of 18.4 ppm (18,417 $\mu g/l$). In total, 1.16 x 10^3 m^3 of freshwater and 21.4 kg of dye were discharged to the surface water during the 8.5 day release. During the study, two storms passed through the area, producing high winds and freshwater runoff from the Acushnet River. One storm occurred during the dye discharge, and the other occurred after the discharge had stopped. Wind and freshwater runoff data from these two storms were recorded; however, the available information was such that it was difficult to determine the duration of the elevated freshwater runoff and winds. Table 6.2 summarizes the available data from the ASA dye study; the wind data has been interpreted from a wind vector plot.

Concentration data were recorded at 45 stations throughout the harbor during low tide for the ASA study. The sampling locations are shown in Figure 2-2 in Section 2.3.2. The sampling times and the corresponding times for low tide can be found in Table 6.3. No sampling occurred on 19 and 25 December 1986 because of unsafe boating conditions during the two storms. All times are given in Eastern Standard Time (EST).

6.3.2 Simulated Dye Study

The ASA dye study was simulated in the ECOM-si model using an offshore discharge to the surface water ($\sigma = 1$) with a flow rate of 1580 cm^3/s, a salinity of 0 ppt, and a conservative tracer concentration of 18,417 $\mu g/l$, and a vertical diffusivity constant, **umol**, of 5 x 10^{-5} m^2/s after (Chan 1995). These values provide a total mass of the tracer in the model simulation that is equal to that of the dye study. The dye was discharged for 8.5 days under minimal meterological forcing. ASA (1987) does provide wind vector plots, total rainfall, and flow rates for the Acushnet River, but lack of specific time series precludes an accurate simulation. Wind and runoff effects were not incorporated into the model for this reason. The exclusion of these forcings are important to note because they influence the dye study and resulting residence time of the estuary as discussed in Section 4.5. Figure 6-1 shows the build-up and decay of the modeled dye study.

Figures 6-2 to 6-13 show the comparisons between the model and the ASA study for 15 to 28 December 1986; ASA observations at 10 locations appear as bold values

Start/End (1986)	Wind (m/s)	Rain (cm)	Runoff (m^3/s)
Dec. 18, 14:00 EST Dec. 19, 12:00 EST	12.5 to SW, ~14 h 6.0 to SSE, ~10 h	5.3	3.7
Dec. 24, 24:00 EST Dec. 25, 09:00 EST	7.5 to NE, ~8 h 10 m/s N, ~6 h 7.5 m/s NE, ~6 h 15 m/s NE, ~1 h	2.2	1.5

Table 6.2: **ASA (1987) Wind and Runoff Data from Dye Study**

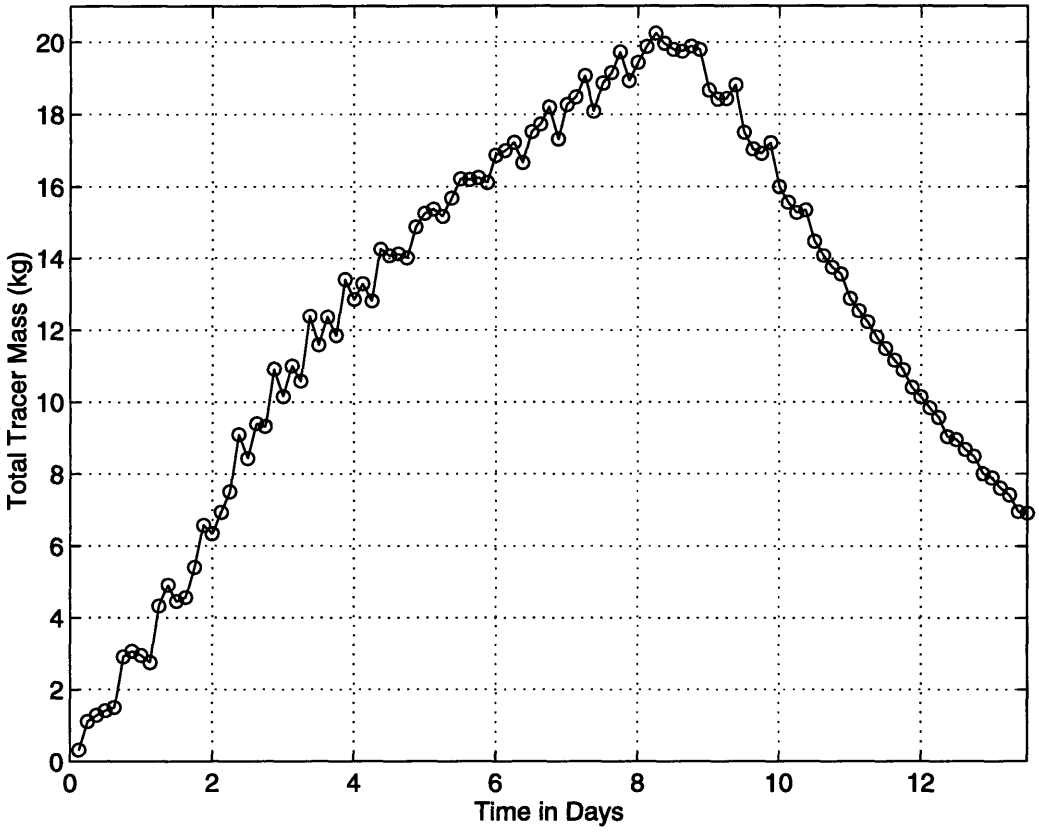

Figure 6-1: **Simulated Dye Study**
Build-up over 8.5 days, decline over 5 days

Day of December 1996	Sampling Time (EST) Start Time	Stop Time	Time of Low Tide in Newport,RI*
15	1140	1224	1302
16	1205	1548	1330
17	1330	1630	1402
18	1300	1724	1434
19	-	-	1506
20	1440	1800	1543
21	1430	1810	1543
22	1430	1905	1705
23	0535	0920	0520
24	0522	0955	0624
25	-	-	-
26	0630	1058	0840
27	0625	0940	0949
28	0750	1150	1052
29	1030	1345	1151

Table 6.3: **ASA Dye Study Sampling Times (ASA 1987)**
***New Bedford low tide approximately 12 minutes later**

over the model's concentration contours. The ten ASA sampling locations were chosen at key points in the harbor to provide an indication of the observed concentration field. These ten locations correspond to ASA (1987) sites 1, 7, 10, 18, 22, 27, 32, 33, 35, and 44 (see Figure 2-2).

The first three observations (Figures 6-2 to 6-4) agree quite well, and the model approximates concentrations accurately at all locations in the harbor. On the fourth day of observation (Figure 6-5), however, differences can be seen in the form of higher-than-observed (roughly doubled) concentrations in the western half of the lower harbor and lower-than-observed concentrations in the eastern half. This may be a result of a no-return-flow regime on the open boundary (the hurricane barrier), which imposes a zero-concentration on incoming water. The model appears to under-predict concentrations through the opening on the eastern side of Pope's Island, though north of Pope's Island, agreement is good. Concentrations through the Coggeshall Street Bridge are over-predicted (almost four times) as well, possibly due to the artificially shallow depth through this region. Examination of the concentration field over the

depth of the Coggeshall Street Bridge cell reveals a fairly uniform value within 1 ppb over $\sigma = 1$ to $\sigma = 10$. Figure 6-6 is similar to Figure 6-5, but agreement in the lower harbor is generally better with the exception of the Coggeshall Street Bridge where concentrations are still four times higher than the observed values.

Figure 6-7 is a snapshot the day after the first storm on 19 December 1986. The elevated runoff rates from the rainfall are manifested in decreased upper estuary observed concentration fields. The storm could also explain the higher concentrations observed (3.88 ppb) south of the source (1.97 ppb), driven downstream by the storm's south-directed winds (see Table 6.2). Lower harbor values have increased, but only slightly since the previous sampling time. The effect of the storm on the lower harbor is seen in the next observation (Figure 6-7), when concentrations remain mostly unchanged and do not increase as one might expect. In the upper estuary, concentration fields are in better agreement as conditions return to normal (i.e., no wind or rain). In both Figures 6-6 and 6-7, the concentrations in the western half of the lower harbor are approximately 50% of the observed values while the eastern half conentrations are approximately 200% that of the observed values. This pattern suggests that the concentration is not effectively moving through the opening on the eastern side of Pope's Island, and artificially shallow bathymetry on the east side of Pope's Island may be the controlling factor. Figures 6-8 and 6-9 show good agreement north of the New Bedford/Fairhaven Bridge. No ASA data were collected in the upper estuary because of shallow water depths during the observations in Figure 6-9. The northernmost recorded value (5.02 ppb), the value recorded at the Coggeshall Street Bridge (2.39 ppb), and the value north of Pope's Island (1.73 ppb), appear to be in good agreement with the simulated concentration field. In both figures, concentrations in the lower harbor still differ by a factor of two from the observed values.

Figure 6-10 is the first observation (approximately six hours) after termination of the dye discharge. The simulated concentration field in the upper estuary varies greatly from 2 to 12 ppb. These values are in contrast to the observed values of 0.74, 3.46, and 3.31 ppb. The simulated concentrations do not decrease as rapidly as the observed concentrations immediately following the cessation of the dye input.

Concentrations in the lower harbor, while not exact, approximate the observed data fairly well. Figure 6-11 shows the concentration field the day after the second storm which occurred on 25 December 1986. As expected, the simulated concentrations are an order of magnitude larger than the observed values in the upper estuary, with concentrations of 2 to 3 ppb compared to ASA's values of 0.22, 0.29, and 0.28 ppb. This difference is primarily due to excess runoff from the second storm event. Observed concentrations in the lower harbor appear to drop by 50% or more except at the hurricane barrier where the concentration increases four-fold from 0.12 to 0.52. After the first storm, the observed concentration field returned to predicted levels because the dye discharge continued long after the storm. Because the second storm occurred after the termination of the dye injection, it was impossible to regain predictable concentration levels as is seen in the remaining figures.

Figure 6-12 shows slightly better agreement in the lower harbor than Figure 6-11; observed values have decreased significantly due to the freshwater dilution from the storm. Upper estuary values, however, are still an order of magnitude higher than the observed values which have changed little since the previous measurement. Figure 6-13, the final comparison snapshot, shows fairly good agreement in the lower harbor; however, the upper estuary concentrations are still an order of magnitude higher that the observed values.

Figure 6-14 shows concentration time-series of the two dye studies (i.e., ASA and the simulated) at the same ten ASA locations in the harbor as in Figures 6-2 through 6-13. In Figure 6-14, the dotted line represents the modeled dye study while the solid line represents the observed and measured concentrations from the ASA 1986 study. The thin vertical lines approximate the start and end times of the two storms. Figure 6-14 generally shows good agreement between the observed and simulated dye studies; however, clear differences exist. Storms that occurred on the fourth to fifth and ninth to tenth days of the dye study brought excess freshwater runoff to the system and diluted concentrations. These storms can be seen in the ten concentration time-series plots as large decreases in the solid-line observed concentrations near day five, particularly at the upper estuary locations (i.e., 1, 2, and 3). The decreases are

seen later (i.e., day 5-6) in the lower harbor. Following the storm, the concentrations peak around day seven. Because the simulated dye study mimics this build up, it is likely that a smaller tidal range is responsible for the build up. Examination of the tidal elevation for this period verifies that the tidal range was relatively small at just 0.7 meters during this period. As a result, less water is exchanged during the tidal cycle, the dye in the harbor is not diluted as much, which, when combined with additional dye from the discharge, creates a peak in concentration; this peak is seen at all ten locations in Figure 6-14.

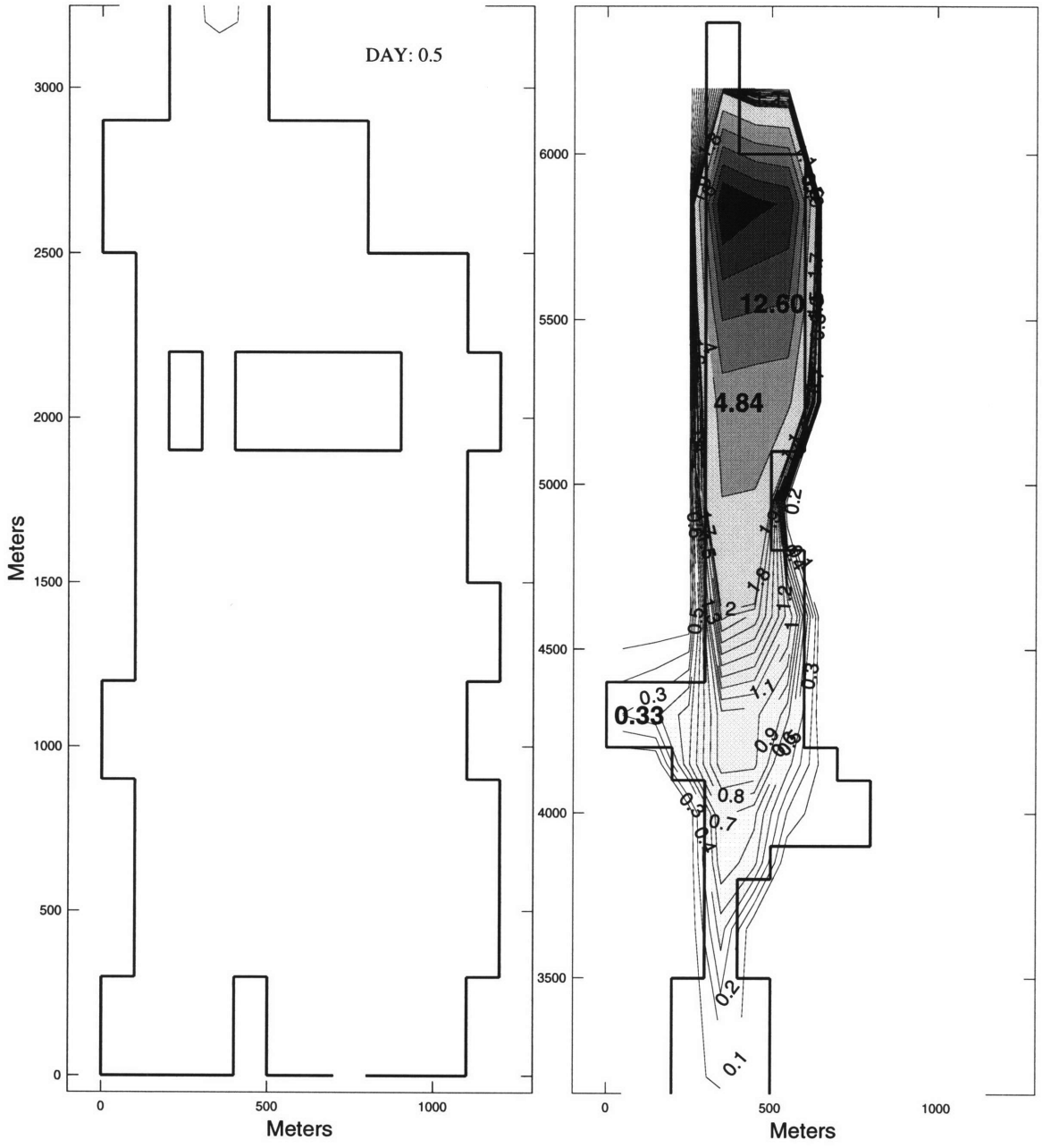

Figure 6-2: **Simulated contours vs. ASA observations: December 15, 1986 Contours are simulated dye study. Values in bold are ASA (1987) observations**

Figure 6-3: **Simulated contours vs. ASA observations: December 16, 1986 Contours are simulated dye study. Values in bold are ASA (1987) observations**

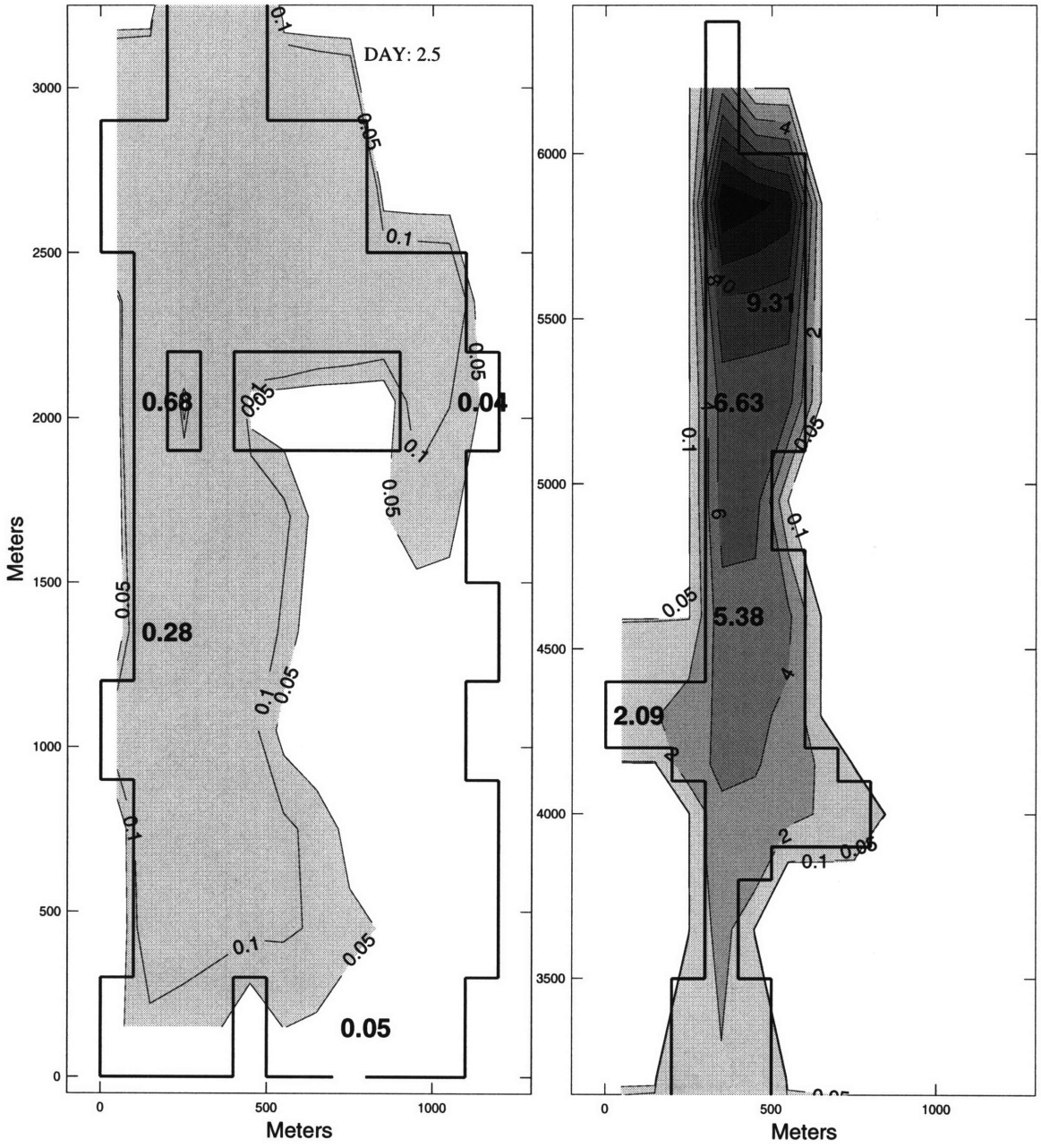

Figure 6-4: **Simulated contours vs. ASA observations: December 17, 1986 Contours are simulated dye study. Values in bold are ASA (1987) observations**

Figure 6-5: **Simulated contours vs. ASA observations: December 18, 1986 Contours are simulated dye study. Values in bold are ASA (1987) observations**

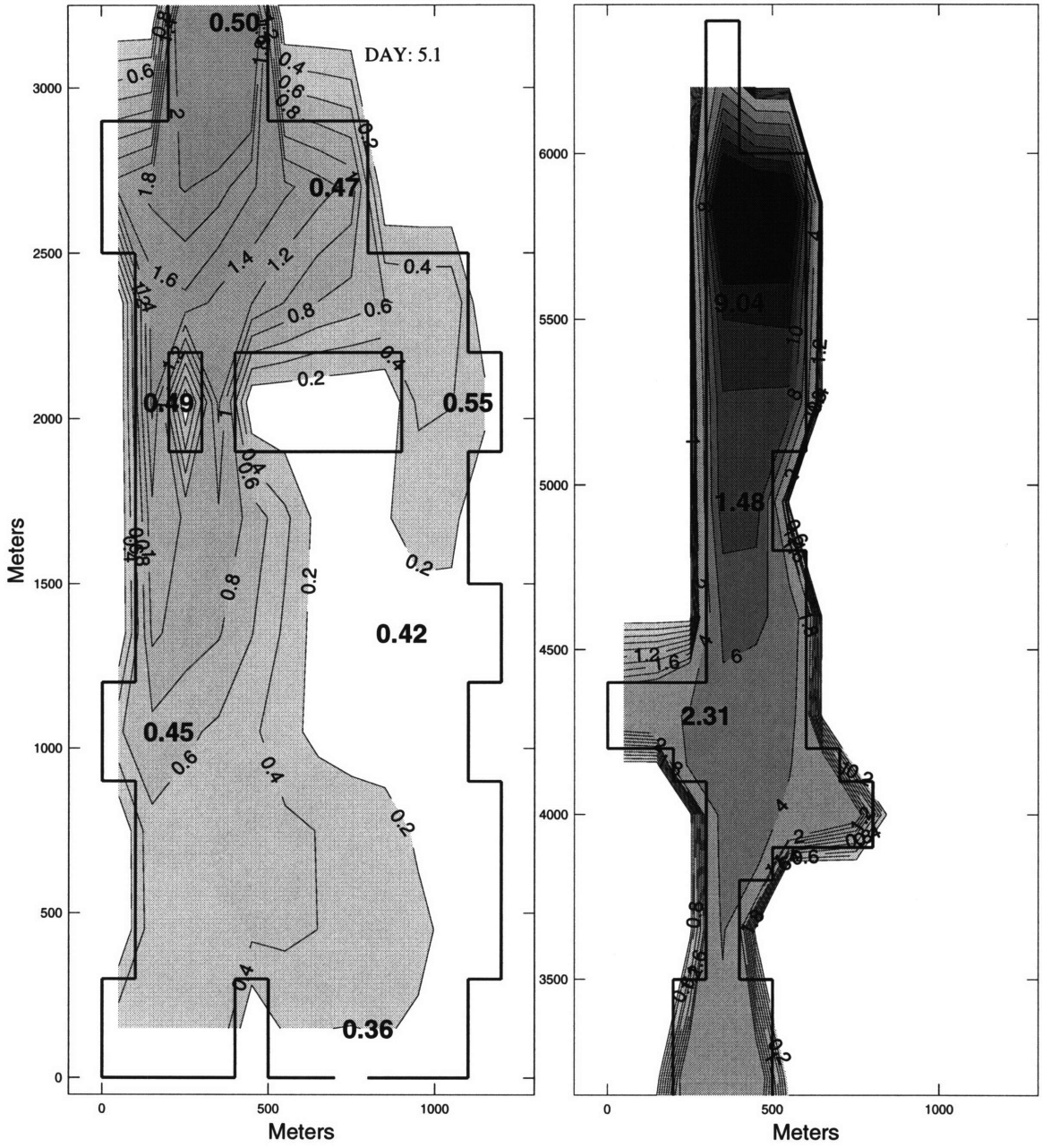

Figure 6-6: **Simulated contours vs. ASA observations: December 20, 1986 Contours are simulated dye study. Values in bold are ASA (1987) observations**

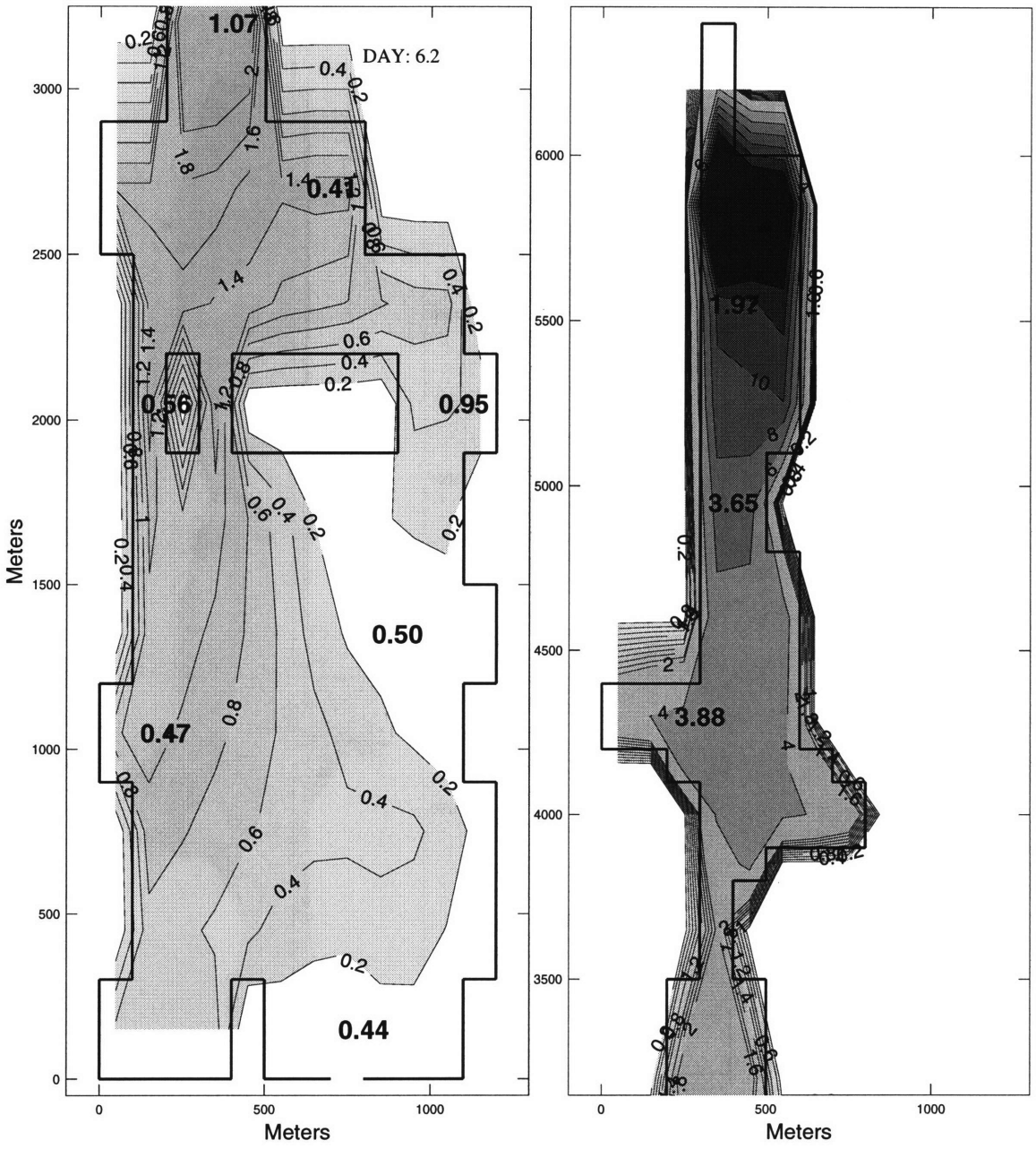

Figure 6-7: **Simulated contours vs. ASA observations: December 21, 1986**
Contours are simulated dye study. Values in bold are ASA (1987) observations

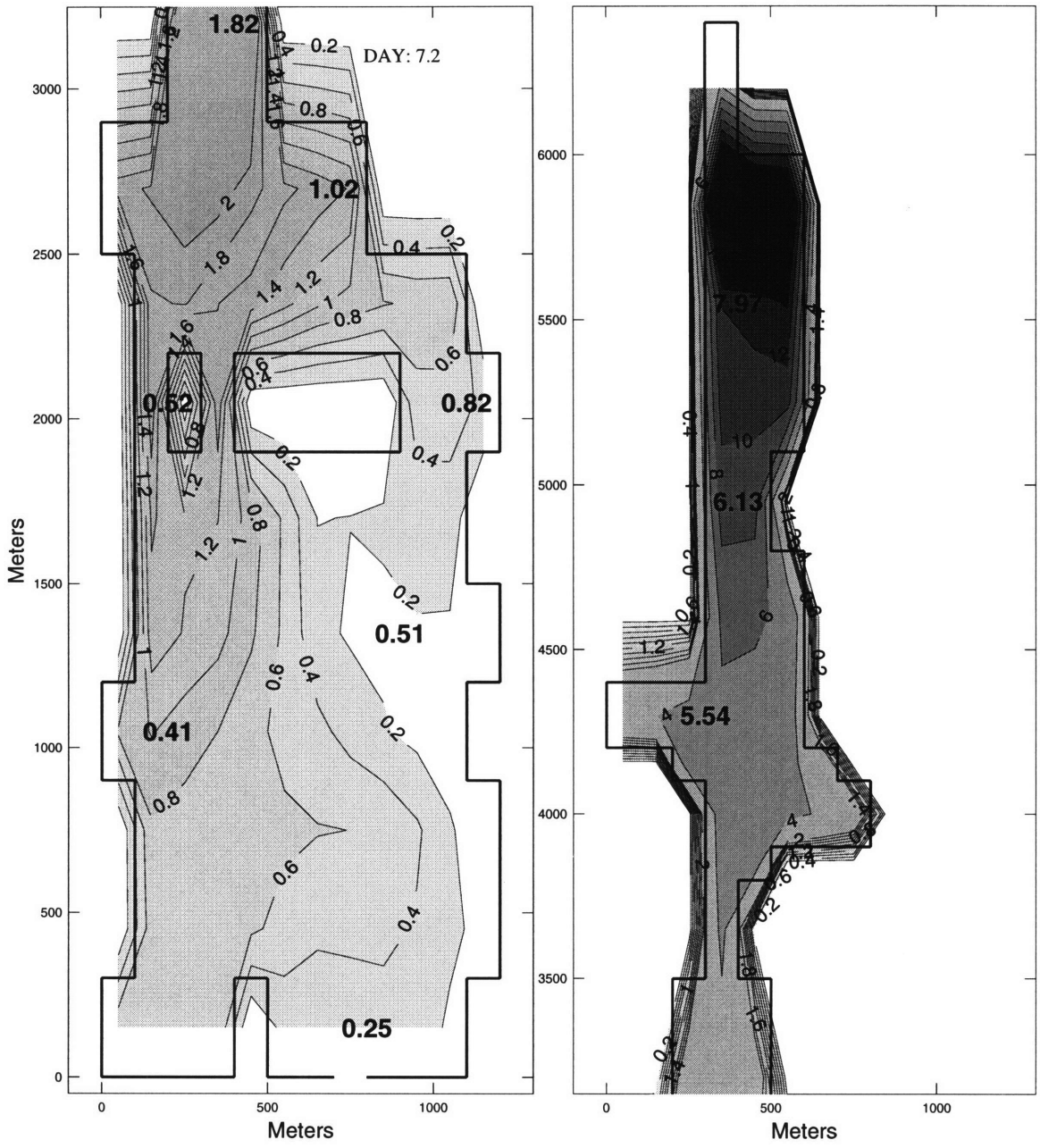

Figure 6-8: **Simulated contours vs. ASA observations: December 22, 1986 Contours are simulated dye study. Values in bold are ASA (1987) observations**

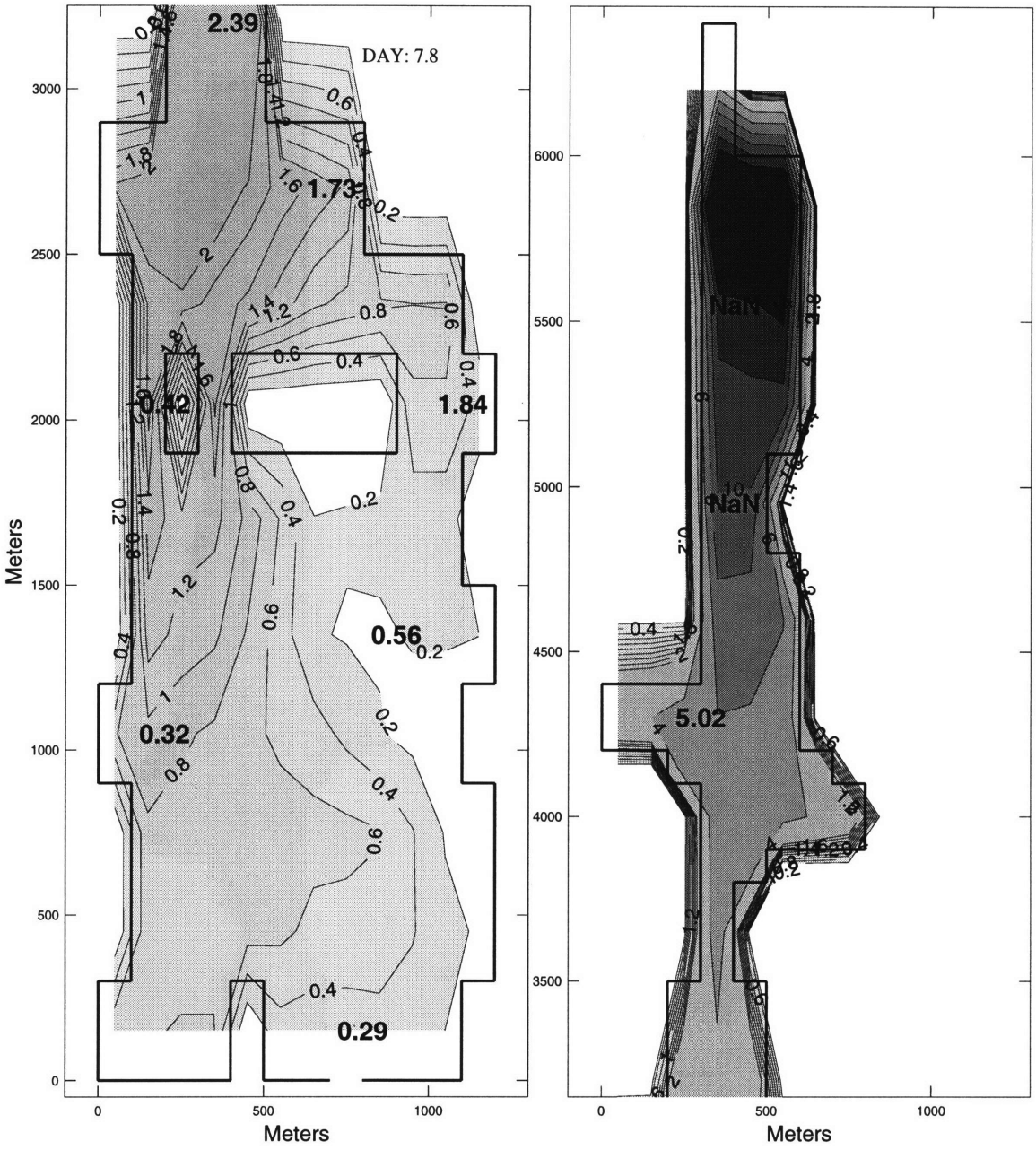

Figure 6-9: **Simulated contours vs. ASA observations: December 23, 1986 Contours are simulated dye study. Values in bold are ASA (1987) observations**

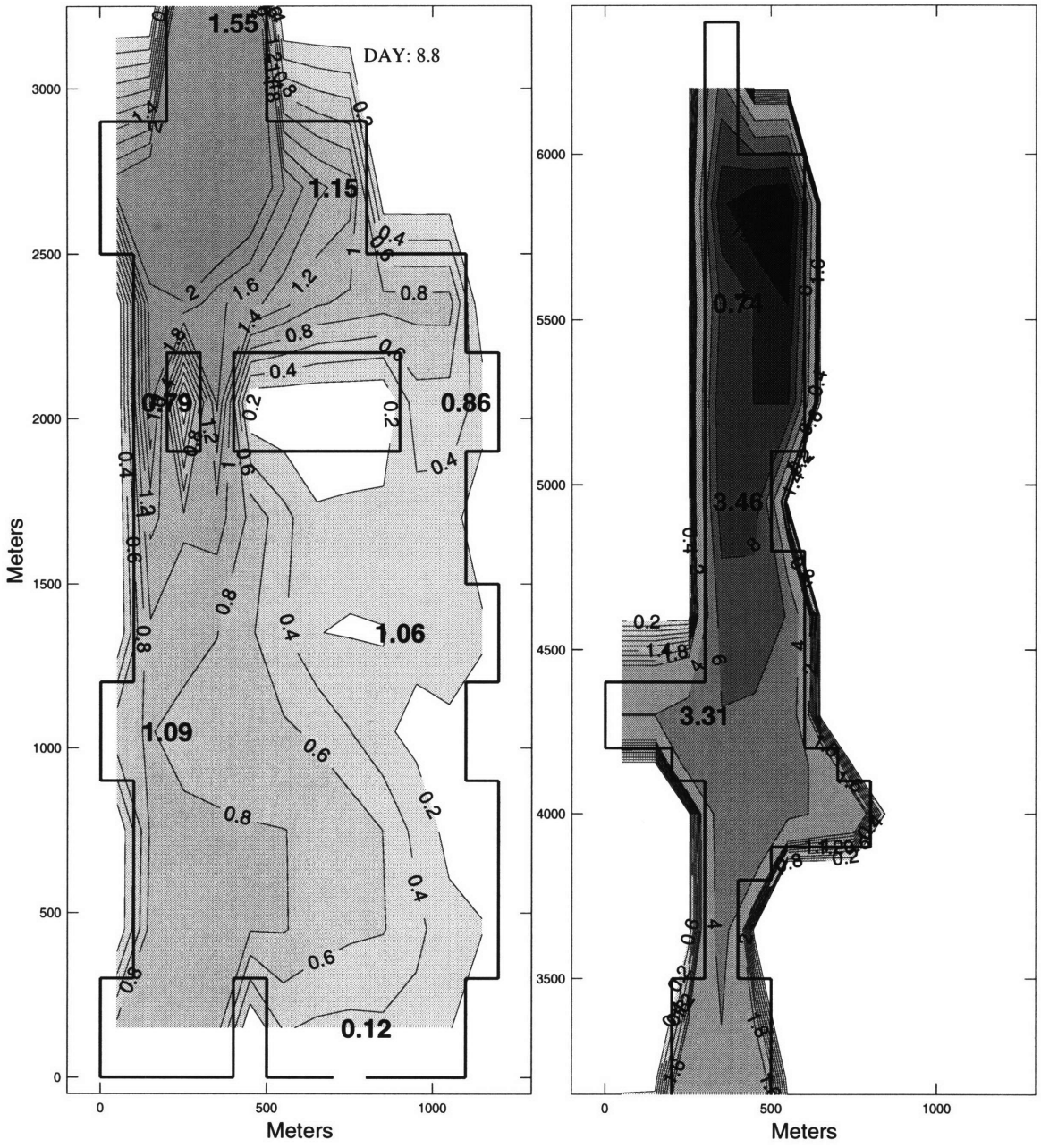

Figure 6-10: **Simulated contours vs. ASA observations: December 24, 1986 Contours are simulated dye study. Values in bold are ASA (1987) observations**

Figure 6-11: **Simulated contours vs. ASA observations: December 26, 1986 Contours are simulated dye study. Values in bold are ASA (1987) observations**

Figure 6-12: **Simulated contours vs. ASA observations: December 27, 1986 Contours are simulated dye study. Values in bold are ASA (1987) observations**

Figure 6-13: **Simulated contours vs. ASA observations: December 28, 1986 Contours are simulated dye study. Values in bold are ASA (1987) observations**

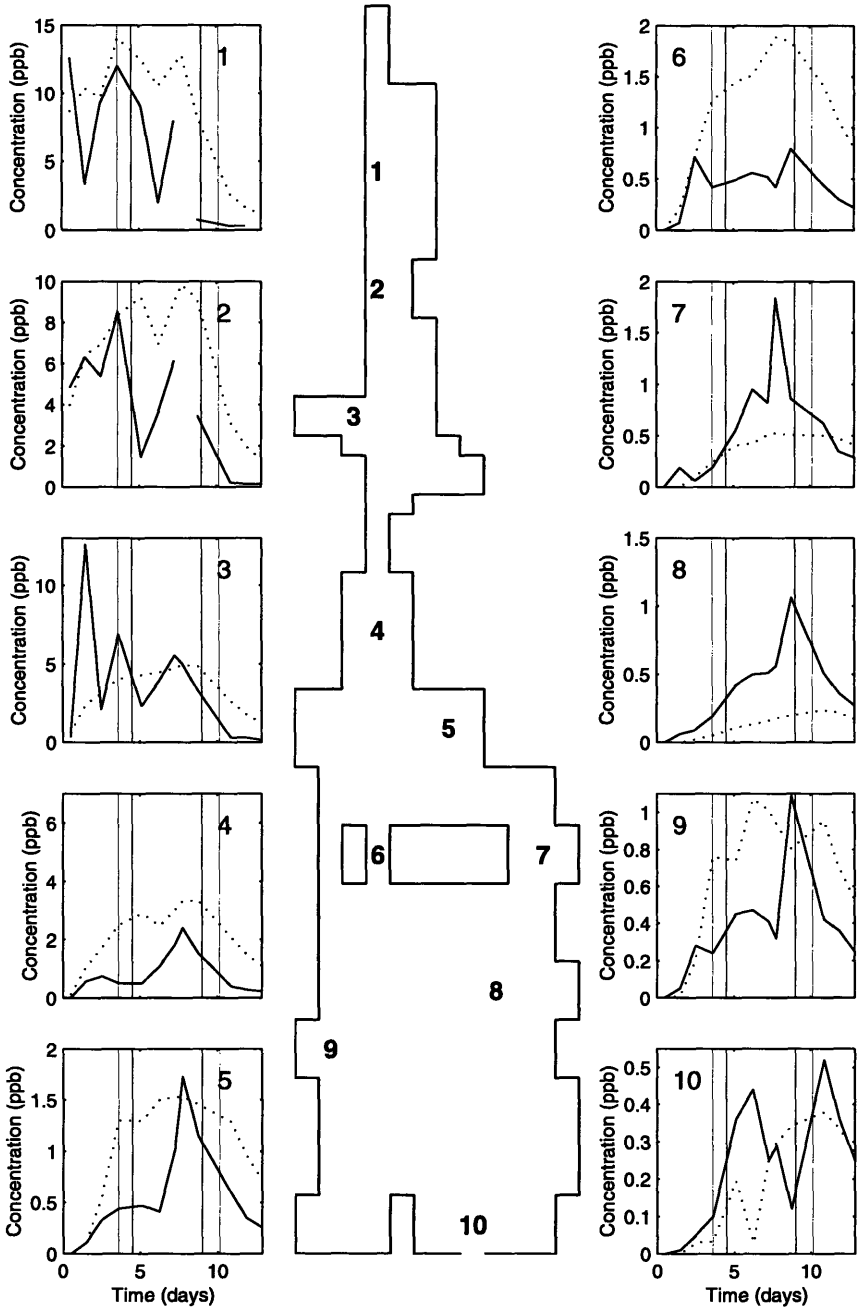

Figure 6-14: **Comparison of ASA dye study and modeled dye study Solid lines indicate the observations from ASA (1987) and dotted lines indicate the simulated dye study concentrations. Vertical lines indicate the approximate start and end times of two storms**

6.3.3 Discussion

While model limitations exist which make exact comparison difficult, agreement between the simulated and observed concentration fields is generally good. Limitations include the somewhat coarse 100 meter grid and bathymetry (as well as artificially shallow areas), the difference in meteorological forcing between the studies, and the no-return regime at the open boundary. Of these limitations, the meteorological differences are probably the most significant, followed by the artificially shallow areas. The no-return regime may have been responsible for diluting lower harbor (perhaps eastern lower harbor) concentrations. Because the horizontal mixing coefficents of the model depend on the horizontal spacing, according to Smagorinsky (1963), these coefficients may be smaller than the values expected for a coastal model with grid sizes on the order of 1-10 km. The simulated dye study clearly shows low horizontal diffusion; this may be an artifact of applying the ECOM-si model to a small estuary.

The model preserves the longitudinal representation of the concentration field fairly well. This argument is supported by comparison of concentrations in the upper estuary and at the hurricane barrier (locations 1 and 10, respectively) in Figure 6-14 which agree well considering different meteorological forcing. The lateral, or cross-estuary, concentrations, however, are consistently under- or overestimated such as at locations (8) and (9), respectively. This discrepancy may be the result of a combination of the limitations (i.e., artificial depths and no-return flow regime). Location (9) in the lower harbor suffers from overestimation of the concentration field by the model, most likely a result of the flow field in this area, where the majority of the tracer-tagged water is directed from the Coggeshall Street Bridge opening down through the New Bedford/Fairhaven Bridge opening on ebb tide. Little water is flushed over the area just north of Pope's Island (location 5) most likely because of shallow areas, resulting in lower concentrations on the eastern side of the lower harbor. To further dilute the eastern harbor concentrations, the flow field from flood tide flushes upward through the opening east of Pope's Island. Figure 6-15 shows the depth-averaged velocity fields on maximum flood and ebb tides. Additional discussion on these figures

can be found in Section 6.1. These circulation effects are better illustrated by the concentration contours in Figures 6-2 through 6-13. These figures show a "tongue" of concentration moving swifly down the western shoreline; equivalent concentrations follow approximately 1.5 days later on the eastern side.

The movement of the simulated tracer through the harbor is helpful in determining the dominant circulation mechanisms. Uniform offsets in concentrations are seen between the simulated and observed dye studies in Figure 6-14 supporting prior evidence that the harbor is primarily tidal-driven. These offsets are seen primarily in the upper estuary where an incoming tide may change the depth and cross-sectional area by a factor of two. As seen in Figure 6-14, an unusually low tide resulted in a peak in concentrations.

6.3.4 Residence Time

A residence time for New Bedford Harbor was calculated using the modeled dye study concentration field. The total mass of the dye was calculated by spatially integrating surface concentrations over the volume. The total dye mass is plotted as a function of time in Figure 6-16 for low tide measurement times and Figure 6-17 for every three hours. Recall that this study used a continuous 8.5 hour dye release. Upon termination of the dye injection, the dye mass declines over a period of several days. For a well mixed estuary, the dye mass should decline exponentially. This exponential decline can be plotted on a natural log scale, and a staight line can be fit to it, the slope of which is the negative inverse of the residence time. Using this method at ASA low tide observation times results in a residence time calculation of 4.6 days. Calculation using all data points (every three hours) after the termination of the discharge results in a residence time of 4.5 days; this latter value introduces less aliasing to the measurement and the low tide measurements provide some smoothing. These values are both two days longer than the ASA dye study residence time calculation of 2.4 days and one day longer than Case's (1998) 3.4 day calculation of residence time from an analysis of the ASA data in Section 4.5. Additionally, the calculated value is roughly twice the value calculated in Section 4.5

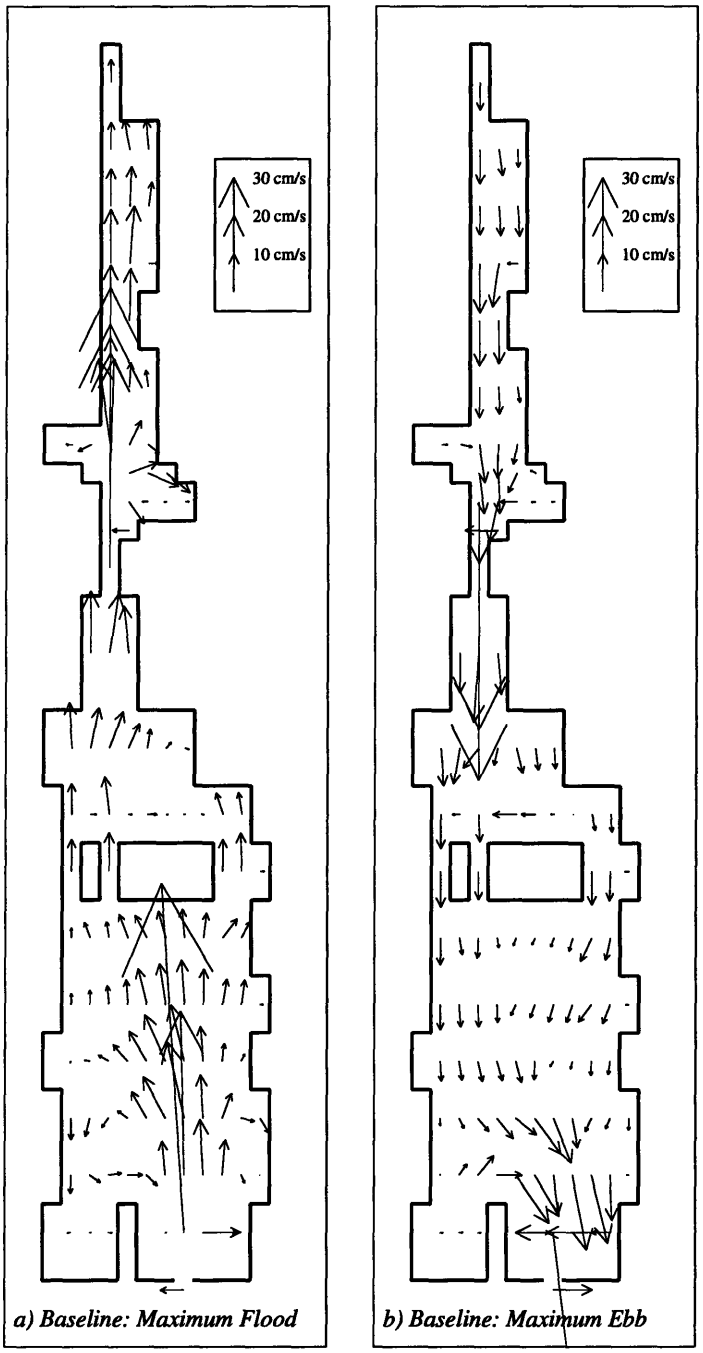

Figure 6-15: **Simulated Depth-Averaged Velocity Fields a) Maximum flood; b)Maximum Ebb**

using the tidal prism method. A value of 4.56 days is, however, within Cochrane's (1992) analysis of the 1991 Aquatec dye study, in which he calculated a residence time of 4±1 days.

As expected the modeled residence time is longer because of missing meteorological data. A no-return regime, however, decreases the model's residence time slightly because tagged volumes of water that normally return on flood tide are replaced by clean, zero-concentration volumes. With these considerations, a residence time of 4.6 days is a reasonable representation of the true residence time of the system.

6.4 Model Results

6.4.1 Baseline

A baseline model scenario has been run to simulate normal, pre-CDF conditions. Normal conditions, in this case, refer to a freshwater flow rate of 0.85 m^3/s from the Acushnet River, normal tidal conditions as described in Section 4.2, and a low wind condition with 1 m/s winds from the southwest.

Flood tide Figures 6-18 and 6-19 show the maximum flood velocity fields under baseline conditions for surface ($\sigma = 1$) and near-bottom ($\sigma = 8$), respectively. Both figures show two hours prior to maximum flood velocity (see Figures 6-18a and 6-19a), maximum flood velocity (6-18b and 6-19b), and two (2) hours after maximum flood velocity (6-18c and 6-19c) for the specified sigma-level. Recall that the maximum flood velocities lead the maximum elevation (high water) by approximately three hours, meaning that Figures 6-18a and 6-19a also represent one hour after flood tide starts (i.e., one hour after low water); Figures 6-18b and 6-19b: mid-flood; and Figures 6-18c and 6-19c: one hour prior to high water.

The one-dimensional tidal prism analysis in Section 4.2.1, predicted extreme velocities for ebb flow at the hurricane barrier and Coggeshall Street Bridge. These extreme velocities can be seen in Figure 6-18b at the bottom and middle center of the flow field. Figures 6-18 and 6-19 indicate a surface return flow in the lower harbor.

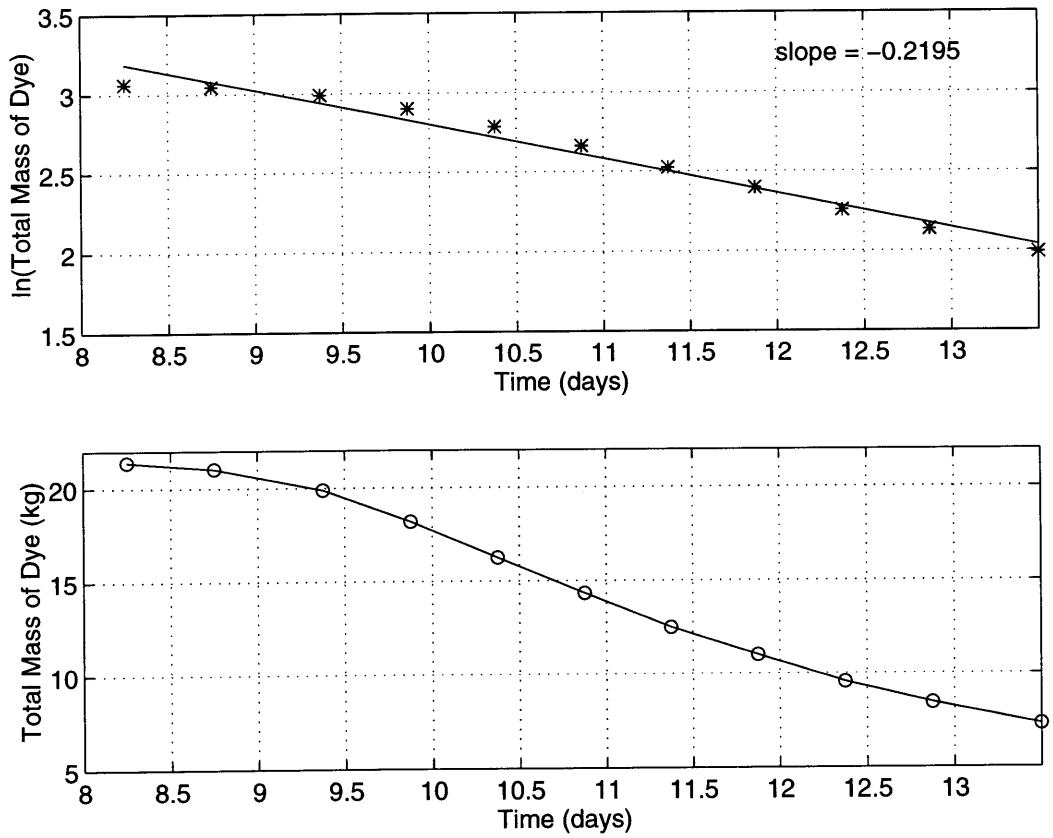

Figure 6-16: **Model-Simulated Total Mass (Low Tide)**

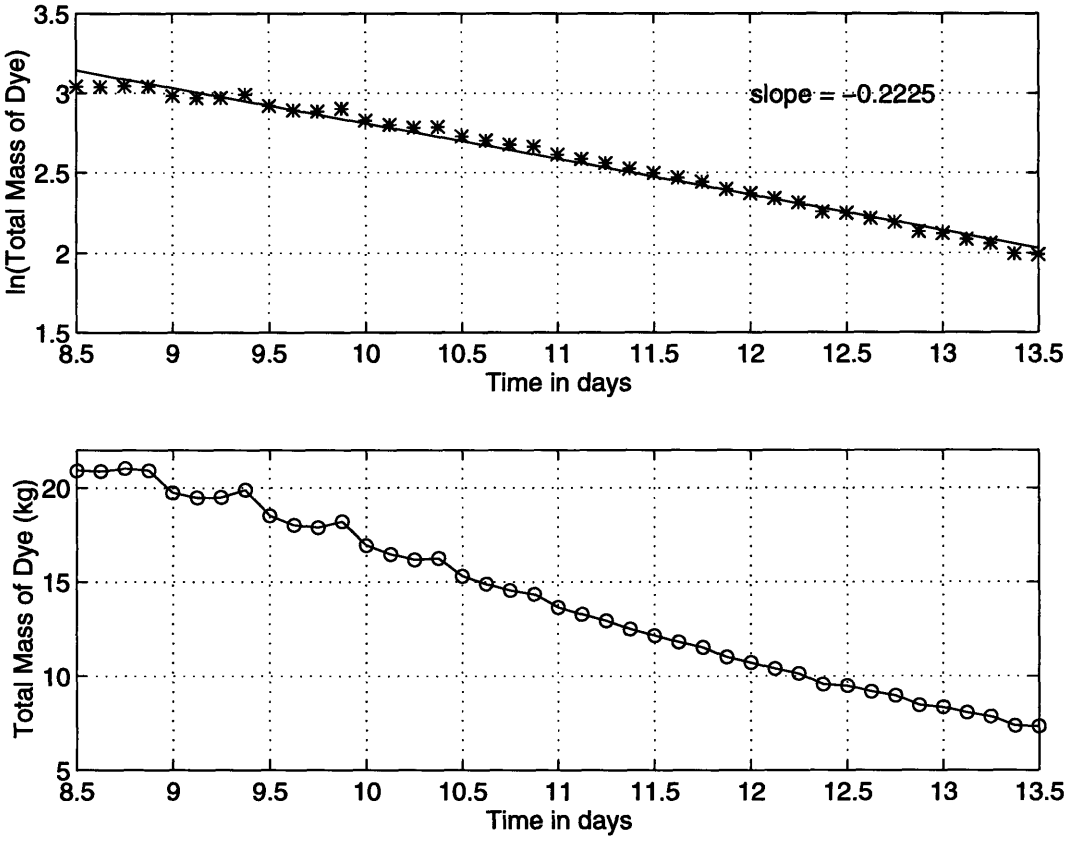

Figure 6-17: **Model-Simulated Total Mass (every 3 hours)**

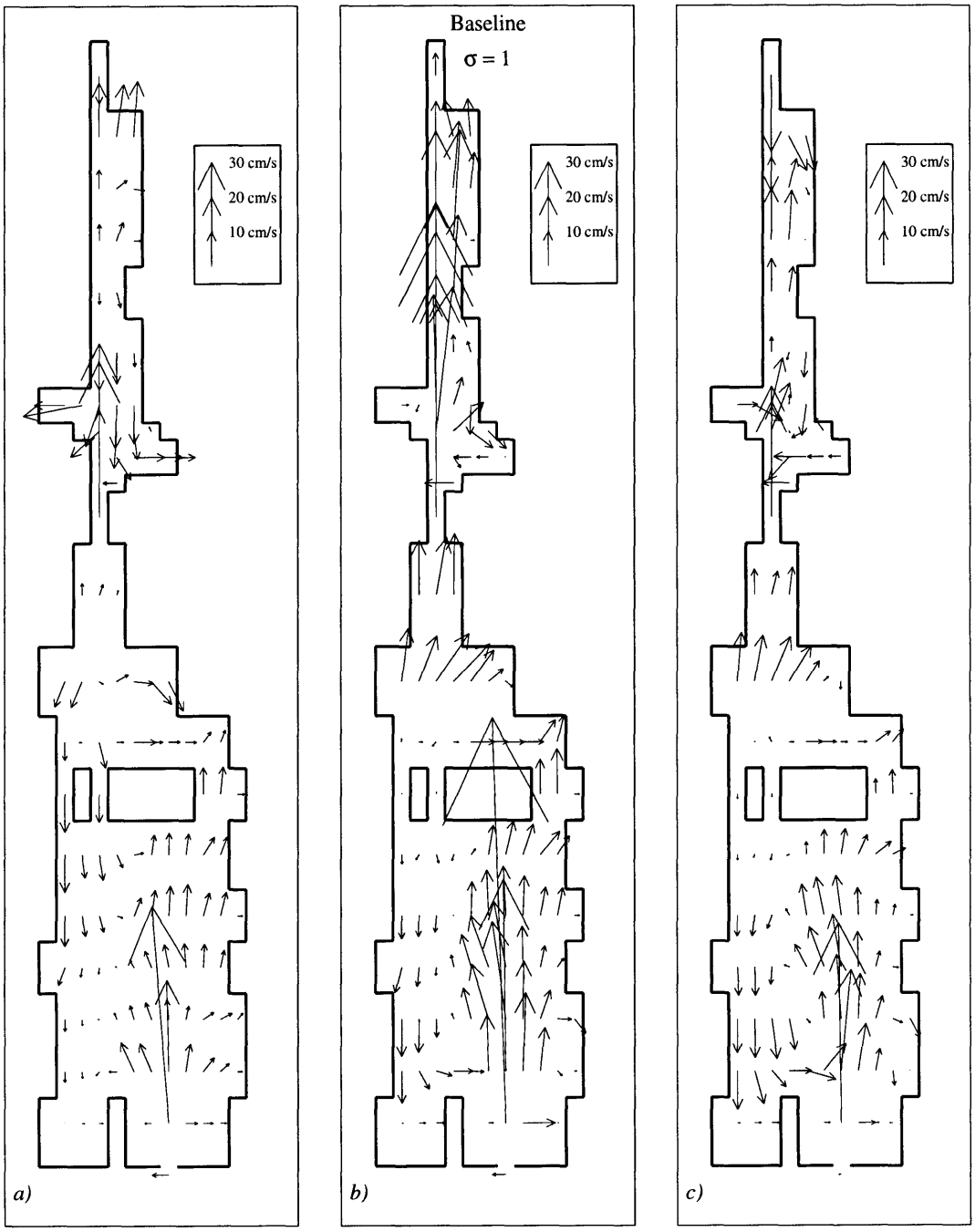

Figure 6-18: **Baseline: Maximum Flood Velocities $\sigma = 1$**
a) 2 hours prior to maximum flood; b) maximum flood; c) 2 hours after maximum flood

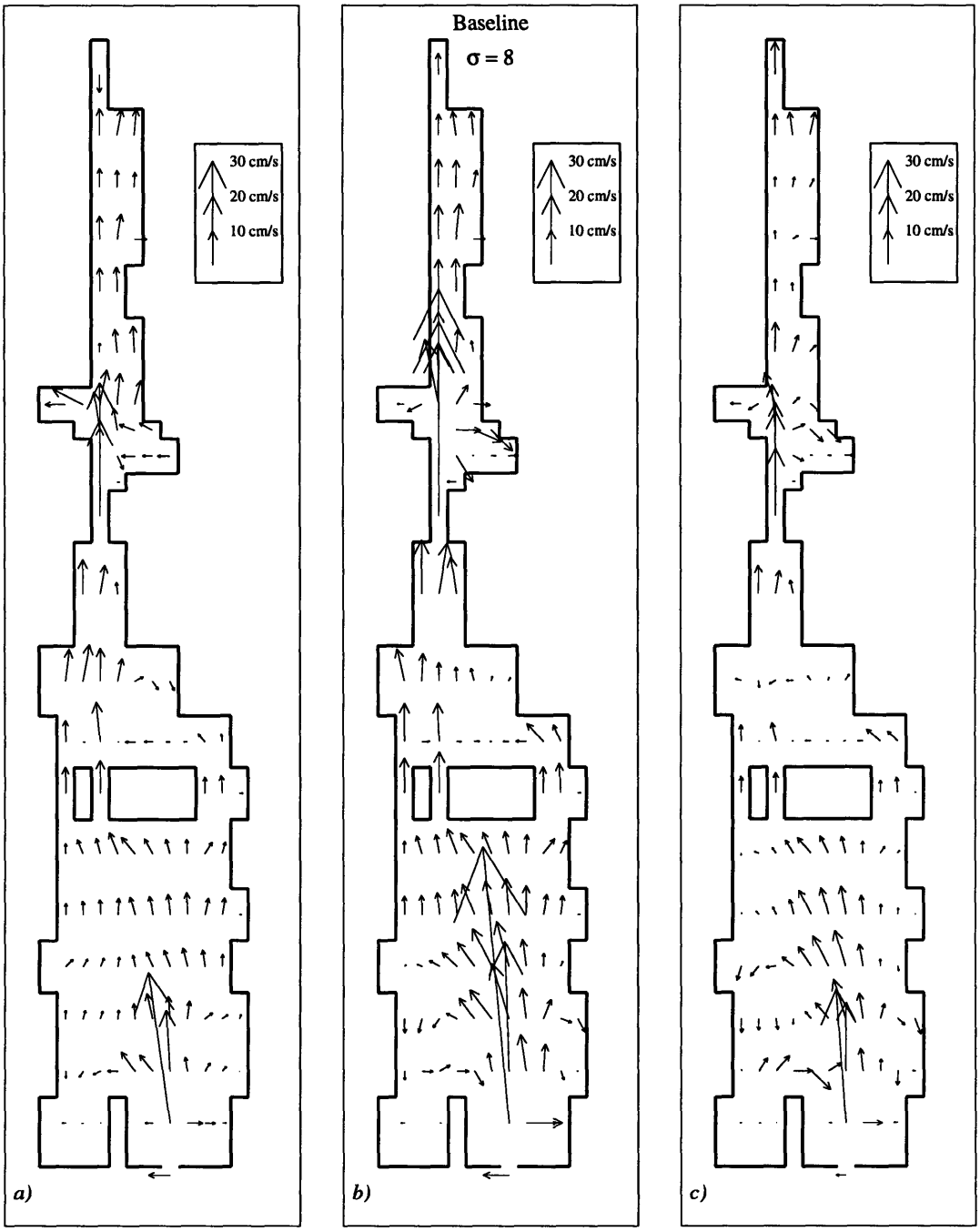

Figure 6-19: **Baseline: Maximum Flood Velocities $\sigma = 8$**
a) 2 hours prior to maximum flood; b) maximum flood; c) 2 hours after maximum flood

Both surface and bottom water are driven around the eastern side of Pope's Island and slow northeast of the island because of shallow areas. South of the New Bedford/Fairhaven Bridge opening (west of Pope's Island), the surface water is mostly still (non-moving), while the bottom water is flushed northward through the opening. Additionally, a southern return flow develops along the western shore of the lower harbor, creating a small counter-clockwise (CCW) gyre at the tip of Palmer's Island. The return surface flow and still surface water are most likely results of the 1 m/s wind forcing from the southwest. Examination of deeper σ-levels ($\sigma = 2$ through $\sigma = 8$) support this theory that the wind is driving the surface circulation patterns, and that the depth averaged flow is better characterized by Figure 6-19. At all σ-levels, a CCW gyre is present at the tip of Palmer's Island, generated by the incoming flow on the east side and still water west of the island (not to mention the wind-driven return flow on the surface).

Focusing on Figure 6-19, the flow is fairly evenly distributed between east and west sides of Pope's Island; however slightly higher velocities occur through the New Bedford/Fairhaven Bridge opening. Circulation in the lower harbor favors the deeper navigation channel only slighly more than shallower areas, however, its influence can be seen in Figure 6-19 cutting diagonally across the harbor from the hurricane barrier to the bridge opening. Once north of the bridge and islands, the flow is funneled towards the Coggeshall Street Bridge, via the deeper navigation channel, where maximum (modeled) velocities of 81 cm/s are attained. From the Coggeshall Street Bridge north, the flow is uniform at approximately 20 cm/s, though accelerating slightly (> 28 cm/s) for surface waters at the northernmost end.

Velocities in excess of u_{crit} occur at the hurricane barrier and Coggeshall Street Bridge openings during flood tide as well as to the north of both of these constrictions. Of special consideration are those velocities in excess of u_{crit} that occur in the upper estuary where PCB sediment concentrations are greatest. Figure 6-18 shows the fastest water on the surface ($\sigma = 1$) half way between the Coggeshall Street Bridge and the upper reaches of the estuary (~ 31 cm/s). Analysis of a time-series of the v-component of the velocity through the Coggeshall Street Bridge shows that it exceeds

u_{crit} for approximately four hours during flood tide.

Ebb tide Figures 6-20 and 6-21 show the maximum ebb velocity fields under baseline conditions for surface ($\sigma = 1$) and near-bottom ($\sigma = 8$), respectively. Both figures show two (2) hours prior to maximum ebb velocity (see Figures 6-20a and 6-21a), maximum ebb velocity (6-20b and 6-21b), and two (2) hours after maximum ebb velocity (6-20c and 6-21c).

As in Figures 6-18 and 6-19, the maximum ebb velocity leads the minimum elevation (low water) by approximately three hours, meaning that Figures 6-20a and 6-21a also represent five (5) hours prior to low water (2 hours after high water); Figures 6-20b and 6-21b: mid-ebb; and Figures 6-20c and 6-21c: one (1) hour prior to low water. Unlike the flood velocities, the ebb velocities appear to be unaffected by the southwest wind imposed on the surface water. As the water moves south from the upper estuary, it is again funneled through the Coggeshall Street Bridge opening, resulting in a maximum velocity of 78 cm/s. South of this constriction, the flow slows as it enters into a wide section.

Differences between Figures 6-20 and 6-21, as well as examination of the remaining σ-layers, indicate that the surface water is moving faster than the bottom water, especially between the hurricane barrier and the Coggeshall Street Bridge. On the surface, Figure 6-20, the flow separates around Pope's Island and merge back together on the south side of the island before heading out of the hurricane barrier. The effect of the deeper navigation channel in the lower harbor is significant, acting as a conduit for the falling water, and can be seen in Figures 6-20a, b, and c; and 6-21a and b.

In the hours after maximum ebb Figure 6-20c, the velocities have increased in the upper estuary (21 cm/s) and the lower harbor; however, they have decreased to 58 cm/s through the Coggeshall Street Bridge opening. More interesting is the flow field Figure 6-20c in the lower harbor, where the prism from the upper estuary is begin flushed down the western shore of the harbor. This phenomena has also been observed in the modeled dye studies in Section 6.3, where a "tongue" of concentration moves along the western shore before being moved inward towards the middle of the

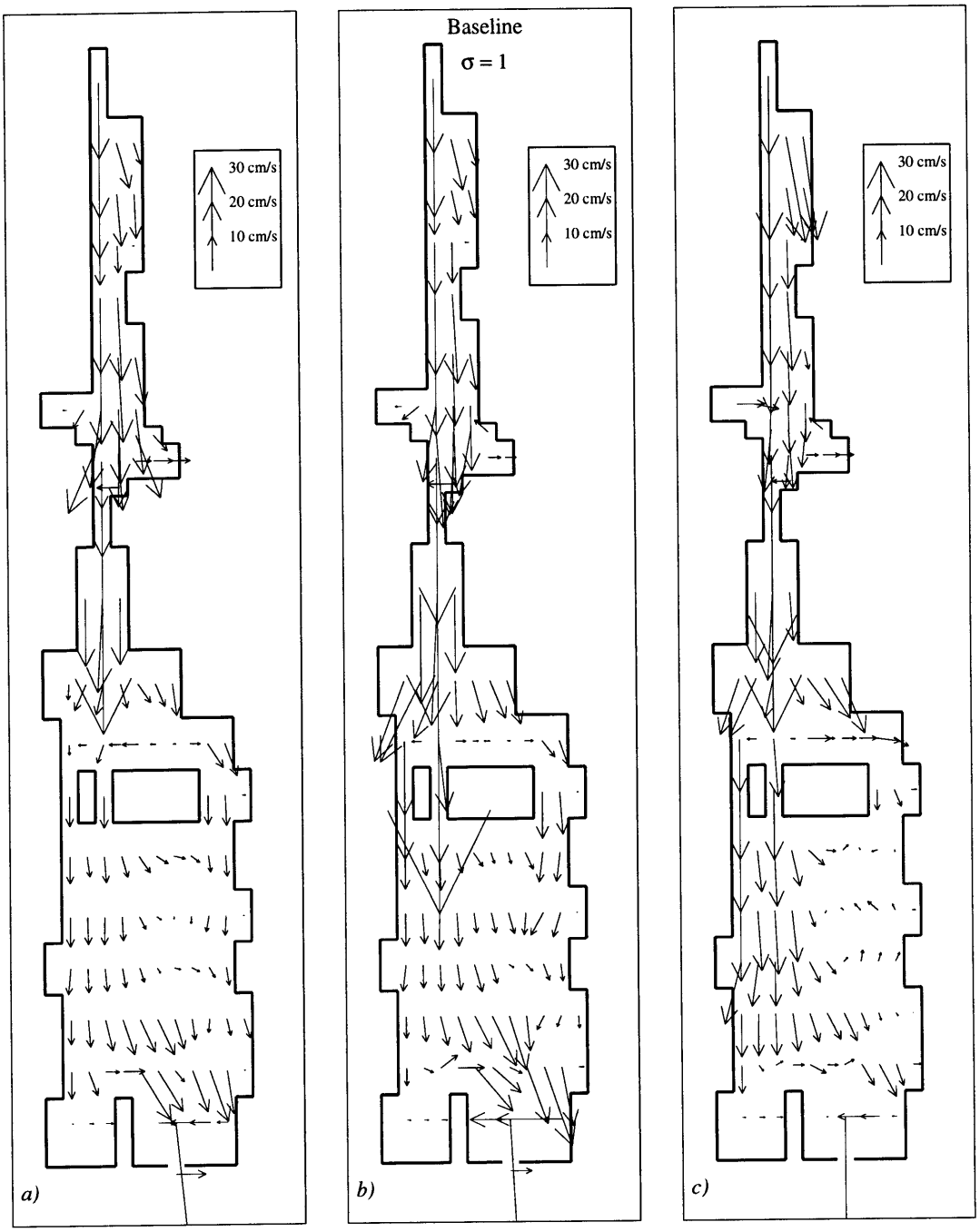

Figure 6-20: **Baseline: Maximum Ebb Velocities $\sigma = 1$**
a) 2 hours prior to maximum ebb; b) maximum ebb; c) 2 hours after maximum ebb

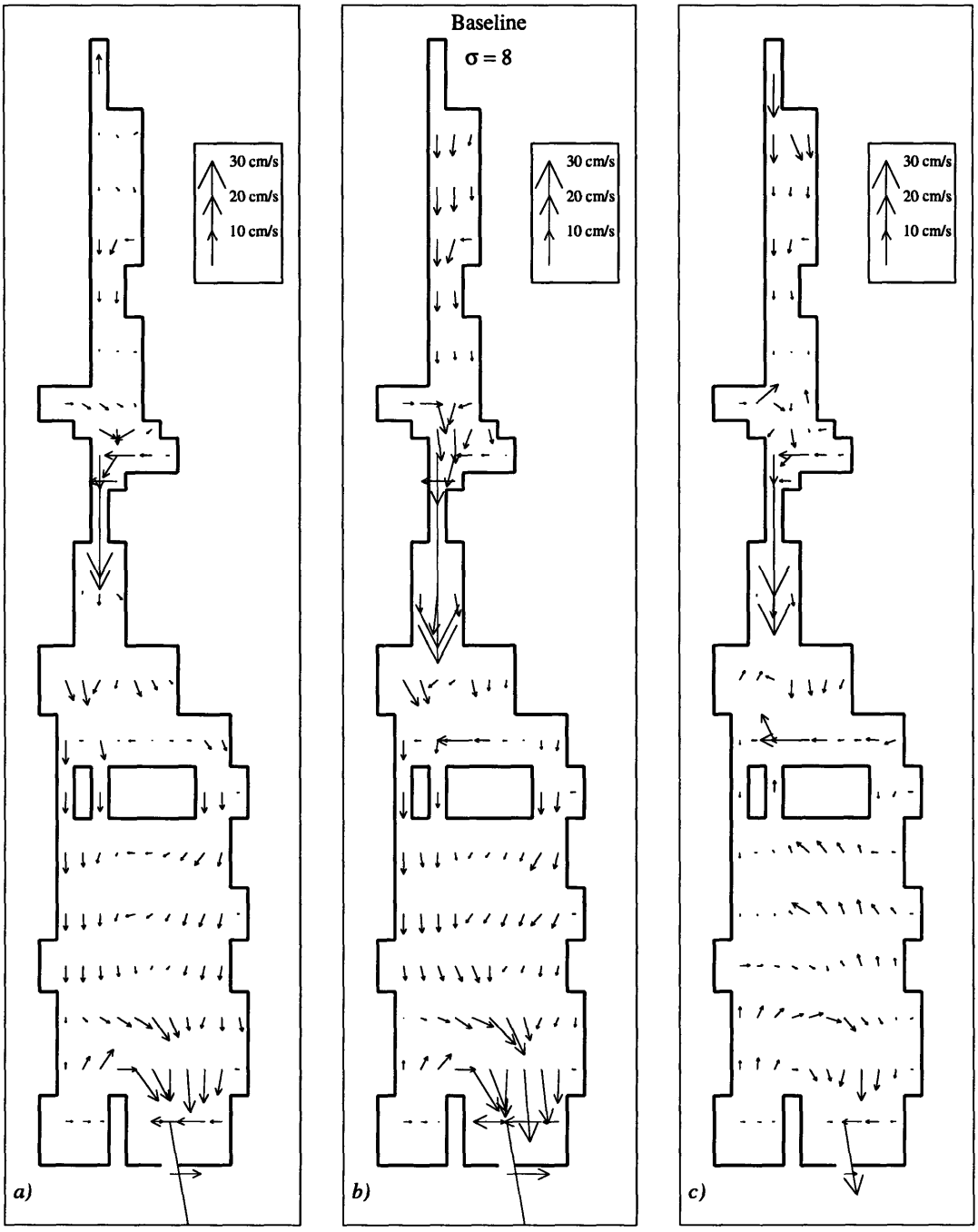

Figure 6-21: **Baseline: Maximum Ebb Velocities $\sigma = 8$**
a) 2 hours prior to maximum ebb; b) maximum ebb; c) 2 hours after maximum ebb

channel. Careful examination of Figure 6-20c and 6-21c indicates a small CCW gyre just north of the hurricane barrier, most probably a result of the changing tide.

Again, velocities in excess of u_{crit} occur at the hurricane barrier and Coggeshall Street Bridge openings during flood tide as well as to the south of both of these constrictions. Velocities in mid- and upper estuary approach u_{crit} ($\sim$ 25 cm/s), but do not equal or exceed it until two hours after maximum ebb Figure 6-20c when velocities in the northernmost reaches equal u_{crit}. A time-series of the v-component of the velocity through the Coggeshall Street Bridge shows that it exceeds u_{crit} for approximately five hours during ebb tide, resulting to high levels of PCB flushing down into the lower harbor.

6.4.2 Baseline Versus CDF Case #1

Flood Tide The effects of the CDFs in CDF Case #1 during the flood tide are limited to the upper estuary, and they are mostly uniform over depth in these areas. There are slight increases in velocity adjacent to the CDFs where PCB-concentration levels are greatest. While the increases do not exceed u_{crit}, they are important because this scenario is forced under normal, or baseline, conditions. Under extreme events, only slightly higher velocities are necessary to suspend sediments. The velocities are generally greater in the surface waters than in the lower sigma levels, which are slowed by bottom friction. Through the Coggeshall Street Bridge, however, the velocities are decreased with the CDFs. Figures 6-22 and 6-23 show the differences between the baseline, present day harbor layout, and a harbor with CDFs, under normal conditions for the surface and bottom flood velocities, respectively. In both figures, there are three subplots: a) the maximum flood velocity field for the baseline case; b) the difference in velocity fields between the baseline case and the CDF Case #1; and c) the maximum flood velocity field for the CDF Case #1. Note that in subplots 6-22b and 6-23b, the arrows represent the positive difference in velocity fields, and while they reflect the direction in which one velocity vector is greater, they do not necessarily reflect that the velocity field for CDF Case #1 is higher or lower than the baseline case.

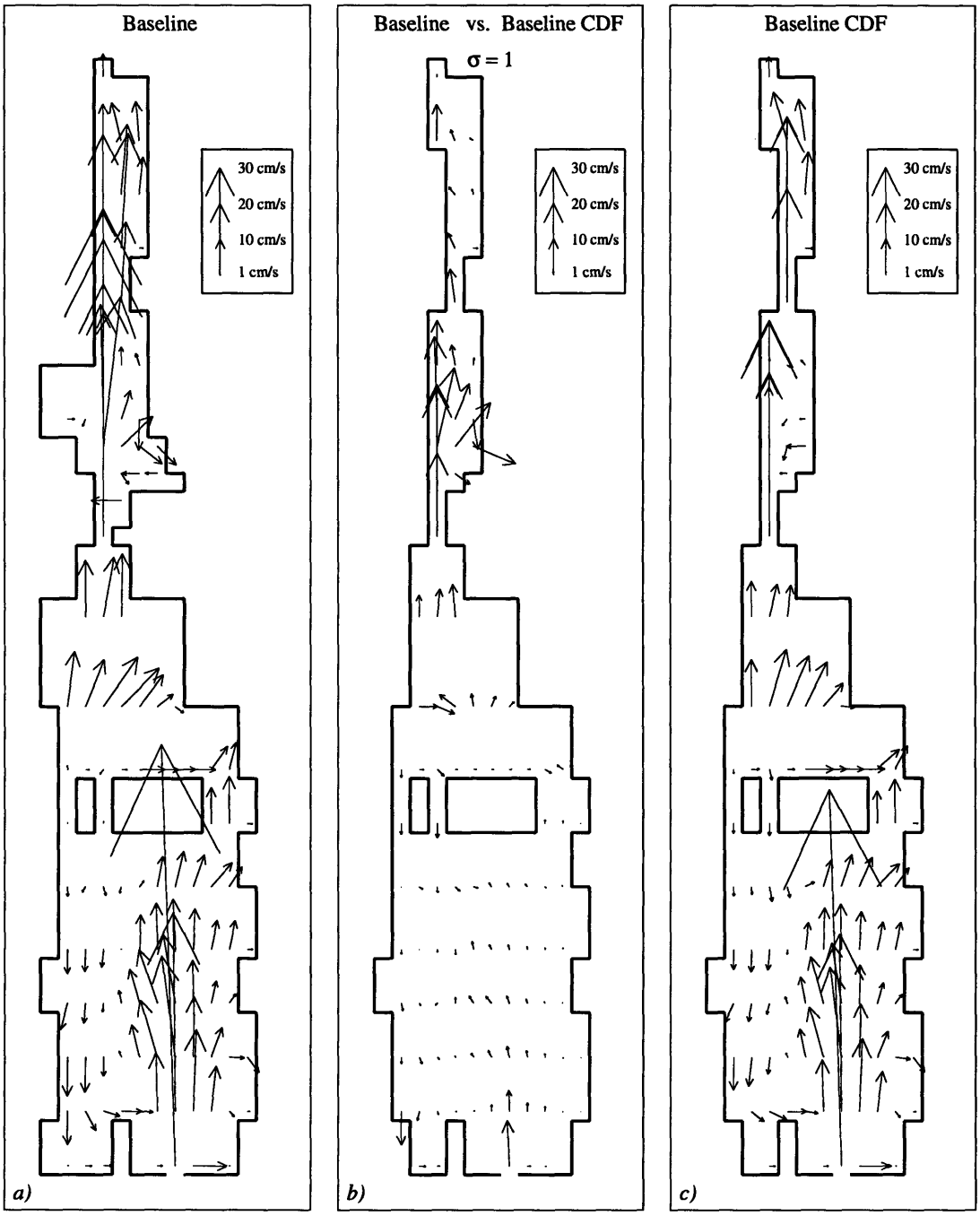

Figure 6-22: **Baseline vs. CDF Case #1: Maximum Flood Velocities $\sigma = 1$ a) Baseline maximum flood ; b) $V_{baseline} - V_{CDFs}$; c) Baseline with CDFs maximum flood**

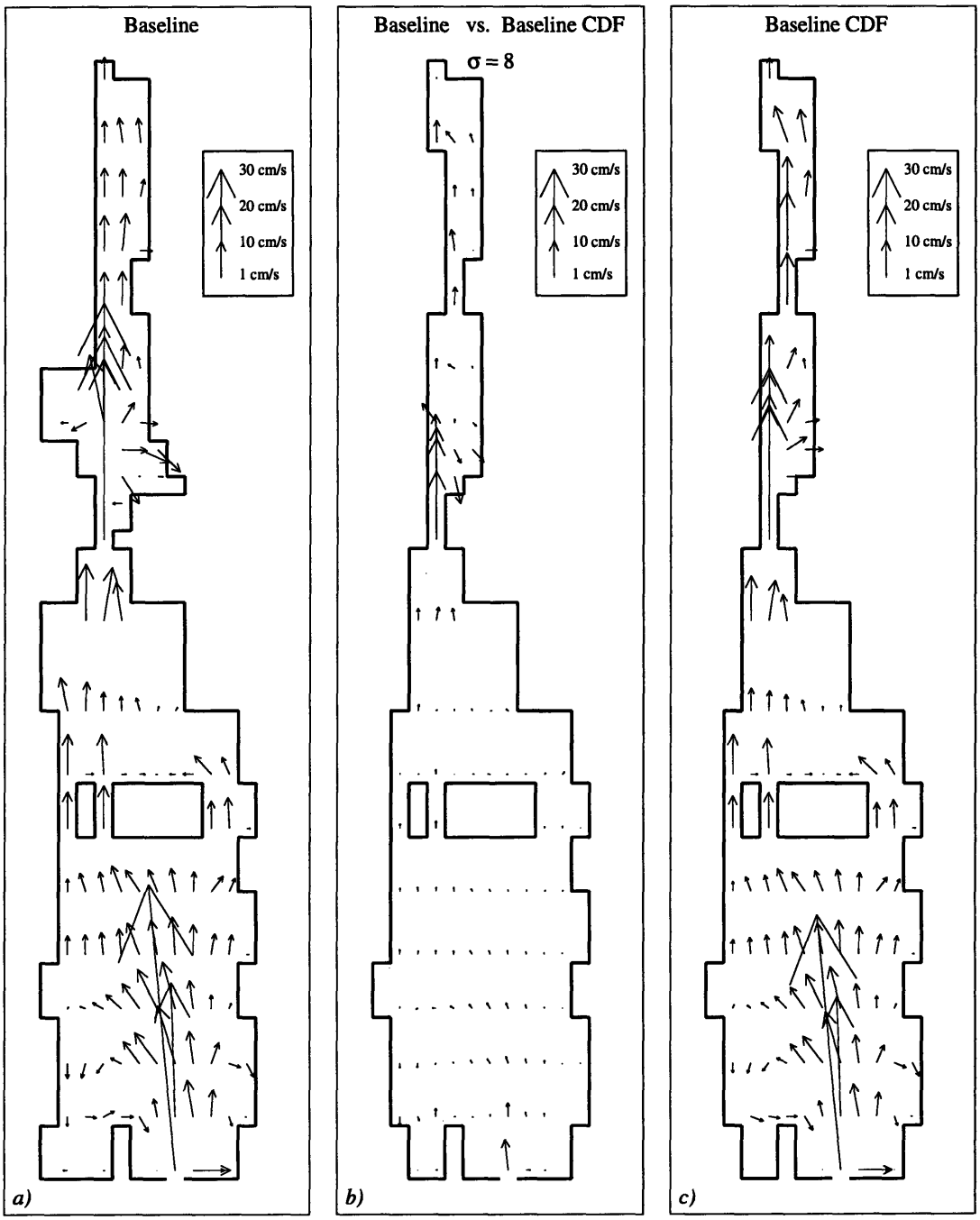

Figure 6-23: **Baseline vs. CDF Case #1: Maximum Flood Velocities $\sigma = 8$ a) Baseline maximum flood ; b) $V_{baseline} - V_{CDFs}$; c) Baseline with CDFs maximum flood**

Subplots 6-22b and 6-23b have been constructed based on the following MATLAB routine:

$$
\begin{aligned}
&\text{if ABS}(V_{baseline}) > \text{ABS}(V_{CDF}) \\
&\quad \Delta \text{ V} = V_{baseline} \text{ - } V_{CDF} \\
&\text{elseif ABS}(V_{baseline}) < \text{ABS}(V_{CDF}) \\
&\quad \Delta \text{ V} = V_{CDF} \text{ - } V_{Baseline} \\
&\text{else} \\
&\quad \Delta \text{ V} = NaN + iNaN
\end{aligned}
$$

where $i = \sqrt{-1}$, and NaN stands for Not-A-Number in MATLAB, in essence giving equal velocity vectors a difference of zero. Figure 6-22 shows differences mostly in the upper estuary. In general, the baseline case produces higher velocities than CDF Case #1. CDF Case #1 does have higher velocities, however, around the northernmost CDF: there is an increase from 32 to 36 cm/s. The velocity through the Coggeshall Street Bridge decreases from 80 to 60 cm/s.

Ebb Tide As predicted in the tidal prism analysis of Section 4.2.1, the construction of CDFs in the upper estuary result in increased velocities adjacent to those facilities and decreased velocities at the Coggeshall Street Bridge on ebb tide from 75-80 cm/s to 55-65 cm/s. Table 6.4 shows the comparison of the tidal prism and ECOM-si velocities.

The decreases are due to the smaller prism volume in the upper estuary. The increases are significant because they exceed u_{crit}, leading to resuspension. In general, the changes are mostly in the upper estuary, with little effect on the lower harbor. The exception to this is at the New Bedford/Fairhaven Bridge, where velocities are also reduced. Because of CDF 7 southwest of the Coggeshall Street Bridge and northwest of the New Bedford/Fairhaven Bridge, more water is forced east of Pope's Island, resulting in elevated velocities. Figures 6-24 and 6-25 show the differences between the baseline, present day harbor layout, and a harbor with CDFs, under normal conditions for the surface and bottom ebb velocities, respectively. Very little difference exists between the bottom velocity fields. In Figure 6-24, an increase is

Location	Prism Baseline Velocity	Prism CDF #1 Velocity	ECOM-si Baseline Ebb	ECOM-si Baseline Flood	ECOM-si CDF Ebb	ECOM-si CDF Flood
Aerovox (CDF1b)	14	28	9.5	6	9	7.5
CDF1 and 3	11	17	14	13	24	24
Coggeshall St.	73	45	56	65	40	43
CDF7	13	9	13	16	10	11
US Rte 6	16*	14*	10	12.5	6	7
Pope's Is. East	16*	14*	8.5	7.2	9	6.4
Hurricane Barrier	120	112	51	71	46	63

* average velocity of 3 openings.

Table 6.4: **ECOM-si vs. Tidal Prism Velocities**

seen just north of the Coggeshall Street Bridge from 38 to 42 cm/s and from 26 to 29 cm/s. Though not large increases, they are nevertheless above u_{crit} for sediment suspension. Figure 6-24 also shows elevated velocities adjacent to the northernmost CDF on the order of 35-40 cm/s versus 20-25 cm/s for the baseline case. These are significant changes because this is one of the most sensitive areas in the upper estuary.

6.4.3 CDF Case #1 vs. CDF Case #2

Flood Tide In CDF Case #2, surface water is forced towards the east side of Pope's Island because of the CDF located in the southwestern corner of the lower harbor. Bottom water appears to be fairly evenly distributed between the east and west sides of Pope's Island, and surface water favors the east side as in the baseline harbor case, though in a more extreme manner. CDF Case #2 does not exhibit the navigation channel-following characteristic that the baseline case does, though a western harbor return flow can be seen. Comparing the two CDF cases for the lower harbor, then, shows that the introduction of a larger CDF 10 in the lower southwest corner results in less surface water flow through the New Bedford/Fairhaven Bridge via the navigation channel and elevated velocities in the eastern lower harbor. In the upper estuary, velocities through the Coggeshall Street Bridge opening are slightly higher (7-10 cm/s) for CDF Case #2. Further upstream, velocities are significantly

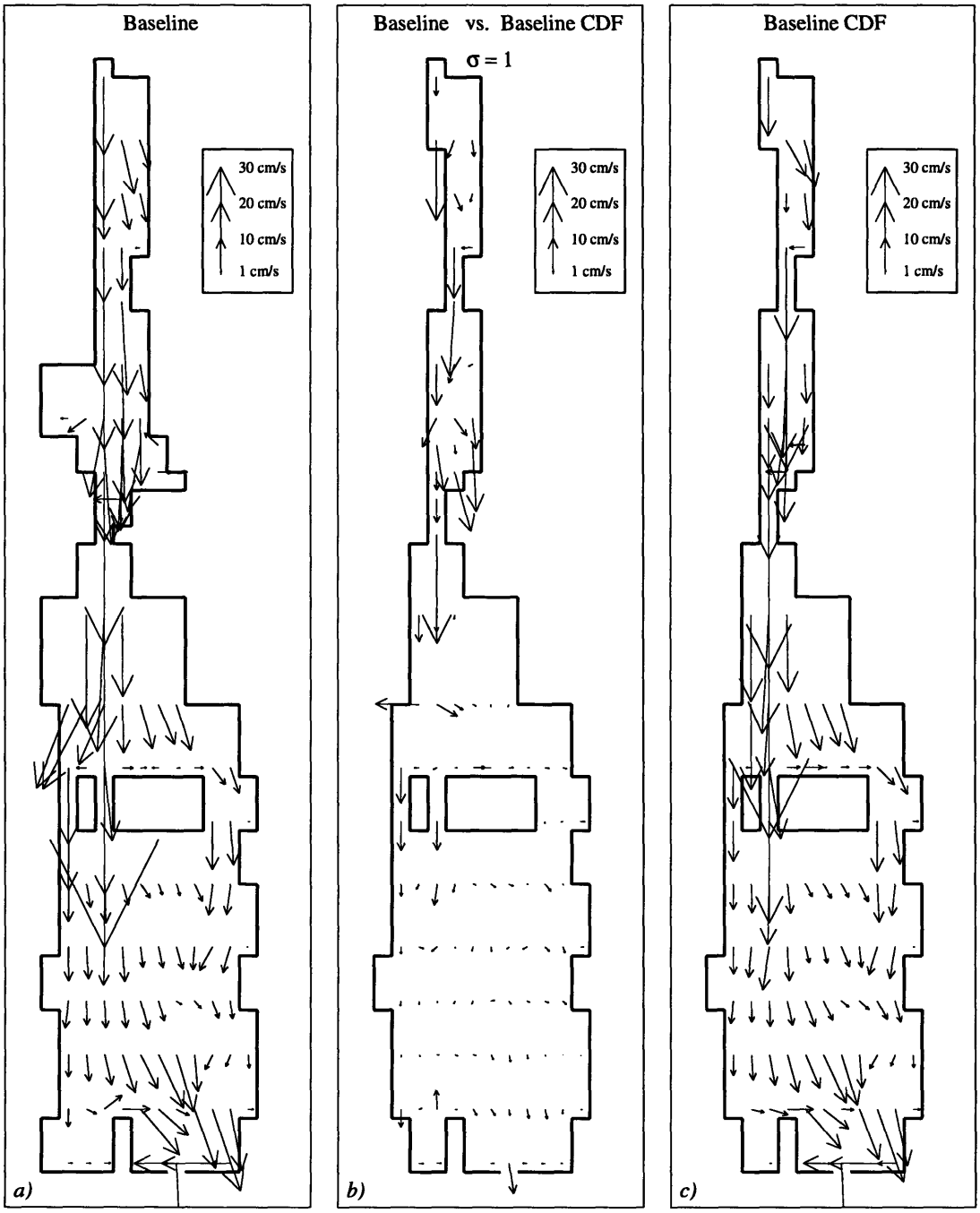

Figure 6-24: **Baseline vs. CDF Case #1: Maximum Ebb Velocities $\sigma = 1$ a) Baseline maximum ebb ; b) $V_{baseline} - V_{CDFs}$; c) Baseline with CDFs maximum ebb**

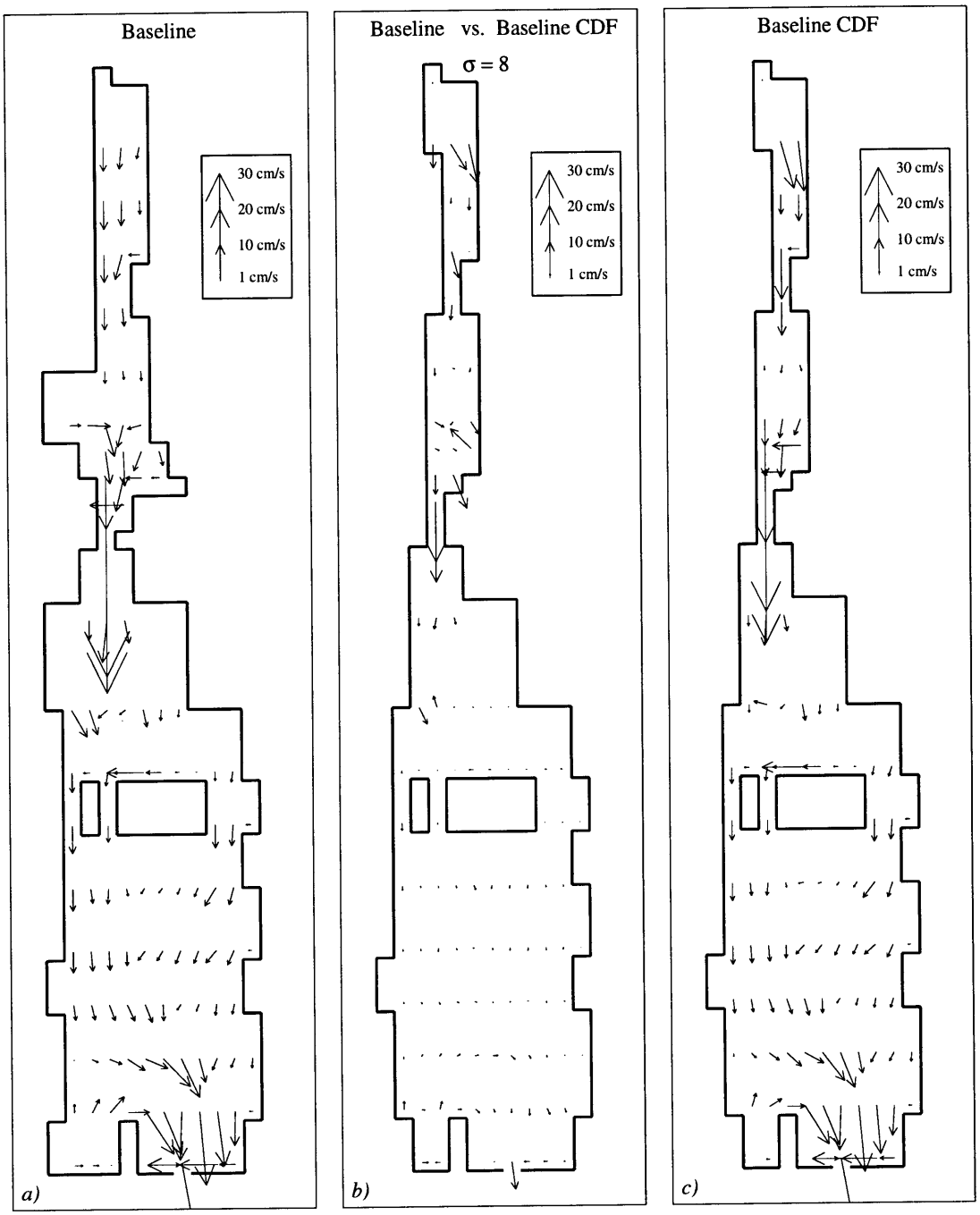

Figure 6-25: **Baseline vs. CDF Case #1: Maximum Ebb Velocities $\sigma = 8$ a) Baseline maximum ebb ; b) $V_{baseline} - V_{CDFs}$; c) Baseline with CDFs maximum ebb**

higher (32 vs. 10 cm/s) for CDF Case #1 because of CDF site 1b. The last difference occurs in the northernmost estuary where velocities for CDF Case #2 exceed 100 cm/s, however, this is most likely an erroneous result because neither the baseline nor the CDF Case #1 reflect velocity increases of this magnitude, and the constrictions have been decreased (i.e., the cross-sections increased) in the CDF Case #2 from CDF Case #1. Ignoring these last findings, the results generally indicate that for the upper estuary, CDF Case #2 provides a better siting arrangement from an environmental impact because current velocities do not reach u_{crit} as they would in CDF Case #1.

Ebb Tide At maximum ebb flow, the most significant differences between the baseline and CDF Case #2 occur in the northernmost section of the estuary, where velocities exceed 100 cm/s for the CDF Case #2. As mentioned previously, the other models do not show this magnitude of velocities though the CDF Case #1 model has tighter constrictions. As such, these upper estuary velocity fields are ignored for the remainder of the analysis.

For the rest of the harbor (i.e., south ofthe Coggeshall Street Bridge), the velocity field produced by CDF Case #2 is lower in magnitude than the baseline velocity field. Almost identical flow patterns are seen for both surface and bottom waters in the lower harbor. Compared to CDF Case #1, CDF Case #2 exhibits slightly higher velocities in the northern lower harbor where the additional CDF site is located. These small differences in velocity fields are almost non-existent by the time they reach the Pope's Island openings. So, by comparison, the two CDF cases do not differ significantly for the ebb flow, giving them an equivalent environmental impact stance.

6.4.4 Flood

The flood scenario was simulated by increasing the freshwater flow rate from the Acushnet River to 18.4 m^3/s over the period of one hour. This flow rate represents the 100 year flood rate described in Section 4.4. The effect of this extreme freshwater discharge can be seen in slightly elevated ebb velocities at the Coggeshall Street

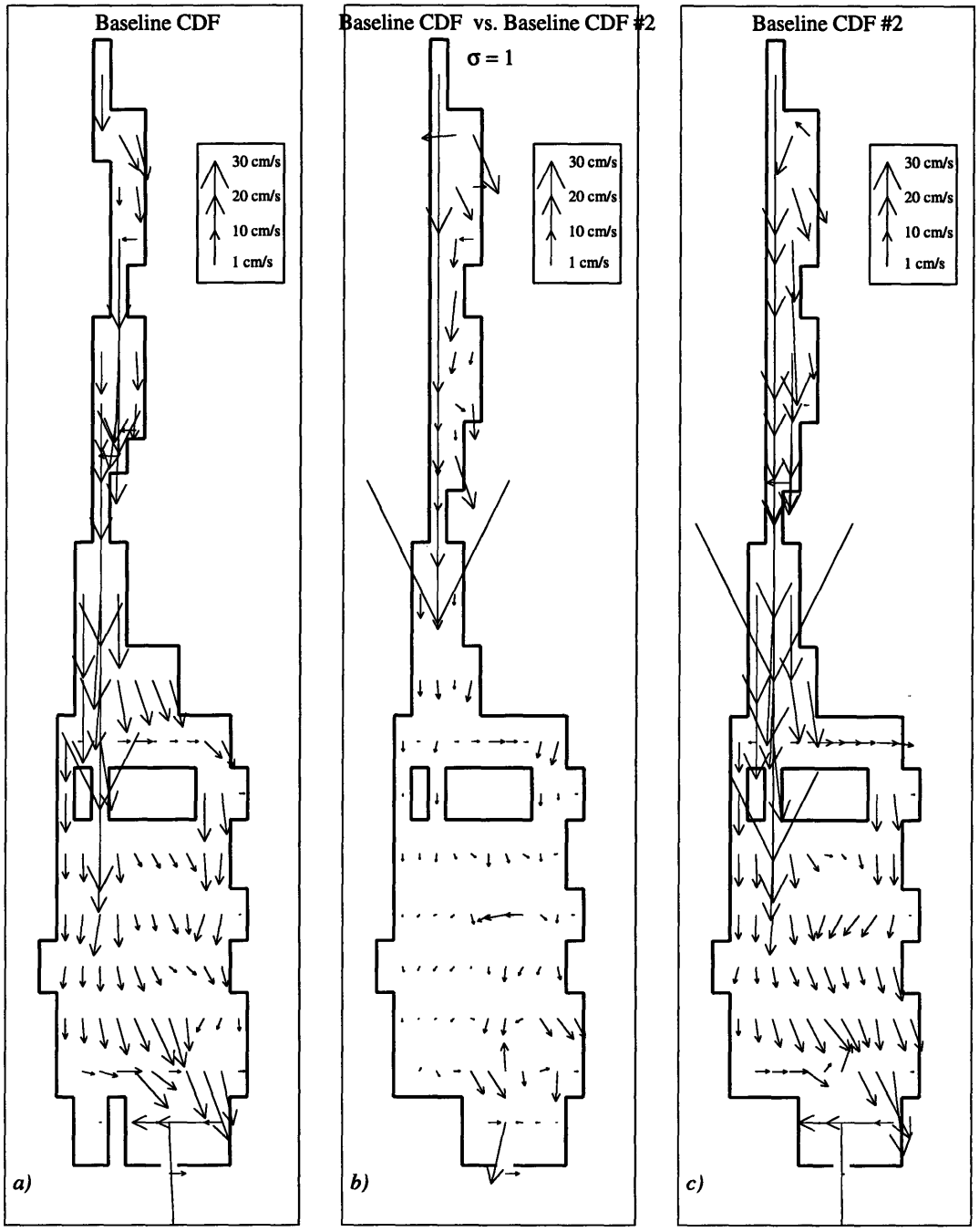

Figure 6-26: **CDF Case #1 vs. CDF Case #2: Max Flood Velocities $\sigma = 1$ a) CDF Case #1 ; b) $V_{CDFCase\#1} - V_{CDFCase\#2}$; c) CDF Case #2**

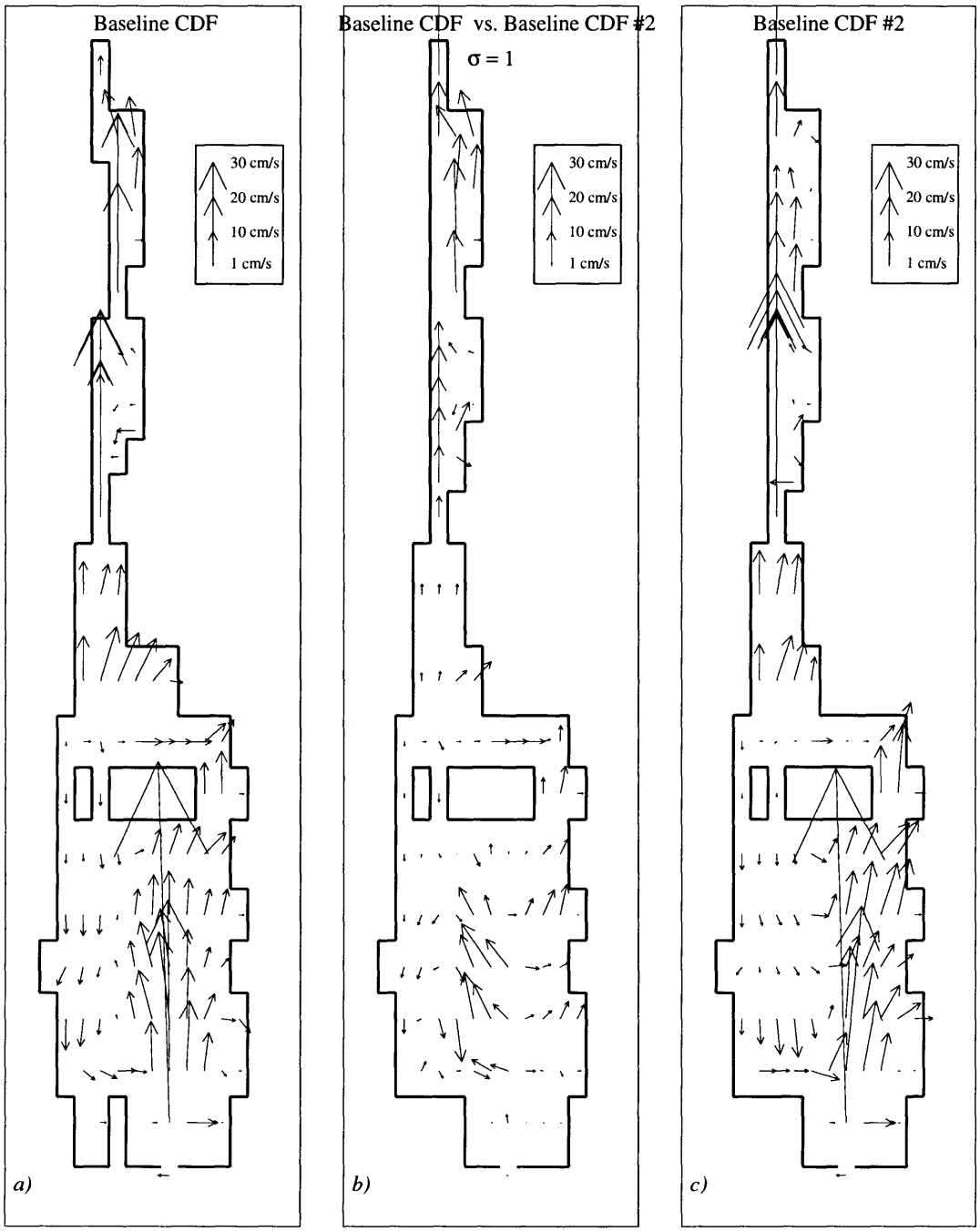

Figure 6-27: **CDF Case #1 vs. CDF Case #2: Max Ebb Velocities $\sigma = 1$ a) CDF Case #1 ; b) $V_{CDFCase\#1} - V_{CDFCase\#2}$; c) CDF Case #2**

Bridge and Pope's Island and decreased flood velocities near Pope's Island. The extreme runoff also decreases tidal flood velocities in the upper estuary.

Interestingly, by hour 15 (i.e., during flood tide) of the extreme runoff event, the phase of the tidal velocities has shifted roughly one hour earlier that the baseline tidal velocities in the upper estuary. By hour 19, this phenomena is visible on the east of Pope's Island. It does not occur, however, at the Coggeshall Street Bridge nor does it occur at the New Bedford/Fairhaven Bridge. This suggests that the runoff is begining to have an effect on the tide by slowing its progress upstream and reducing flood velocities.

In general, the circulation patterns of the flood scenario are similar to those under baseline conditions. Increases in elevation due to the flood waters, however, are smaller than expected – on the order of a millimeter in the upper estuary and negligible at the hurricane barrier. Little information has been found in the ECOMsi-related literature regarding flooding.

Baseline vs. Flood with CDF Case #1 At maximum ebb tide, the placement of the CDFs result in increased velocities adjacent to the upper estuary sites. As in the baseline scenario, the velocities are velocities are reduced in the CDF flood scenario. Recall that in the baseline flood condition, the velocities through the Coggeshall Street Bridge are increased approximately 10 cm/s by the excess freshwater runoff.

At maximum flood, CDF Case #1 also creates higher velocities adjacent to the sites. While elevated, a phase shift in the tidal velocity is still seen in the upper estuary and east of Pope's Island.

Baseline vs. Flood with CDF Case #2 Comparing CDF Case #2 to the baseline and CDF Case #1 during a flooding event (on flood tide) reveals some interesting differences. In the upper estuary, the tight constriction formed by the disposal sites in the CDF Case #1 arrangement causes velocities in excess of u_{crit} (32 cm/s) compared with baseline and CDF Case #2 velocities of 24 and 5 cm/s, respectively. In this case, the velocity field from the CDF Case #2 is lower than

the baseline case in the upper estuary, most likely a result of the decreased volume in the lower harbor from the larger CDF 10 and new CDF north of Pope's Island. This effect is less apparent at the Coggeshall Street Bridge opening with maximum velocities reaching 76, 57, and 58 cm/s for baseline, CDF Case #1, and CDF Case #2, respectively.

Comparison of the CDF cases during ebb tide is not as significant. On the whole, velocity fields are very similiar. For example, at the Coggeshall Street Bridge, velocities reach 73, 65, and 65 cm/s for baseline, CDF Case #1, and CDF Case #2, respectively. In the upper estuary, maximum velocities all range from 10 to 15 cm/s during the ebb cycle of a flood event. The effect of the CDFs compounded with the flood event is minimal during ebb tide.

6.4.5 Hurricane Winds

After an initial two day startup of the model, the tidal forcing (and elevation) was stopped abruptly between model runs. Because this change occurred at low tide, elevations are all below mean water. Hurricane wind was simulated by increasing wind speed from zero to 33.5 m/s over two hours. No tidal forcing was included because the harbor is protected by a hurricane barrier which protects against tidal surge. Additionally, river flow rates were maintained at baseline levels in order to assess the circulation effects from hurricane winds only. Under hurricane forcing, the major circulation patterns occur in the lower harbor. The wind from the south drives flow symmetrically northward around Pope's Island on the surface ($\sigma = 1$), while at the lower levels ($\sigma = 8$), water returns along the southeast edge of the lower harbor. The effect of the wind in the upper estuary can be seen in Figure 6-28, which shows an increase in free-surface elevation at a location adjacent to Aerovox. This phenomena, called setup and described in Section 4.3.1, reached 6 cm over three days of model runtime, similar to that calculated in Section 4.3.1 for the upper estuary (5 cm). Equation (4.4) in Section 4.3.1 was used to calculate a setup of 12 cm for a 15 m/s wind from the south. Using a 33.5 m/s wind under the same conditions, i.e., depth and fetch, Equation (4.4) results in a setup of 56 cm for unlimited duration.

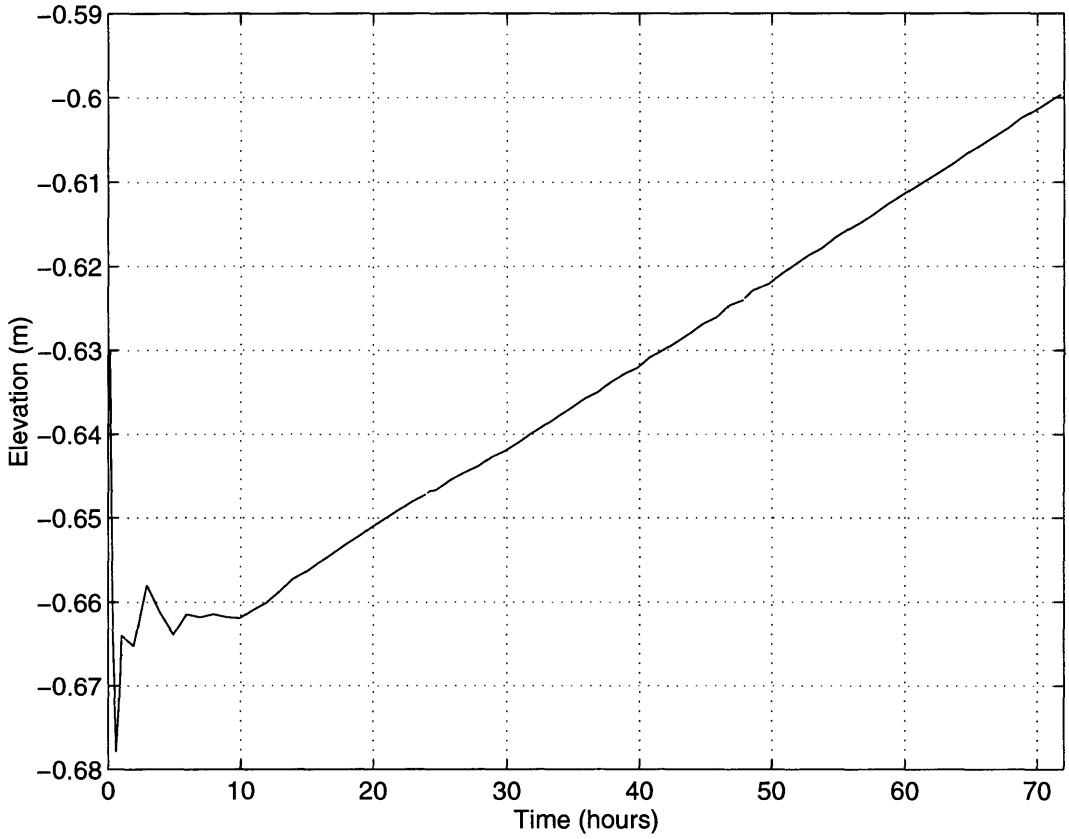

Figure 6-28: **Setup in the Upper Estuary**

By the end of one day (24 hours) of model runtime, an elevation of 1.5 cm (from steady state level after transients) had occurred in the upper estuary, and by the end of the second and third days of runtime, the free surface elevation had risen almost 4 and 6 cm, respectively. By the end of the third day of runtime, the elevation is still rising by approximately 1 mm/hour. At this rate of increase, an elevation rise of 56 cm would take approximately 23 days.

Figures 6-29 and 6-30 shows a comparison of the maximum flood tide for the baseline case compared to the peak velocities produced by the hurricane case. As expected, most of the movement for the hurricane case occurs in the upper layers where the wind's influence is greatest. The flow is evenly distributed around Pope's

Island, though faster velocities (28-33 cm/s)are encountered in the eastern half of the lower harbor. Near the bottom, however, water tends to recirculate around the lower harbor in a clockwise pattern (see Figure 6-30). The highest velocities in the bottom layer occur just north of Pope's Island towards the east (18 cm/s) and in the southeast corner of the lower harbor (29 cm/s).

Baseline vs. Hurricane with CDF Case #1 The CDFs do not have significant impact during periods of high winds because they are located in the upper estuary where velocities, and subsequently circulation, are minimal. The important factor under wind forcing of this type is the setup that occurs in the upper estuary. During a hurricane event with similar winds, water is piled up in the upper estuary. If the tidal surge passes, and the hurricane barrier gates open, the added elevation of water may cause resuspension as it drains out of the upper estuary.

Baseline vs. Hurricane with CDF Case #2 As with CDF Case #1, most of the effects from CDF Case #2 are limited to the lower harbor. Surface water velocities in the lower harbor reach 22-26 cm/s and 28-32 cm/s for CDF Cases #1 and #2, respectively. This difference in surface water velocities is due to the significantly larger CDF 10 in the southwestern corner of the lower harbor. In the upper estuary, little differences are seen between the two CDF cases. There is, however, a small setup height difference of 1 mm between the two cases.

6.5 Recent Developments in New Bedford

Since the completion of several of the models, there have been new developments in the EPA preferred sites. As of 26 July 1996, a proposal to develop CDFs 1a, 1b, and 7 had been suggested (Dickerson, 1996). In this proposal, CDFs 1b, 1a, and 7 (see Figure 1-3) had been renamed A and B (CDF 1b), C, and D, respectively. CDFs A, B, C, and 7 (D is slightly larger) would then provide an approximate volume of 300,000 cubic yards, roughly one-third of the volume needed for both remediation and maintenance dredging projects, suggesting the need for additional facilities. The

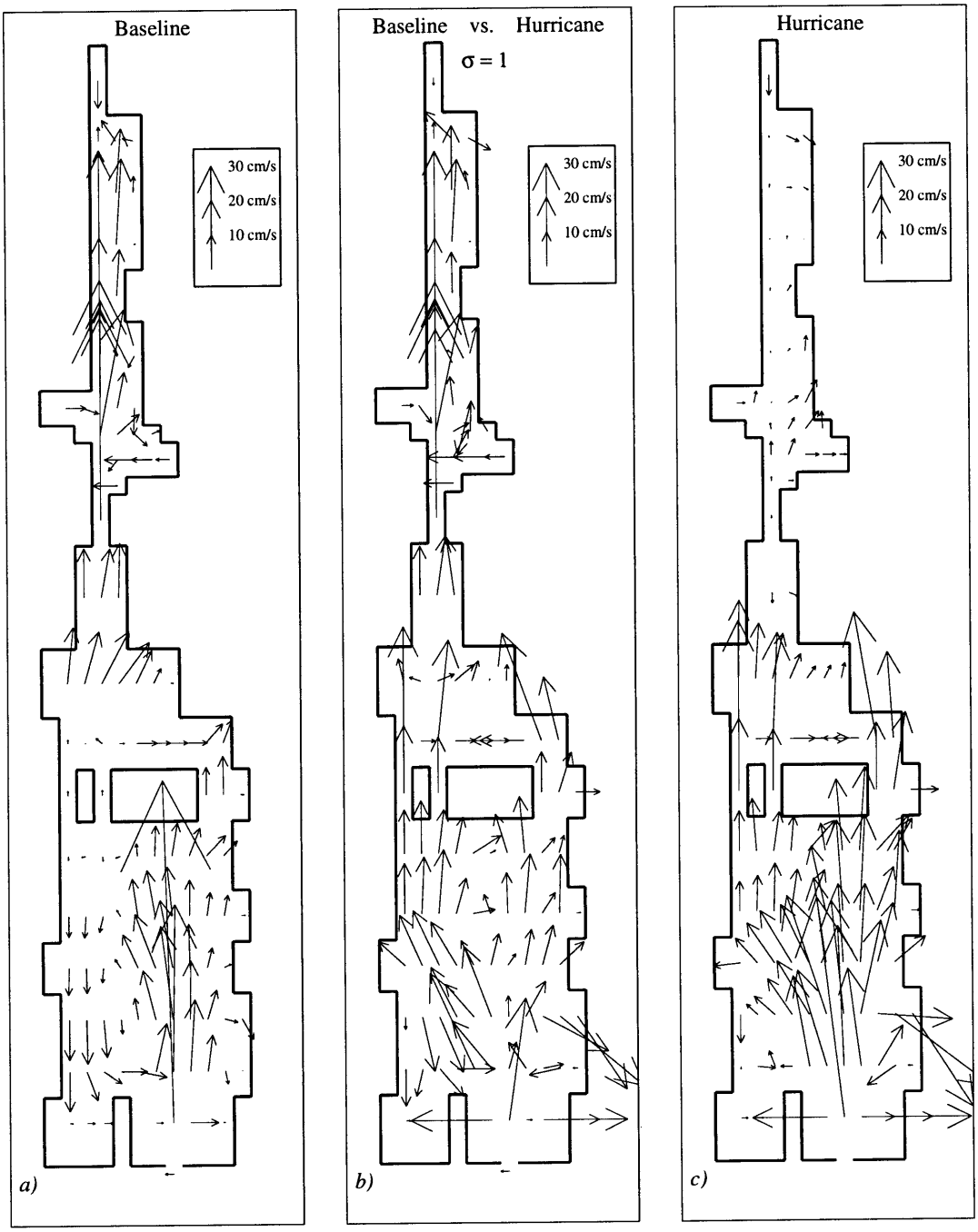

Figure 6-29: **Hurricane Case vs. Maximum Flood Velocities: $\sigma = 1$ a) Baseline maximum flood ; b) $V_{baseline} - V_{hurricane}$; c) Hurricane maximum velocity**

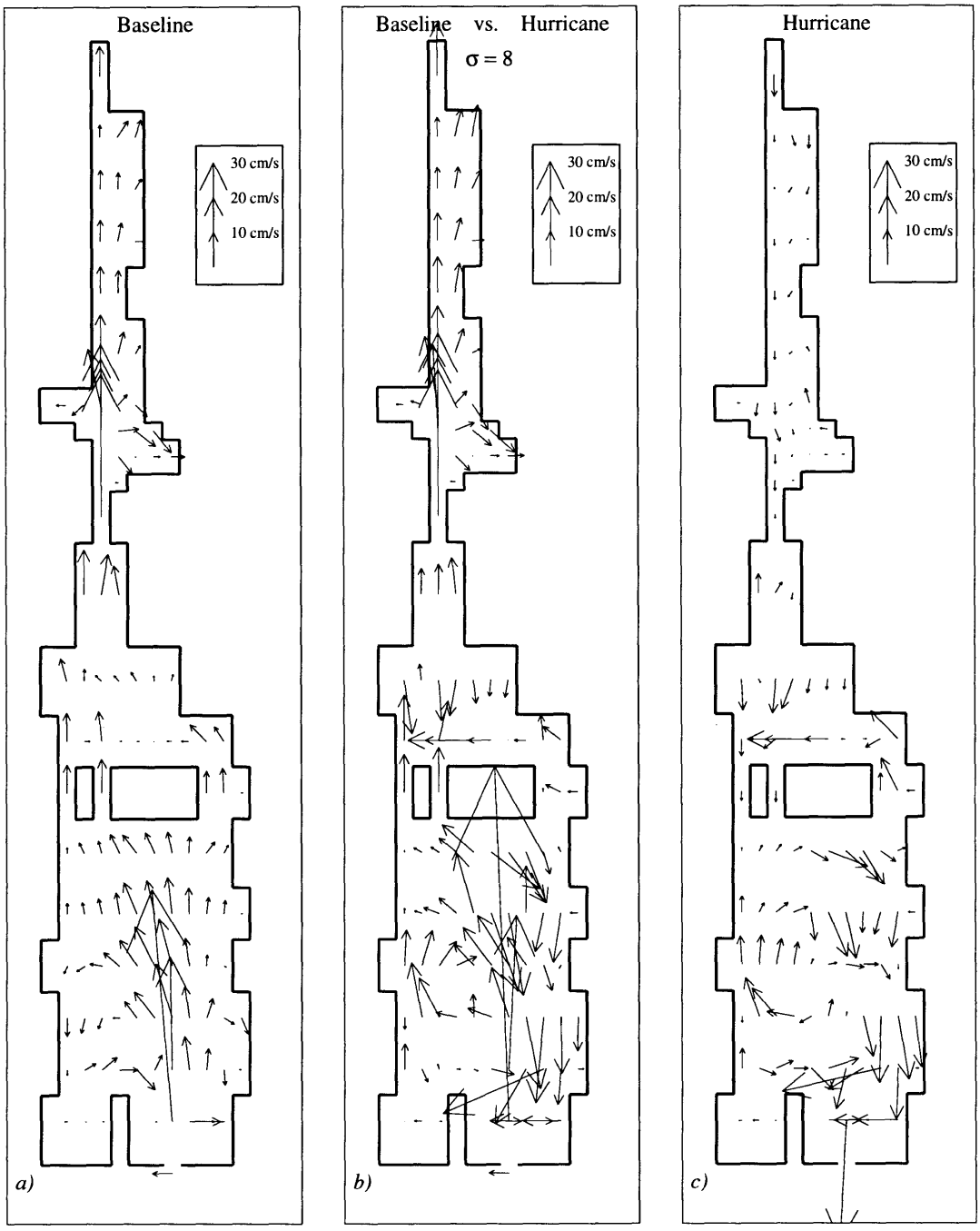

Figure 6-30: **Hurricane Case vs. Maximum Flood Velocities: $\sigma = 8$ a) Baseline maximum flood ; b) $V_{baseline} - V_{hurricane}$; c) Hurricane maximum velocity**

placement of sites A, B, C, and D are not vastly different from the CDF Case #1 model (such as in Figure 5-3). Thus, it is likely that the introduction of sites A and B in the upper estuary (in essence CDF 1b) along the western shoreline will result in elevated velocities in the upper estuary. CDF B (the lower half of CDF 1b) is located at one of the narrowest spots in the upper estuary, resulting in a reduction of cross-section and elevated velocities. As Figures 6-24 and 6-25 show, the this geometric constriction results in velocities that exceed u_{crit}. Additionally, CDF D has been enlarged from the former CDF 7. This increase in volume is similar to that seen in CDF Case #2, with the addition of a CDF north of Pope's Island, which did not have a significant effect on the circulation. CDF D is likely to have a negligible effect, however, its expansion will mean routing the navigation channel in the upper harbor around the CDF, and this may have other consequences.

6.6 Model Improvements

While the model appears to duplicate (limited) observations fairly well, it is clear from both the simulated dye study and the velocity fields in the lower harbor that the model is overestimating the circulation and transport along the western shore and underestimating the circulation along the eastern shore. Unfortunately, velocity data from previous studies are only available for constrictions and key navigational areas, providing little to which to compare simulated mid-harbor and mid-estuary velocity fields. The ASA (1987) dye study, however, does provide valuable information to which simulated data can be compared. As discussed in Section 5.1.1, ECOM-si has been developed and used mostly for ocean shelf studies, where grid sizes are on the order of kilometers. This is a limitation for the New Bedford Harbor model because its smaller grid sizes result in a small timestep, e.g., 4 seconds, and the model becomes computationally inefficient. Additionally, the grid size controls the horizontal mixing parameters (see Section 5.1), which may be responsible for the differences seen in the simulated dye study versus ASA (1987).

Chapter 7

Summary and Conclusions

7.1 Summary of Study

Much controversy surrounds the disposal of PCB-contaminated sediments into confined disposal facilities along the shoreline of New Bedford Harbor. Public concern remains opposed to the construction of the facilities; however, other disposal options are not cost efficient and introduce unnecessary risks. The volume of contaminated sediments from the Superfund dredging, over 400,000 cubic yards, (and later from maintenance dredging efforts, over 500,000 cubic yards) mandates a local disposal option such as the CDFs. This thesis provides insight into the impacts that the siting of these CDFs will have on the circulation of the harbor.

Several techniques have been employed to assess the impact of confined disposal facilities on the circulation in New Bedford Harbor. The effects of the CDFs on the three dominant forcing factors have been evaluated using both analytical and numerical techniques, and two extreme events have been studied. Furthermore, two arrangements of CDFs have been modeled to reflect 1) 1995 USEPA proposed CDF site locations and 2) an alternative arrangement based on modeling results from the 1995 arrangement. Finally, recommendations have been made based on comparisons of the baseline harbor model to these two CDF siting scenarios.

Adverse environmental impacts from the CDFs have been quantified based on the exceedance of a critical parameter; for this study, the most important parameter

governing further contamination of the harbor and surrounding areas is the critical resuspension velocity, u_{crit}, of 28 cm/s. This value has been used in all modeling efforts, both analytical and numerical. Critical resuspension velocity is deemed the most important because PCBs are generally resuspended along with the sediments. As such, two velocity fields for different cases, e.g., baseline versus CDF #1 or CDF #1 versus CDF #2, are compared based on this critical value. Visual changes in circulation patterns can be qualified as well, providing additional information about the effect of the modifications.

7.2 Results

7.2.1 Upper Estuary CDFs: 1, 1b, and 3

A tidal prism analysis in Section 4.2.1 provides insight into the impacts of the CDFs in the upper estuary. A decrease in the upper estuary tidal prism from the siting of CDFs 1, 1b, and 3 results in decreased velocities through the Coggeshall Street Bridge and I-195 constrictions. These decreases are not sufficient to reduce the velocities in this location below u_{crit}; however, the reduction will reduce the seaward flux of PCBs.

During flood events, the rate of water discharged from the Acushnet River may increase over 2000%, e.g., 0.85 to 18.4 m^3/s. This increase in flow rate results in elevated velocities. A simple calculation in Section 4.4 suggests that the velocities will increase from 19 cm/s without CDFs to 39 cm/s with CDF 1b in place. ECOM-si supports this calculation, though not quite to the same extreme, with ebb velocities of approximately 14 cm/s and 23 cm/s with and without CDF 1b, respectively. As for the tidal case, velocities downriver at the Coggeshall Street Bridge are reduced from 56 cm/s to 41 cm/s at maximum ebb from the siting of CDFs in the upper estuary.

Hurricane winds from the south impose a setup condition on the upper estuary. Section 4.3.1 calculated a setup of 12 cm for unlimited duration winds over the length of the harbor and estuary; this equates to approximately a 5 cm height dif-

ferential from the Coggeshall Street Bridge north into the upper estuary. This value is similar to that calculated by ECOM-si, e.g., 6 cm, for 72 hours of wind forcing; however, at 72 hours of model runtime, the simulated elevation is still rising steadily at 1 mm/hour. The impact of setup depends greatly on the initial surface elevation of the harbor: if a hurricane wind event is concurrent with a high tide, setup may result in flooding of nearby wetlands, releasing additional PCBs into the water column.

7.2.2 Upper and Lower Harbor CDFs: 7 and 10

There is one USEPA-potential site, i.e., there has been current Superfund discussions about using CDF 7, in the upper harbor, and one USEPA-proposed site, i.e., there has been previous (pre-1995) discussions about using CDF 10, in the lower harbor. According to analytical and numerical models in this thesis, the siting of CDFs 7 and 10 will result in minimal circulation changes in the harbor. Additionally, neither siting will not alter current velocities sufficiently such that the velocities exceed u_{crit}. The extension of CDF 7, **CDFBIG** in Section 6.1, will create slightly higher velocities that the original CDF 7, but again, not sufficient enough to exceed u_{crit}. In modeling **CDF7BIG**, no changes were made to surrounding bathymetry; however, current 1996 proposals call for the deeper navigational channel adjacent to the proposed CDF 7 site to be moved eastward to accommodate the larger CDF. Recall that modeling efforts indicated that the flow is driven mostly by bathymetry (see Figure 5-2); a shift in the location of the navigation channel may redirect the flow towards Pope's Islan, though this is out of the scope of this thesis.

CDF 10, though potentially more visible than the other facilities, does not result in any adverse hydrodynamic effects, although other air quality issues may be more important in this area because of the New Bedford fish auction at South Terminal. This facility, air qualilty issues aside, provides a large storage capacity in an unused area of the harbor, making it ideal for a large disposal facility. Its distance from the contaminated areas, however, makes it an unlikely candidate.

7.3 Recommendations

Of the upper estuary CDFs, CDF 1 and 1b have similar impacts on harbor velocities (see Figure 4-6) because they both reduce the overall cross section significantly. CDF 1 is potentially better suited because it is larger than CDF 1b, and it is further south of the heavily contaminated areas. If the upper estuary CDFs are necessary, elevated velocities that result from these facilities are better located in the southern extremes of the upper estuary to avoid resuspension of residual PCB-contaminated sediments. In the modeling scenarios, CDF case #2 provided lower velocities in the upper estuary because of the elimination of CDF 1b and a slight decrease in the sizes of CDFs 1 and 3.

The trade-offs between CDFs 1 and 1b are elevated velocities in the upper estuary versus containment of all contaminants (and CDFs) to a few contaminated areas of the river, such as CDF 1b. Containment to already-contaminated sections of the river reduces the somewhat unlikely risk of PCBs from the CDFs leaching into cleaner sediments, further contaminating the harbor. Long term, however, it is more likely that several storms each year will bring high winds and runoff to the area, resuspending sediments adjacent to the CDFs. Therefore, CDF 1 provides the best long term environmentally sound answer (over CDF 1b) if an upper estuary CDF is necessary.

Because the upper and lower harbor are significantly wider and deeper than the upper estuary, modification of the shoreline geometry and/or harbor (prism) volume do not result in adverse conditions, i.e., no CDF-induced velocities $> u_{crit}$. Because of this fact alone, CDFs 7 and 10 offer the best siting alternatives. While these facilities are much further south that the majority of the dredging and highly contaminated areas (see Figure 1-2), they offer the best long-term siting solutions because there is room for expansion, if needed. Given the total volume of contaminated sediments, e.g., ~1,000,000 cubic yards, larger and fewer facilities will be more cost effective in the long term because each facility will require maintenance indefinitely. The additional distance, however, introduces risk of contamination during dredging operations as

well as costs to the project. These trade-offs must be determined by local, USEPA Superfund, and USACE officials.

References

Applied Science Associates (ASA). 1986. Circulation and Pollutant Transport Model of New Bedford Harbor. Prepared by Applied Science Associates, Inc., Narragansett, RI, for Ropes and Gray, Boston, MA.

Applied Science Associates (ASA). 1987. Selected Studies of PCB Transport in New Bedford Harbor. Prepared by Applied Science Associates, Inc., Narragansett, RI, for Ropes and Gray, Boston, MA.

Aquatec, Inc. 1991. New Bedford Dye Study During 26 February - 19 March 1991. Prepared for the Department of Justice, Washington, D.C. Aquatec Project # 91024. Aquatec, Inc., South Burlington, VT.

Ariathurai, R., R.C. MacArthur, R.B. Krone. 1977. Mathematical Model of Estuarine Sediment Transport. Technical Report D77-12. U.S. Army Engineer Waterways Experiment Station, Vicksburg, MS.

Averett, Daniel E., M.R. Palermo, M.J. Otis, P.B. Rubinoff. 1989. "New Bedford Harbor Superfund Project, Acushnet River Estuary Engineering Feasibility Study of Dredging and Dredged Material Disposal Alternatives; Report 11, Evaluation of Conceptual Dredging and Disposal Alternatives," Technical Report EL-88-15, U.S. Army Engineer Waterways Experiment Station, Vicksburg, MS [NTIS AD No. A211 895].

Battelle Ocean Sciences (Battelle). 1990. Modeling of the Transport, Distribution, and Fate of PCBs and Heavy Metals in the Acushnet River/New Bedford Harbor/Buzzards Bay System. Volumes I-III. Submitted to EBASCO Services, September 21, 1990.

Beaudoin, Maurice. 1996. Personal Communication. Resident Engineer, USACE NED New Bedford Residence Office, New Bedford, MA. August 23, 1996.

Blumberg, A.F. and D.M. Goodrich. 1990. Modeling of Wind-Induced Destratification in Chesapeake Bay. *Estuaries*, **13**, pp. 1236-1249.

Blumberg, A.F. and L.H. Kantha. 1985. Open Boundary Condtion for Circulation Models. *J. Hydraulic Engineering*, **111**, pp. 237-255.

Blumberg, A.F. and G.L. Mellor. 1980. A Coastal Ocean Numerical Model, in *Mathematical Modelling of Estuarine Physics, Proceedings of an International Symposium.* Hamburg, Germany, August 24-26, 1978. J. Sundermannn and K.P. Holz, Eds., Springer-Verlag, Berlin.

Blumberg, A.F. and G.L. Mellor. 1983. Diagnostic and Prognostic Numerical Circulation Studies of the South Atlantic Bight. *J. Geophys. Res.*, **88**, pp. 4579-4592.

Blumberg, A.F. and G.L. Mellor. 1985. A Simulation of the Circulation in the Gulf of Mexico. *Israel J. of Earth Sciences*, **34**, pp. 122-144.

Blumberg, A.F. and G.L. Mellor. 1987. A Description of a Three-Dimensional Coastal Ocean Circulation Model, in *Three-Dimensional Coastal Ocean Models*, N. Heaps, Ed. American Geophys. Union, pp. 1-16.

Blumberg, A.F., R.P. Signell, and H.L. Jenter. 1993. Modelling Transport Processes in the Coastal Ocean. *J. Marine Env. Engg.*, **1**, pp. 3-52.

Blumberg, A.F. 1994. *A Primer for ECOM-si.* Hydroqual, Inc., New Jersey.

Case, E. 1989. Final Report on Independent Study and Research. 1.999 Special Undergraduate Projects. MIT Student Report. Advisor E.E. Adams.

Casulli, V. 1990. Semi-implicit Finite Difference Methods for the Two-dimensional Shallow Water Equations. *J. Comput. Phy.*, **86**, pp. 56-74.

Casulli, V. and R.T. Cheng. 1992. Semi-implicit Finite Difference Methods for Three Dimensional Shallow Water Flow. *Int. J. for Numer. Meth. in Fluids*, **15**, pp. 629-648.

Chan, A.B.J. 1995. A Numerical Investigation of the Effects of Freshwater Inflow on the Flushing in Boston's Inner Harbor. Masters Thesis, Dept. Civil and Environmental Engineering, MIT, Cambridge, MA, September 1995.

Cochrane, M. 1992. Evaluation of the Aquatec dye study in the New Bedford Harbor. MIT Project. September 4, 1992.

Condike, B.J. 1986. "New Bedford Superfund Site, Acushnet River Estuary Study," US Army Engineer Division, New England, Materials and Water Quality Laboratory, Hubbardston, MA.

Jason M. Cortell and Associates. 1982. Waterfront Park, New Bedford - Draft Environmental Impact Report. Prepared for Massachusetts Division of Waterways.

Dickerson, David. 1996. Memo to Brona Simon, State Archaeologist, Massachusetts Historical Commission, Re: Proposed Cleanup of the New Bedford Harbor Superfund Site. From David Dickerson, Remediation Manager, USEPA Region I, Boston, MA, July 25, 1996.

Dolin, E.J. and J. Pederson. 1991. Marine-Dredged Materials Management in Massachusetts: Issues, Options, and the Future. MIT Sea Grant MITSG 91-25, MCZM 91-01.

Ellis, J.P., B.C. Kelley, P. Stoffers, M.G. Fitzgerald, and C.P. Summerhayes. 1977. "Data File: New Bedford Harbor, Massachusetts," Technical Report WHOI-77-73, Woods Hole Oceanographic Institution, Woods Hole, MA.

Fischer, H.B., E.J. List, R.C.Y. Koh, J. Imberger, N.H. Brooks 1979. *Mixing in inland and coastal waters.* Academic Press, New York, New York, 483 pp.

Fowler, Alan S. 1991. "ARCS I: New Bedford Harbor Post FS Support Evaluation of Footprint Adjustments." EBASCO Services, Interoffice Correspondence #M91-329.

Francingues, Norman R., Jr., D.E. Averett, M.J. Otis. 1988. "New Bedford Harbor Superfund Project, Acushnet River Estuary Engineering Feasibility Study of Dredging and Dredged Material Disposal Alternatives; Report 1, Study Overview" Technical Report EL-88-15, U.S. Army Engineer Waterways Experiment Station, Vicksburg, MS [NTIS AD No. A211 895].

Galperin, B. and G.L. Mellor. 1990a. A Time-Dependenat, Three-Dimensional Model of the Delaware Bay and River System. *Estuarine, Coastal Shelf Sci.*, **31**, pp. 231-281.

Galperin, B. and G.L. Mellor. 1990b. Salinity Intrusion and Residual Circulation in Delaware Bay During the Drought of 1984, in *Residual Current and Long Term Transport*, R.T. Cheng, Ed. Springer-Verlag New York, Inc., **38**, pp. 464-482.

Germano, J.D., D.C. Rhodes, J.D. Lunt. 1994. An Integrated, Tiered Approach to Monitoring and Management of Dredged Material Disposal Sites in the New England Region. Science Applications International Corporation (SAIC) contribution #82, SAIC-90/7575&234. Submitted to USACE-New England Division.

Geyer, W.R. and W.D. Grant. 1986. A Field Study of the Circulation and Dispersion in New Bedford Harbor. Final Report Submitted to Battelle Ocean Sciences on September 30, 1986.

Graber, H.C. 1987. Improvement on Bottom Stress Calculations in the Presence of Waves Using a Simplified Form of the Grant-Madsen Boundary Layer Model. Woods Hole Oceanographic Institution, Woods Hole, Massachusetts.

Jenter, H. L. and R. P. Signell, 1992. NetCDF: A Freely-Available Software-Solution to Data-Access Problems for Numerical Modelers. Proceedings of the American Society of Civil Engineers Conference on Estuarine and Coastal Modeling. Tampa, Florida.

Ketchum, B.H. 1951. The exchanges of fresh and salt waters in tidal estuaries. *Journal of Marine Research.* **10**, pp. 18-38.

Mehta, A.J., E.J. Hayter, W.R. Parkes, A.M. Teeter. 1986. Cohesive Sediment Transport Processes. *Proceedings, Sedimentation Control Committee*, National Research Council, Washington, D.C.

Mirick, B. 1996. Personal Communication. USACE, NED, Waltham, MA, 13 August 1996.

MIT Department of Urban Planning and Studies (DUSP). 1996. New Bedford/ Fairhaven Harbor Planning Study. D.M. Frenchman, P. Roth, R.K. Burch, J.M. Carpenter, J. Lee-Chibli, R.M. Lohse, R. Singh, J.P. Vandermillen. July 1996.

National Marine Fisheries Service (NMFS). 1996. "Recovery Measures for New England Groundfish Approved," Press Release 96-R139, May 16, 1996. National Oceanic and Atmospheric Administration, U.S. Department of Commerce.

National Oceanic and Atmospheric Administration (NOAA). 1991. U.S. East Coast: Massachusetts: New Bedford Harbor and Approaches. National Ocean Survey, U.S. Department of Commerce. Navigational Chart #13232. February 1991, 1st Edition.

O'Donnell, E. 1996. Personal Communication regarding maintenance dredging operations in New Bedford Harbor. USACE-NED, Waltham, MA, October 11, 1996.

Oey, L.-Y., G.L. Mellor, and R.I. Hires. 1985a. Tidal Modeling of the Hudson-Raritan Estuary. *Estuarine Coastal Shelf Sci.*, **20**, pp. 511-527.

Oey, L.-Y., G.L. Mellor, and R.I. Hires. 1985b. A Three-Dimensional Simulation of the Hudson-Raritan Estuary. Part I: Description of the Model and Model Simulations. *J. Phys. Oceangr.*, **15**, pp. 1676-1692.

Oey, L.-Y., G.L. Mellor, and R.I. Hires. 1985c. A Three-Dimensional Simulation of the Hudson-Raritan Estuary. Part II: Comparison With Observations.*J. Phys. Oceangr.*, **15**, pp. 1693-1709.

Oey, L.-Y., G.L. Mellor, and R.I. Hires. 1985d. A Three-Dimensional Simulation of the Hudson-Raritan Estuary. Part III: Salt Flux Analyses. *J. Phys. Oceangr.*, **15**, pp. 1711-1720.

Rhodes, D.C. and D.K. Young. 1970. The influence of deposit-feeding organisms on sediment stability and community trophic structure. *J. Mar. Res.* **28**:15-176.

Roache, P. 1982.*Computational Fluid Dynamics.* Revised Printing, Hermosa, Albuquerque, NM.

Signell, Richard P. 1987. Tide- and wind-forced currents in Buzzards Bay, Massachusetts. MIT Master's Thesis, EAPS, Cambridge, MA.

Smagorinsky, J. 1963. General Circulation Experiments with the Primitive Equations, I. The Basic Experiment. *Mon. Weather Rev.*, **91**, pp. 99-164.

Speer, Paul Edward. 1984. Tidal distortion in shallow estuaries. MIT Ph.D. Thesis, EAPS, Cambridge, MA.

Summerhayes, C.P., J.P. Ellis, P. Stoffers, S.R. Briggs, and M.G. Fitzgerald. 1977. Fine-grained Sediment and Industrial Waste Distribution and Dispersal in New Bedford Harbor and Western Buzzards Bay, Massachusetts. Woods Hole Oceanographic Institution. WHOI-76-115. 110 p.

Summerhayes, C.P, J.P. Ellis, P. Stoffers. 1985. Estuaries as sinks for sediment and industrial waste : a case history from the Massachusetts coast, in *Contributions to sedimentology*, **14**. Schweizerbart, Stuttgart, 47 p.

Taylor, Captain Michael. 1996. Personal communication regarding commercial ship navigation within New Bedford Harbor.

Teeter, Allan M. 1988. "New Bedford Harbor Superfund Project, Acushnet River Estuary Engineering Feasibility Study of Dredging and Dredged Material Disposal Alternatives; Report 2, Sediment and Contaminant Hydraulic Transport Investigations," Technical Report EL-88-15, US Army Engineers Waterways Experiment Station, Vicksburg, MS [NTIS AD No. A205 136].

U.S. Army Corps of Engineers. 1989. Survey of New Bedford Harbor and Approaches. USACE New England Division. December 1989.

U.S. Army Coastal Engineering Research Center (USACERC). 1977. Shore Protection Manual. Department of the Army. Corps of Engineers.

U.S. Department of Commerce, NOAA, NMFS. 1996. "Recovery Measures for New England Groundfish Approved," Press Release 96-R139, May 16, 1996.

U.S. Environmental Protection Agency. 1983. "Aerovox PCB Disposal Site; Acushnet River and New Bedford Harbor, Massachusetts; Tidal Cycle and PCB Mass Transport Study," Environmental Response Team, Edison, NJ.

U.S. Environmental Protection Agency. 1987. Description of Alternative Disposal Sites for the New Bedford Harbor Feasibility Study. EPA Region I, Superfund Program, New Bedford Harbor Site, New Bedford, MA.

U.S. Environmental Protection Agency. 1990. Superfund record of decision : New Bedford Harbor, MA. USEPA Office of Emergency and Remedial Response. EPA/ROD/R01-90/045. March 1990.

U.S. Environmental Protection Agency. 1992a. "EPA Proposes Cleanup Plan to Address Contamination in the Estuary and Lower Harbor/Bay at the New Bedford Harbor Site," Proposed Plan. EPA Region I, Superfund Program, New Bedford Harbor Site, New Bedford, MA, January 1992.

U.S. Environmental Protection Agency. 1992b. Draft Final Supplementary Feasibility Study Evaluation for Upper Buzzards Bay and New Bedford Harbor RI/FS. Prepared by EBASCO Services for EPA Region I, Superfund Program, New Bedford Harbor Site, New Bedford, MA, May 1992.

U.S. Environmental Protection Agency. 1992c. "EPA Proposes Cleanup Plan to Address Contamination in the Estuary and Lower Harbor/Bay at the New Bedford Harbor Site," Addendum Proposed Plan. EPA Region I, Superfund Program, New Bedford Harbor Site, New Bedford, MA, May 1992.

U.S. Environmental Protection Agency. 1995. New Bedford Harbor Superfund Site: Community Forum: November 29, 1995 Poster Session. New Bedford, MA.